Decay of Nonsense-Containing β-Globin mRNA in Erythroid Cells

PhD Dissertation

Presented in Partial Fulfillment of the Requirements for the Degree Doctor of Philosophy in the Graduate School of The Ohio State University

By

Julie Ann Dougherty

Biomedical Sciences

The Ohio State University

2014

Dissertation Committee:

Daniel R. Schoenberg, Advisor

Juan D. Alfonzo

Dawn S. Chandler

Denis C. Guttridge

Abstract

mRNAs targeted by endonuclease decay generally disappear without detectable decay intermediates. Nonsense-containing human β-globin mRNA is a unique exception. Detectable 5' truncated β-globin RNAs are stabilized in the cytoplasm of erythroid cells of transgenic mice and in transfected erythroid cell lines. A quantitative assay was developed to study the relationship of the truncated RNAs to the full-length mRNA. Addtionally, an inducible erythroid cell system was developed to allow for kinetic analysis of a precursor-product relationship. Results verified that a 5' truncated β-globin RNA is indeed a metastable decay product of the full-length transcript. The inducible cells allowed for knockdown to occur prior to expression of nonsense β-globin mRNA. Upf1 is the master regulator of NMD and its knockdown revealed an increase in full-length β-globin and a decrease in the truncated RNA, confirming involvement of NMD. SMG6 has been identified as an endonuclease of the NMD pathway, thus SMG6 knockdown was performed prior to inducing nonsense-containing β-globin mRNA expression. Full-length nonsense-containing β-globin was increased during SMG6 knockdowm while the truncated species was decreased; which is consistent with SMG6 being involved in their generation. Next, endogenous SMG6 was knocked down and complemented back with siRNA-resistant constructs, either wild type or a SMG6 mutant with an inactive endonuclease activity. Complementation with wild type SMG6 was able to rescue the increased accumulation of the truncated RNA with the associated decrease in full-length transcript. The inactivated enzyme was unable to reverse the effects of SMG6 knockdown and the full-length mRNA was stabilized and the amount of the shortened RNA decreased. These results demonstrate that the endonuclease activity of SMG6 is responsible for

the generation of the 5’ truncated decay products. Notably, none of the SMG6 manipulations altered the phosphorylation state of Upf1. As a whole, these data provide the first proof for generation of stable NMD decay products by SMG6 endonuclease cleavage.

Dedication

I dedicate this document to those who look at the world with wonder.

Acknowledgments

I would first like to acknowledge and thank my advisor, Dan, for all his guidance and encouragement over the years. Thank you for challenging me, pushing me, and believing in me as I could not have asked for a better advisor. I would also like to acknowledge present and former members of the lab for all their advice and support. Roshan for his teamwork on the SMG6 project and for pushing me forward. Deepak for sharing his sequencing and PCR expertise to help me get through implementation of the MBRACE assay. Daniel for giving me lessons in scientific writing and rigorously reviewing my drafts. I would also like to acknowledge Chandrama, ShanQing, Baskar, Juny, Sean, Jennifer, and Jackson for their support and encouragement. I would also like to acknowledge my committee members – Dawn, Juan, and Denis – for their counsel and rigor to push me to understand my project at all levels.

I would like to thank Beth being a great friend and willing to listen when I needed someone to talk to. I am so very grateful to Leslie for her unwavering belief in me and understanding of the tribulations of graduate school. I am ever greateful to Rob, my better half, for all his love and understanding, especially through the stressful times. Finally, I sincerely appreciate the wonderful support and love I have had from my family. I am utterly grateful to my parents for allowing me to be inquisitive as a child, nurturing my mind and my heart, and *always* being there for me no matter what. I want to thank my sister for knowing how to improve my mood with humor and offering guidance for the professional world. I am most grateful to my brother for embracing life, taking time to visit me, and being a source of inspiration and love.

Vita

June 2002	Lorain Admiral King High School
March 2006	B.S. Biological Sciences, Ohio University
June 2006 –June 2008	Quality Control Technician, LifeShare Community Blood Services, Elyria Ohio
June 2008 – April 2010	Graduate Research Associate, Department of Molecular Virology, Immunology, and Medical Genetics
April 2010 - present	Graduate Research Associate, Department of Molecular & Cellular Biochemistry

Publications

Youseff BH, **Dougherty JA** and Rappleye CA**.** (2009) Reverse genetics through random mutagenesis in *Histoplasma capsulatum*. *BMC Microbiol*. **9**, 236.

Mascarenhas R*, **Dougherty JA***, and Schoenberg DR. (2013) SMG6 Cleavage Generates Metastable Decay Intermediates from Nonsense-Containing β-Globin mRNA. *PLoS ONE* **8**(9): e74791. doi:10.1371/journal.pone.0074791. *These authors contributed equally to this work.

Dougherty JA, Roshan Mascerenhas, and Schoenberg DR. (2014) Quantitative analysis of deadenylation-independent mRNA decay by MBRACE assay. *Methods in Molecular Biology*. Rorbach, J. and Bobrowicz, A.J. (eds) vo1 1125 Copyright ©2014 Springer+Business Media, New York.

Fields of Study

Major Field: Integrated Biomedical Science Program

Emphasis: Molecular Basis of Disease

Table of Contents

Abstract ..... ***ii***

Dedication ..... ***iv***

Acknowledgments ..... ***v***

Vita ..... ***vi***

List of Tables ..... ***x***

List of Figures ..... ***xi***

Abbreviations and Keywords ..... ***xiii***

Chapter 1: Introduction ***1***

Chapter 2: Quantitative Analysis of Deadenylation-Independent mRNA by Modified MBRACE Assay ***39***

Chapter 3: SMG6 Cleavages Generates Metastable Decay Intermediates from Nonsense-Containing β-globin mRNA ***64***

Chapter 4: Discussion ***92***

List of References ***106***

List of Tables

Table 1. Core NMD Factors 5

Table 2. TAP reaction master mix 43

Table 3. RNA linker ligation reaction master mix 44

Table 4. RT master mix for RNA 45

Table 5. 2x RT reaction master mix 45

Table 6. 2x RT reaction mix 55

Table 7. Molecular Beacon qPCR master mix 57

Table 8. Oligonucleotides and Primers 91

List of Figures

Figure 1. Model of Normal vs PTC-containing mRNA 2

Figure 2. Domain and interaction map of Upf1, Upf2, and UPf3 6

Figure 3. Conformational change of Upf1 upon binding to Upf2 7

Figure 4. Domain map of SMG1 9

Figure 5. Domain map of SMG5 and SMG7. 10

Figure 6. Ribbon representation of PIN domain structures of SMG5 and SMG6 11

Figure 7. EBM domains of Upf3b and SMG6 13

Figure 8. The 50-55 nt rule for PTC determination 14

Figure 9. NMD-sensitivity as a function of PTC position. 15

Figure 10. The faux 3' UTR model of PTC recognition 17

Figure 11. NMD is a branched pathway 21

Figure 12. Normal translation termination. 22

Figure 13. Premature translation termination 24

Figure 14. Mechanisms of mRNA degradation 26

Figure 15. SMG5, SMG7, and PNRC2 target mRNA overlap 27

Figure 16. Biogenesis of miRNAs 30

Figure 17. Phenotype of thalassemic RBCs 33

Figure 18 Schematic of PTC locations along -globin mRNA 34

Figure 19. S1 nuclease protection assay methodology 35

Figure 20. Gel electrophoresis of 5' RLM-RACE products 48

Figure 21. Schematic of Molecular Beacon 49

Figure 22. Theoretical thermal denaturation profile for molecular beacon 51

Figure 23. Workflow of modified MBRACE protocol 54

Figure 24. Calculation and results of MBRACE validation experiments 60

Figure 25. Prolonged cytoplasmic residence of 5' truncated forms of PTC-hBg mRNA 73

Figure 26. Development of a modified MBRACE assay for quantifying full-length and one of the 5' truncated B-globin mRNAs 75

Figure 27. Evidence that NMD is responsible for the accumulation of Δ169 RNA from PTC-hβg mRNA .. 77

Figure 28. Evidence that 5' truncated RNAs are decay intermediates. 80

Figure 29. SMG6-knockdown increases full-length PTC hβg mRNA and decreases Δ169 RNA 82

Figure 30. Complementataion identifies SMG6 is the endonuclease responsible for generating Δ169 RNA from PTC hβg mRNA 84

Figure 31. Upf1 phosphorylation status is unaffected by SMG6 knockdown or overexpression of inactive SMG6 85

Figure 32. Sequence alignment of human beta- and delta-globin mRNA and locations of MBRACE primers 89

Figure 33. Impact of changes in PMR1 on full-length and Δ169 hβG mRNA. 90

Abbreviations and Keywords

ATP – adenosine triphosphate

C. elegans – Caenorhabditis elegans, worms

cCE – cytoplasmic capping enzyme

cDNA – complementary DNA

DN – dominant negative

D. melanogaster – Drosophila melanogaster, fruit flies

DNA – deoxyribonucleic acid

eIF4AIII – eukaryotic initiation factor 4 AIII, EJC component

eIF4E/G – eukaryotic initiation factors 4 E/G

E. coli – Escherichia coli

EJC – exon junction complex

eRF1/eRF3 – eukaryotic release factor 1/3

K562 – human erythroleukemic cell line

MBRACE – molecular beacon rapid amplification of cDNA ends

MEL – murine erythroleukemic cell line

mRNA – messenger ribonucleic acid

mRNP – messenger ribonucleoprotein particle

Norm2 – MEL expressing wildtype human β-globin

NMD – nonsense-mediated mRNA decay

oligo(dt) – thymine oligonucleotide

PABPC1 – poly(A) binding protein cytoplasmic 1

PCR – polymerase chain reaction

qPCR – quantitative polymerase chain reaction

hPMR1 – human polysomal ribonuclease 1

PTC – premature termination codon

5'-RLM-RACE – 5'- RNA-linker-mediated rapid amplification of cDNA ends

RNA – ribonucleic acid

RNase(s) – ribonuclease(s)

RNAi – RNA interference

RNPS1 –RNA-binding protein with serine-rich domain 1, EJC component

S. cerevisiae – *Saccharomyces cerevisiae*, yeast

S. pombe – *Schizosaccharomyces pombe*, budding yeast

S1 NPA – S1 nuclease protection assay

TAP – tobacco acid pyrophosphatase

Thal10 – MEL cell line expressing PTC60/61 human β-globin

WT – wildtype

Xrn1 – 5'-3' exonuclease

Y14/Magoh – heterodimer component of the EJC

Units

kDa – kilo Dalton

nt - nucleotide

mL - milliliter

µL – microliter

mM - millimolar

nM – nanomolar

µM – micromolar

µg – microgram

ng - nanogram

h – hour

min – minute

sec - second

g - acceleration due to gravity

v/v – volume per unit volume

w/v – weight per unit volume

Chapter 1: Introduction

Messenger RNA Surveillance and Quality Control

The primary purpose of messenger RNAs (mRNAs) is to act as a template for protein synthesis. Numerous cellular processes are required to generate, modify, survey, and destroy mRNAs. An incomplete list includes transcription, capping, splicing, polyadenylation, editing, export, cytoplasmic localization, translation and degradation. Errors are inherent in all of these processes and amount to a significant number of abnormal mRNAs that challenge the fidelity of gene expression. Quality control mechanisms, therefore, are important for recognizing and destroying these erroneous mRNAs. Cells have evolved myriad means to this end but the focus here will be on one such pathway, nonsense-mediated mRNA decay (NMD).

NMD is a post-transcriptional surveillance mechanism that recognizes and targets transcripts harboring premature termination codons (PTCs), also known as nonsense codons, for rapid degradation (Figure 1). The pathway was discovered over 30 years ago in worms, budding yeast, and human bone marrow cells of β-thalassemia patients. Analysis of RNA metabolism revealed that the stability of mRNAs that contained a PTC was greatly reduced compared to their normal counterparts [26, 27]. This destabilization of PTC-containing mRNAs has been observed in many eukaryotic species indicating that NMD emerged early on in eukaryote evolution. This quality control system functions to prevent the production of truncated proteins, which can pose several threats to the cell and whose synthesis would be a waste of cellular resources. Additionally, truncated proteins can have dominant negative effects inhibiting the function(s) of their wildtype equivalent and have potentially deleterious effects in cells. Lastly, the truncation

may actually impose a gain of function or constitutively active phenotype; which could be harmful to the cell by disrupting regulation of normal protein function. Therefore, it is vitally important for cells to survey, recognize, and degrade these aberrant mRNAs.

Figure 1. Model of Normal vs PTC-containing mRNA

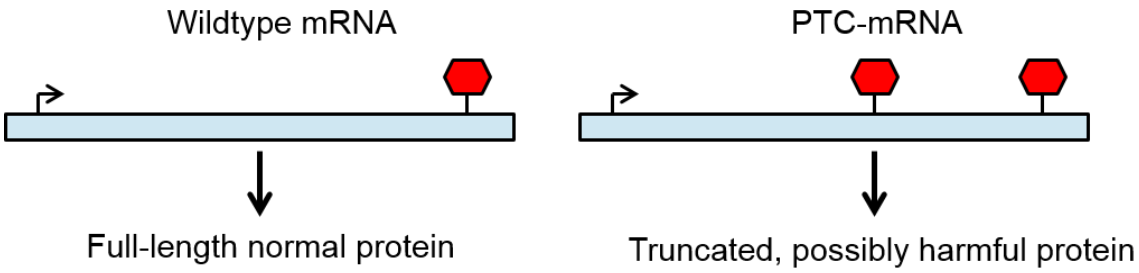

Translation starts at arrow. Stop codon represented by red stop sign

The increasing practicality of sequencing technology allowed for the discovery that NMD also functions to regulate physiological mRNAs, which encode full-length proteins. mRNA profiling studies of NMD-defective *S. cerevisiae*, *C. elegans*, *Drosophila* and human cells revealed between 3-10% of all mRNAs are regulated by NMD [28-36]. These findings expand the role of NMD beyond a mere quality control mechanism into one that influences a range of biological processes by influencing gene expression.

NMD is an Essential and Conserved Pathway Among Metazoans

Simpler organisms with NMD deficiencies are still viable and have mild phenotypes. NMD-deficient strains of *S. pombe* have not shown a detectable phenotype under laboratory conditions [37], most likely due to the lack of alternative splicing occurring in budding yeast. *C. elegans* undergo moderate alternative splicing and mutations in NMD genes have several mild phenotypic

defects including embryonic patterning defects [38], morphological alterations of genitalia [39], reduced brood size [40], and abnormal maintenance of RNAi [41]. Conversely, perturbing NMD is more detrimental in more complex organisms, presumably due to a larger extent of alternative splicing. Many believe alternative splicing is a mechanism by which organisms can expand their proteome by expressing new protein isoforms [42]. For example, *Drosophila* Dscam pre-mRNA can undergo extensive alternative splicing; it contains 95 alternative exons to generate 38,016 unique mRNAs [43]. Alternative splicing is also proposed to act as a regulatory mechanism by affecting the localization, activity, stability, or even function of a gene depending on the exons that are retained or removed by splicing [44-46]. Studies show 70-90% of human genes undergo alternative splicing and 25-35% of alternative exons introduce a PTC [47, 48]. This is a likely explanation for the increased importantce of NMD in higher order species. Zebrafish with knocked down NMD factors suffer severe embryonic developmental abnormalities including early patterning defects and loss of cell viability, and die during embryonic development [49]. *Drosophila* with null mutations for certain core NMD factor genes die during larval development [50, 51] and knockout experiments in mice have shown that losing particular core NMD factors is embryonic lethal [52-54]. In mammals, however, elucidation of the biological requirement of NMD is further complicated by the involvement of NMD factors in telomere maintenance, DNA repair, and genome stability [55-58]. Collectively, these findings support the concept that the need for intact NMD is important for normal development and this need is conserved.

NMD factors

In mammals, the core proteins of the NMD surveillance complex are Upf1, Upf2, Upf3a/3b, SMG1, SMG5, SMG6, and SMG7 (Table 1). All are evolutionarily conserved, the Upf proteins from eukaryotes and the SMG proteins from metazoan. Other peripheral factors utilized by the NMD pathway include translational release factors, components of the exon-exon junction

complex (EJC), additional SMG factors, and factors that bind the 5' and 3' ends of mRNAs. An overview of the factors and their importance to NMD will be presented.

The Upf Protein Family

The Upf proteins were originally identified in budding yeast [59] in a genetic screen for translation frameshift suppressors, thus the name Upf for up-frameshift. Upf1, Upf2, and Upf3 are the principle NMD regulators in eukaryotes [40, 60-64]. Upf1 is the key effector and master regulatory protein of NMD. Upf1 is absolutely required for NMD to occur [65] as deletion or mutations in Upf1 are embryonic lethal in flies and mammals. Upf1 is capable of binding RNA in the presence or absence of ATP [66-68]. The protein has two principal domains (Figure 2) a cysteine and histidine rich zinc finger domain (CH domain) followed by a flexible linker sequence and a domain with conserved motifs common to super family I helicases [69-71]. The helicase core contains two recombinase A (RecA)-like domains, common to all super family I helicases, and there are also two Upf1-specific regulatory domains 1B and 1C [72]. The CH domain plus the RNA-dependent ATPase and RNA helicase activities of Upf1 are all essential for NMD [65, 67, 68, 73]. The CH domain of Upf1 interacts with Upf2, which acts as a molecular bridge to potentiate Upf1's interaction with Upf3 [61]. In the absence of Upf2 binding, Upf1 exists in a closed state where domain 1B binds RNA, which increases overall RNA binding but decreases ATPase and helicase activities [66, 74, 75]. Upon binding to Upf2, Upf1 undergoes a significant conformational change (Figure 3); resulting in decreased RNA binding and stimulating its helicase activity [74]. Thus transitioning it from a state where it tightly binds RNA to one where it can unwind RNA.

Table 1. Core NMD Factors

Factor	Cellular localization	Biochemical characteristics	Function(s) during NMD	Non-NMD functions	refs
Upf1	Shuttling, mainly cytoplasmic	RNA helicase, RNA-dependent ATPase, RNA binding	Master regulator, links the EJC and translation termination machinery by binding to Upf2 and eRF3	Promotes translation; histone mRNA decay; genome stability; telomere maintenance	[52, 56, 67, 76-86]
Upf2	Cytoplasmic, mainly perinuclear but has NLS	phosphoprotein	Binds to Upf3 and Upf1, promotes Upf1 phosphorylation	Translation; telomere maintenance	[35, 56, 79, 87-90]
Upf3a	Mainly nuclear	RNA-binding, phosphoprotein	binds Upf2; interacts with EJC core; weaker NMD factor than Upf3b; can partially compensate for Upf3b deletion	Telomere maintenance	[56, 79, 90-92]
Upf3b/ Upf3X	Mainly nuclear	RNA-binding, phosphoprotein	Binds Upf2; interacts with EJC core; stronger NMD factor than Upf3a	Translation; telomere maintenance	[56, 79, 90-94]
SMG1	Cytoplasmic and nuclear	Ser/Thr kinase of PIKK family, ATP binding, phosphoprotein	Directly phosphorylates Upf1	Genotoxic and stress response pathways; TNAα-induced apoptosis; telomere maintenance	[57, 76, 78, 95-99]
SMG5	Mainly cytoplasmic	Inactive PIN domain, 14-3-3-like domain	Promotes Upf1 dephosphorylation; can form heterodimer with SMG7 or PNRC2	Telomere maintenance	[13, 77, 100-103]
SMG6	Mainly cytoplasmic	Active PIN domain, 14-3-3-like domain	Promotes Upf1 dephosphorylation; directly cleaves transcripts	Telomere maintenance	[13, 103, 104]
SMG7	Mainly cytoplasmic	Two 14-3-3-like domains	Promotes Upf1 dephosphorylation; forms heterodimer with SMG5	Telomere maintenance	[8, 78, 100, 105]

EJC: exon-exon junction complex; PIN: PilT N Terminus; PIKK: PI3K-like kinase. Adapted from [106] © The Authors Journal compilation ©Biochemical Society and from [16] with permission license 3333681320786.

Figure 2. Domain and interaction map of Upf1, Upf2, and UPf3

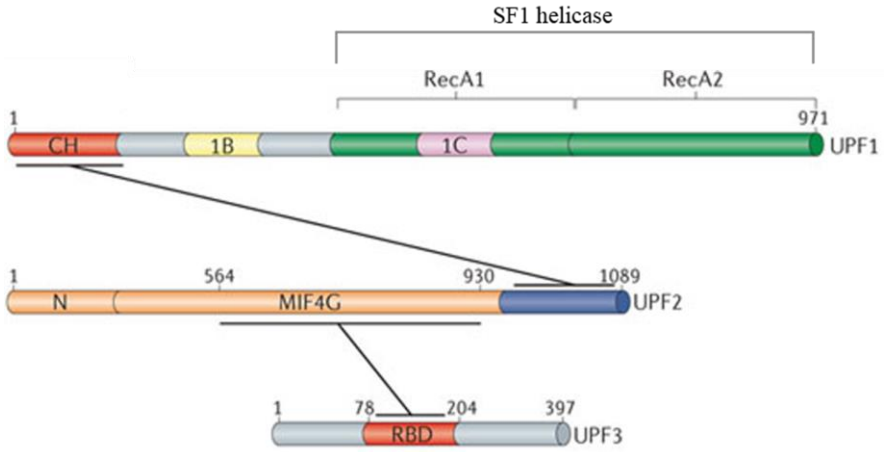

Lines represent interactions between factors. Domains are labeled as such. Reprinted with permission license from 3327161320906 from [14].

In mammals, Upf3 is expressed as two different proteins, Upf3a and Upf3b. The factors are encoded by two different genes located on two separate chromosomes. Both proteins are expressed in multiple isoforms due to alternative splicing. Although highly homologous to Upf3b, Upf3a is not as strong an activator of NMD and is not essential for degradation to occur [91]. Upf3b binds to the EJC core proteins RNPS1 [107] and Y14 [93] during splicing in the nucleus, with Upf2 being recruited to Upf3 soon after mRNA export.

Figure 3. Conformational change of Upf1 upon binding to Upf2

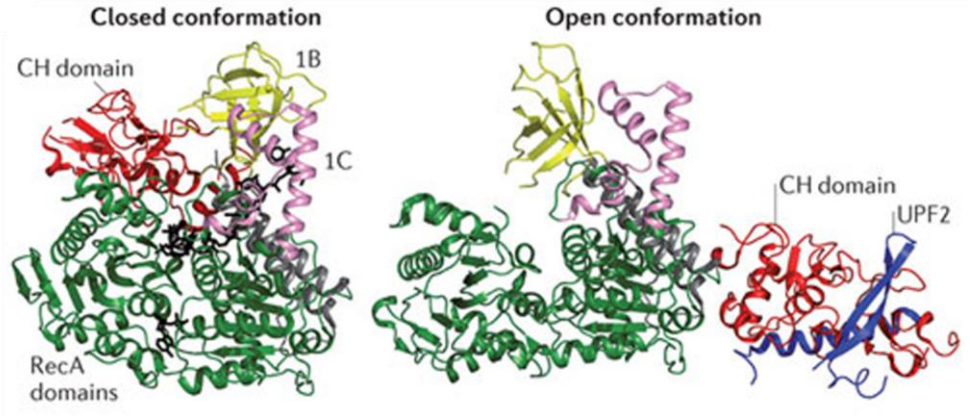

The significant rearrangement of the CH domain of Upf1 upon binding Upf2. Reprinted with permission license 3327161320906 from [62].

The SMG Protein Family

The SMG protein family was originally identified in *C. elegans* [108, 109] and plays a crucial role in NMD. SMG proteins were named for suppressor with morphological effect on genitalia. SMG proteins (Table 1) are believed to modulate the activity of Upf1 through cyclical rounds of phosphorylation and dephosphorylation [77, 108]. SMG1 directly phosphorylates Upf1 while SMG5, SMG6, and SMG7 are involved in factor recruitment for dephosphorylation. Additionally, SMG5, SMG6, and SMG7 are responsible for recruiting degradation factors to the mRNA once NMD has been induced.

SMG1

SMG1 is a phosphatidyl-inositol-3-kinase (PI3K)-related kinase (PIKK) that is directly responsible for the phosphorylation of Upf1 [78, 95]. SMG1 is essential for NMD to occur as inhibitors of this kinase (caffeine and wortmannin) block NMD of PTC-containing reporters [110]. SMG1 is a large protein at 410 kDa that shares structural elements common to all PIKK

proteins (Figure 4). The conserved 600 amino acid FAT (FRAP/TOR, ATM, and TRRAP) domain is followed by the catalytic kinase domain and a short C-terminal FATC (FAT C-terminal domain. The conserved C terminus is preceded numerous, helical, mainly HEAT (huntington, elongation factor 3, a subunit of PP2A and TOR1) repeats [111] providing this region extensive flexibility, which usually acts as scaffolding for protein-protein interactions.

SMG1 is unique among PIKK family members in that it has an approximately 1000 amino acid insertion between the kinase and FATC domains. Tis region has poorly characterized function but has been implicated in Upf1 recognition [76]. Newly identified factors SMG8 and SMG9 form a complex with SMG1, termed the SMG1 complex or SMG1-C [112]. *In vitro* kinase assays show that SMG8 suppresses the kinase activity of SMG1 while in the SMG1-C, in a dose dependent manner. SMG9 stimulates the formation of SMG1-C as its depletion reduces the amount of SMG8 that co-immunoprecipitates with SMG1. Furthermore, depletion of SMG9 causes the accumulation of phosphorylated Upf1, suggesting a role in its cyclical phosphorylation and dephosphorylation [112]. Knockdown of either SMG8 or SMG9 inhibits NMD of PTC-containing reporters, consistent with a requirement for NMD [112]. SMG1 phosphorylation is induced by formation of the decay inducing (DECID) complex [112], which will be discussed later, and triggers assembly of the decay machinery. Phosphorylated Upf1 is recognized by SMG5, SMG6, and SMG7 via a conserved 14-3-3 like domain present in all three proteins. This domain consists of nine parallel α helices and folds in an orientation homologous to 14-3-3 proteins. 14-3-3 proteins are a large family of proteins that interact with phosphorylated serine and threonine residues of their partners [105]. These interactions generally serve to link mRNA surveillance and decay. These interactions also serve an adaptor between Upf1 and protein phosphatase 2A [77, 100, 101], leading to dephosphorylation and inactivation of Upf1.

Figure 4. Domain map of SMG1

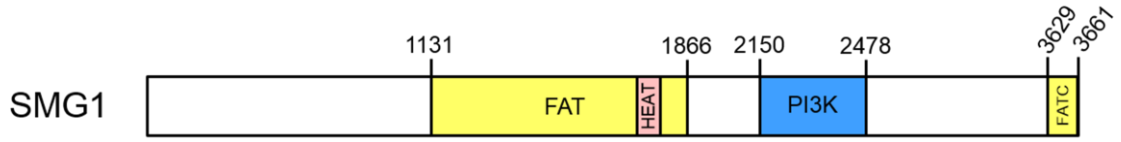

FAT: FRAP/TOR, ATM, TRRAP; HEAT: Huntington, elongation factor 3, a subunit of PP2A, TOR1; PI3K: phosphatidyl-inositol-3-kinase; FATC: C-terminal FAT

SMG5, SMG7

SMG5 and SMG7 can form a heterodimer via their 14-3-3-like domains [101] (Figure 5), which is able to bind phosphorylated Upf1. Whether heterodimerization of SMG5-SMG7 is required for NMD was investigated with complementation assays. A SMG5 variant mutated to disrupt binding to SMG7 and still maintain proper folding of its N-terminal domain was created. Endogenous SMG5 and SMG6 were siRNA-depleted and SMG5 was complemented with wildtype or mutant SMG5. Results showed that the SMG5 mutant was inactive or strongly impaired in rescuing decay of NMD reporters. Reciprocal mutations were made in SMG7 and complementation assays were performed similarly and again showed that disrupting the SMG5-SMG7 interaction abrogated the rescue of NMD [113]. Conversely, experiments from another group showed that SMG5 can heterodimerize with PNRC2 and still elicit mRNA degradation establishing that the SMG5:SMG7 dimer is not essential for NMD, this will be further discussed later.

Figure 5. Domain map of SMG5 and SMG7.

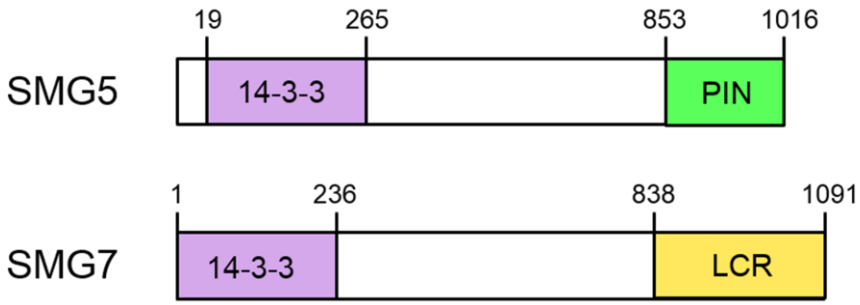

Adapted from [17] permission not needed since >6 months from publication. Copyright ©2010 by Cold Spring Harbor Laboratory Press, New York. PIN: PilT N Terminus; LCR: Low complexity region.

SMG6

Both SMG5 and SMG6 contain predicted PilT N terminus (PIN) endonuclease domains, as judged by sequence homology [77]. PIN domains were named for sequence similarity to the N-terminal domain of a documented pili biogenesis protein, PilT [114]. PIN-domain-containing proteins are present in all three kingdoms of life and their endonuclease activity was predicted by bioinformatic analysis of their sequence and active site similarity to other known endoribonucleases [102]. PIN domain active sites consist of a cluster of invariant acidic amino acid residues, likely as putative metal-binding residues, with ribonuclease activity [115]. Despite overall sequence and structural similarities, further analysis revealed significant differences between SMG5 and SMG6 at their putative active sites [13]. Only SMG6 has the catalytic triad of aspartic acid residues needed to efficiently coordinate endonuclease activity (Figure 6) [13]. Furthermore, i*n vitro* degradation assays showed that only SMG6 is capable of efficiently cleaving ssRNA [13]. SMG6 was found to be the enzyme responsible for NMD cleavage in *Drosophila* S2 cells [116]. Endogenous SMG6 was depleted with a specific siRNA and this was shown to inhibit NMD of PTC-containing reporters [116]. To better establish the role of SMG6 in this pathway, S2 cells were depleted of endogenous SMG6 and were complemented with

wildtype and PIN-inactive mutant siRNA-resistant forms of SMG6. Complementation with wildtype SMG6 was able to rescue NMD of the PTC-containing reporters but NMD was not

Figure 6. Ribbon representation of PIN domain structures of SMG5 and SMG6

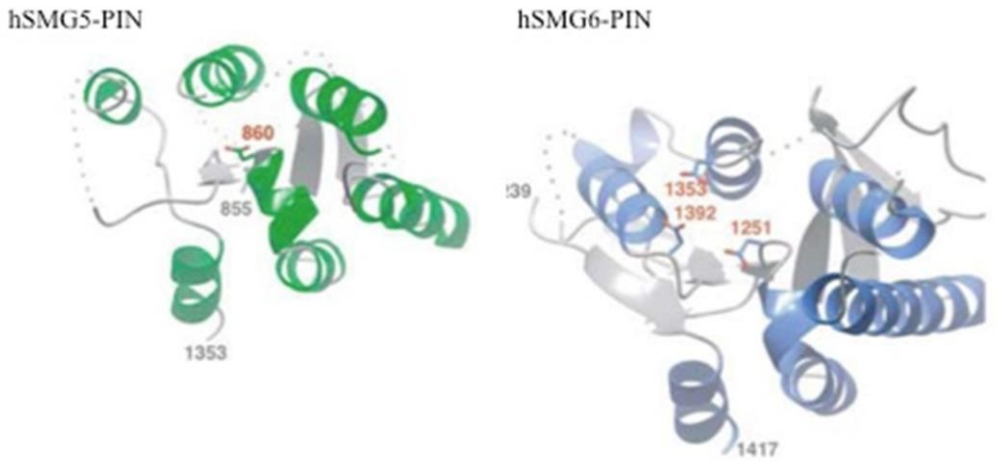

Catalytic core of the PIN domains of SMG5 and SMG6 shown with key aspartic acid residues in red. Reprinted with permission license 3331520387802 from [13].

recoverable during complementation with the inactive PIN-mutant [116]. The PIN domain of SMG6 was replaced with the PIN domain of a known endonuclease with similar structure and complementation experiments were repeated. Results demonstrated that NMD of the reporters was rescued in cells complemented with the exchanged active PIN domain [116]. Similar complementation experiments confirmed SMG6 as an endoribonuclease involved in NMD in human cells [104].

In addition to its 14-3-3-like and PIN domains, SMG6 also has an N terminal domain that plays an important role in the pathway. Experiments with SMG6 deletion mutants and PTC-containing reporters showed that all 3 domains are required for NMD; complementation to

SMG6-depleted cells did not rescue NMD activity [4]. While the roles of the PIN and 14-3-3-like domains were characterized (endonucleolytic RNA cleavage and binding to phosphorylated Upf1 respectively) no function had yet been identified for the N-terminal domain of SMG6. The Izaurralde group continued working with the SMG6 single domain deletion mutants to investigate interactions with other NMD factors. Co-immunoprecipitation (co-IP) experiments demonstrated that SMG6 is able to bind Upf1, Upf2, Upf3b, SMG5, and SMG7, in an RNA-independent manner [76]. Y14, Magoh, and PABP were also identified as binding partners but were lost when treated with RNase A [4]. Normally, a protein-protein interaction that is sensitive to RNase treatment indicates that the interaction is indirect. However, in this case, EJC assembly requires RNA and it may have been destabilized with RNase treatment. Two conserved and related motifs were found in the N-terminal domains from several species suggesting that these motifs within the N-terminal domain may be the source of interaction(s) with NMD surveillance complexes. Interestingly, these motifs exhibited 23% and 38% identity with a Upf3b C-terminal motif known to mediate its binding to the EJC [93, 117]. The motifs were termed EJC binding motifs (EBMs) and designated EBM1 and EBM2 (Figure 7). *In vitro* binding experiments using recombinant proteins and a biotinylated peptide corresponding to EBM2 sequence showed that the N-terminal domain containing the EBMs is required for binding to EJC components [4]. The EBMs were tested for their individual and shared ability to bind the EJC and influence on NMD by deleting one or both motifs. Deleting either motif greatly reduced SMG6 binding to Y14 and Magoh, while double deletion abolished binding altogether. *In vitro* competition experiments with tagged SMG6 and Upf3b were performed against preassembled EJCs to determine if these proteins bind the EJC in a mutually exclusive manner. Results showed that it took a six-fold molar excess of SMG6 to disrupt Upf3b binding, while it only required a two-fold excess of Upf3b to block SMG6 binding [4]. These result support the hypothesis that SMG6 competes with Upf3b to interact with the EJC, via Y14 and Magoh and that Upf3b has a higher affinity for the binding site [4]. Additional experiments with the EBM mutant SMG6 determined that the interaction with the

EJC via the EBMs is required for proper NMD activity. NMD of PTC-containing reporters was greatly inhibited when either of the domains were deleted and was completely abolished when both EBMs were deleted [4].

Figure 7. EBM domains of Upf3b and SMG6

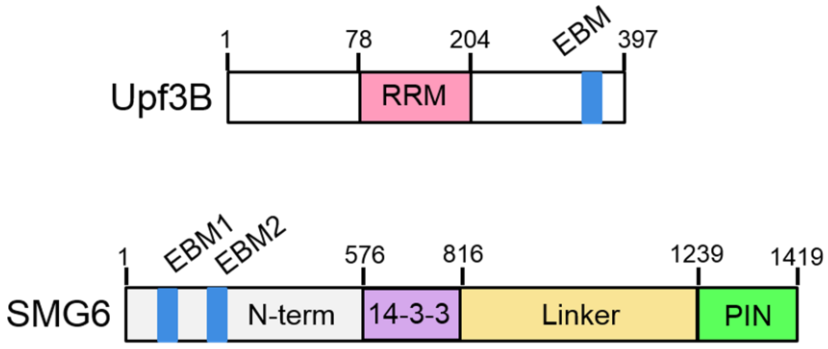

Competitive exon-exon junction binding domains (EBM) are found in Upf3B and SMG6. RRM: RNA Recognition Motif; PIN: PilT N-terminal. Adapted from [4] permission not needed since >6 months from publication. Copyright ©2010 by Cold Spring Harbor Laboratory Press, New York.

Models for PTC recognition

In order for a PTC-containing transcript to be degraded by the NMD pathway the PTC must first be recognized as premature. While NMD is a conserved process, the mechanism of PTC recognition is not. Different organisms have different mechanisms and most utilize multiple means. Studies over the years have identified various *cis* and *trans* factors that demarcate PTCs. Collectively, these data have brought about two leading models of PTC recognition – the 50-55 nucleotide (nt) rule and the faux 3' UTR model.

The 50-55 nt rule

The splicing process alters the composition of the messenger ribonucleoprotein particle (mRNP) by depositing the stable exon-exon junction complex (EJC) 20-25nt upstream of exon-exon junctions [118]. A general rule for recognition by the NMD machinery is the 50-55nt rule, which stipulates that if a termination codon is more than 50-55nt upstream of the 3' most exon-exon junction then it is determined to be premature and the mRNA is targeted for degradation by NMD (Figure 8) [119].

Figure 8. The 50-55 nt rule for PTC determination

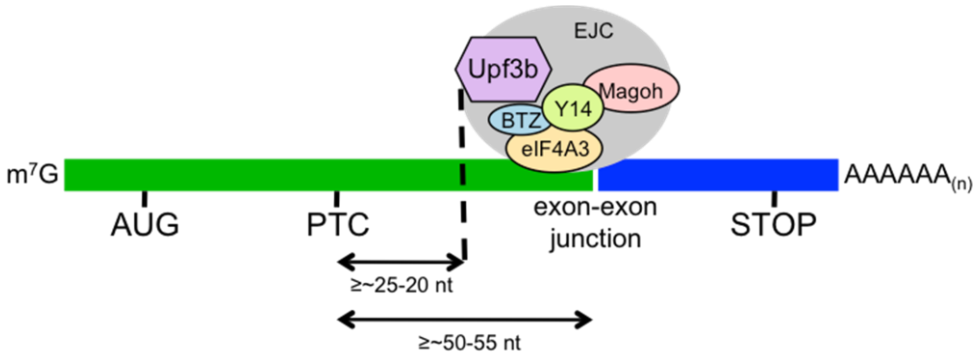

Pre-mRNA splicing results in the deposition of an exon-junction complex (EJC) of proteins upstream of mRNA exon–exon junctions . Core EJC components consist of eIF4AIII, RNA-binding-motif protein Y14, mago nashi homologue (MAGOH) and Barentsz (BTZ). The UPF3b NMD factor, which shuttles to the nucleus, is thought to be recruited to EJCs in the nucleus and is exported with the mRNA to the cytoplasm. UPF3b then recruits UPF2 to the complex. Adapted from [18] with permission license 3367700774749..

The basis for this rule arose from two studies that determined the role of splicing and the EJC in NMD. Early studies from the Maquat lab looked for possible *cis* factors that could be causing decreased stability of PTC-containing human triosephosphate isomerase (TPI) transcripts.

Work with this 7 exon TPI reporter first identified differences in mRNA stability between a PTC located at codon 189 and one located at codon 208 of pentultimate exon 6. PTC189 reduced TPI mRNA levels to 20% of normal and PTC 208 had no effect on TPI abundance [5]. To narrow this margin, PTCs were placed at all codons between 189 and 208 and PTC-containing TPI reporter mRNA was analyzed for stability. The boundary was defined somewhere between codon 192 and 195, or 43 to 55 nt upstream of the last intron [5] (Figure 9) Experiments by the Kulozik group with β-globin mRNAs with PTCs in the second (pentultimate) exon and determined that the nonsense mutation must be at least 50 nt upstream from the last exon junction to trigger NMD [120]. The 50-55nt rule is thought to be the principal mode of PTC recognition in vertebrates, although there are exceptions to the rule.

Figure 9. NMD-sensitivity as a function of PTC position.

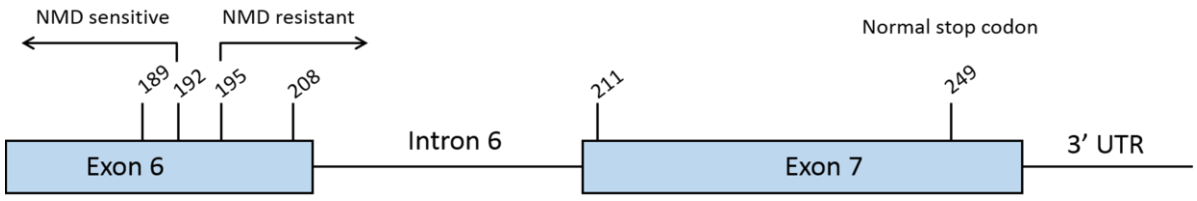

PTC locations as noted, normal translation termination occurs at codon 249. Each PTC construct was analyzed for sensitivity to NMD by assessing mRNA stability. Adapted from [5], permission granted from American Society for Microbiology for academic use. ©1994 American Society for Microbiology.

One exception to the 50-55 nt rule has been well characterized by the Kulozik lab [121] by studying NMD-sensitivity of PTCs within exon I of β-globin mRNA. They identified a strict boundary within exon I of β-globin where PTCs upstream of the boundary were able to escape NMD and reinitiate translation downstream of the PTC [121]. β-globin reporters were constructed

with a PTC present in codons along exon 1 and into the 5' end of exon 2. Northern blot analysis detected β-globin mRNA with a radio-labeled complementary probe and revealed that mRNA with a PTC in codons 2-23 of exon I showed only a slight decrease in abundance, indicating they were escaping NMD. This observation was surprising as all tested PTCs were upstream of one or even two introns at sufficient distance. These findings demonstrate that NMD-sensitivity is influenced by the location of the PTC within the first exon regardless of adherence to the 50-55nt rule.

The faux 3' UTR model

The NMD-sensitivity of transcripts can also be determined by the nature of their 3' untranslated region (UTR). One way premature termination is recognized as abnormal to the absence of regulatory (or other) factors that would otherwise be present on a proper 3' UTR, hence the *faux* 3' UTR model. Poly(A) binding protein complex 1 (PABPC1) binds to the poly(A) tail and its interaction with translation eukaryotic release factor 3 (eRF3) is alleged to signal and induce normal translation termination. A long 3' UTR providing significant physical distance between a termination codon and the poly(A) tail will inhibit PABPC1's interaction with eRF3 (Figure 10). An mRNA is considered to have a "faux 3' UTR" when there is considerable distance between the PTC and the poly(A) tail [122]. Another version of this model is when the ribosome encounters a stop codon but is unable to interact with PABPC1 then the transcript is subject to NMD (Figure 10). To test whether the proximity of a PTC to Pab1p (PABPC1 homolog in yeast) is necessary for NMD, Pabp1 was tethered closely downstream of the PTC. This UTR-based mechanism of PTC recognition is thought to predominate in yeast and *Drosophila*.

An mRNA is considered to have a "faux 3' UTR" when there is considerable distance between the PTC and the poly(A) tail [122]. Another version of this model is when the ribosome encounters a stop codon but is unable to interact with PABPC1 then the transcript is subject to NMD (Figure 10). To test whether the proximity of a PTC to Pab1p (PABPC1 homolog in yeast)

is necessary for NMD, Pabp1 was tethered closely downstream of the PTC. Results showed a 5-11 fold increase in nonsense reporter RNA, indicating that close proximity to Pabp1 allowed for NMD evasion [122]. The Izaurralde lab made a normal termination codon sensitive to NMD by

Figure 10. The faux 3' UTR model of PTC recognition

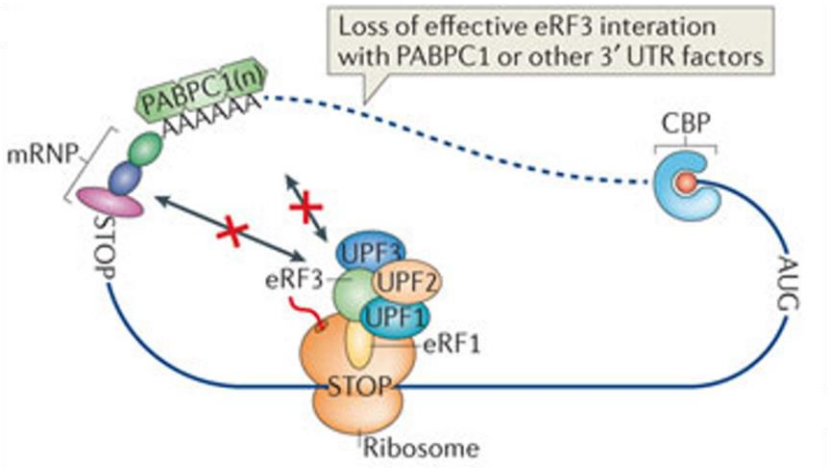

Fig 10. The faux 3' UTR model of PTC recognition. Reprinted with permission license 3327161320906 from [14].

inserting a 198 nt sequence in the 3' UTR. The PTC-containing reporter mRNA was clearly reduced in abundance [123] as it was degraded by NMD. The faux 3' UTR model has also been observed in mammals. Generally speaking, when PABPC1 is bound only 15 codons away from the PTC then the mRNA is able to evade NMD [124]. There are notable exceptions to this rule in mammals as some mRNAs have extensive 3' with many exceeding 1000 bases.

NMD and the "Pioneer round of translation"

The pioneer round of translation model postulates that mRNAs are only susceptible to NMD during their first round of translation while EJCs remain bound to the transcript and the 5' cap is bound by the nuclear cap binding complex (CBC). The nuclear CBC consists of 2 subunits cap binding protein 80 (CBP80) and cap binding protein 20. This model asserts that CBC-bound mRNA undergoes a pioneer, first, round of translation for the purpose of surveillance. CBC is then exchanged for eIF4F, which supports bulk translation. The pioneer round model is based on the assumption that EJCs are stripped from the mRNA by translating ribosomes and thus are no longer present to aid in PTC recognition. Experimental support for this model came from immunoaffinity assays. The Maquat lab performed co-IPs with antibodies to CBP80 and eIF4E (a subunit of eIF4F) to purify RNA and proteins bound to each of them. Expression of human β-globin NMD reporters in monkey and murine cells showed their association with CBP80 but not with eIF4E after pulldown and detection with traditional polymerase chain reaction (PCR) [125]. Later, the Maquat lab performed additional co-IPs using tagged Upf1 in human cells and were able to co-purify CBP80 as evidenced by Western blot [126]. Subsequent co-IPs with tagged Upf1 deletions mutants were able to map the interaction site to amino acids 419-700 of Upf1 [126], which is within its helicase domain. Corresponding co-IPs with tagged CBP80 deletion mutants identified the interaction site on it at amino acids 664-790 [126]. Additionally, the pioneer round model claims the lack of co-purification of eIF4E with EJC components [76, 127] as further support for this model. Recent studies provide positive data in opposition to this model.

The assertion that eIF4F-bound mRNAs are resistant to NMD is based on negative evidence, like the lack of co-precipitating NMD factors after coIP with anti eIF4E antibody [125, 127-129]. Other negative evidence includes expression of eIF4E-BP1, an eIF4F inhibitor, does not inhibit NMD [130]. Evidence that eIF4F-bound mRNA can undergo NMD lies in the observation that the exchange of CBC for eIF4F is independent of translation [131, 132]. A

recent study by Durand and Lykke-Andersen investigated NMD of eIF4F-bound PTC-containing mRNA. One experiment meant to discern if the treatment with translation inhibitors allowed for the exchange of CBC for eIF4E. They investigated the effect of eIF4E-eIF4G inhibitor 1 (4EGI-1) on PTC- β-globin degradation after removal of translation inhibition. 4EGI-1is a translation inhibitor that binds to eIF4E to block its interaction with eIF4G [133], thus precluding formation of the translation initiation complex. The presence of 4EGI-1 increased the half-life of PTC- β-globin mRNA by nearly two-fold compared to control cells after puromycin removal [134]. These results signify that blocking translation intiation with 4EGI-1, allowed for CBC to exchange for eIF4E, and stabilized β-globin mRNA that was bound to eIF4E as translation-dependent NMD could not target it for degradation [134]. These experimental results are inconsistent with the pioneer round model and demonstrate that NMD can occur on eIF4F-bound mRNAs.

Another study by Rufener and Mühlemann also demonstrated NMD occurs on eIF4F-bound RNAs. They first established an efficient, consistent protocol for isolating eIF4F-associated mRNA ribonucleoprotein particles (mRNPs) or CBP80-associated mRNPs [135]. For experiments whole cell extract, anti-CBP80 IP, and anti-eIF4E IP samples were used to investigate the half-life, and therefore NMD, of a TCRβ mRNA reporter with a PTC at codon 68, termed TCRβ68. If NMD were restricted to the pioneer, CBC-bound, round of translation then the half-life for eIF4E-bound TCRβ68 should be the same as that of its wildtype equivalent and half-life of CBC-bound TCRβ68 will be much shorter than wild type. These experiments were conducted with and without Upf1 knockdown to ensure the changes in decay were due to NMD. RNA was assessed by quantitative PCR (qPCR) and results showed that the CBP80-bound TCRβ68 degraded more rapidly than wild type and was stabilized under Upf1 knockdown signifying its decay was due to NMD. The eIF4E-bound TCRβ68 showed similar results thus it was also degraded by the NMD pathway [135]. Further experiments utilized a different NMD reporter that underwent NMD via the faux 3' UTR mechanism of recognition and saw similar

results signifying that NMD occurs on CBP80- and eIF4E-bound mRNAs regardless of method of recognition.

Alternative Branches of NMD

NMD in mammals is not restricted to a single mechanism as there are various branches with differing factor requirements. The use of different branches of NMD may account for some of the observed tissue- and transcript-specific differences in NMD efficiency that have been observed. NMD can be activated independent of Upf2, Upf3b, and some EJC components [2, 3] (Figure 11). Simultaneous tethering and siRNA-mediated depletion experiments identified two branches: one being Upf2-independent and the other being independent of certain EJC components [2]. Transcripts with tethered RNPS1 were dependent upon the presence of Upf2. In contrast, transcripts with tethered Y14, Magoh, Upf3b, or eIF4A3 showed no change in NMD-sensitivity with concurrent Upf2 depletion [2] and thus were Upf2-independent. Another branch was identified in mammalian cells as being independent of Upf3b. These experiments utilized the NMD reporters PTC-TCRβ and PTC-β-globin in cell lines with stable knockdown of Upf3a and/or Upf3b. PTC-containing TCRβ mRNA was expressed at normal levels in cell lines with stable knockdown of Upf3b but PTC-β-globin mRNA was degraded [3]. Both transcripts were destabilized under Upf1 knockdown to support differences were due to decreased NMD [3]. Stable cell line selection can sometimes leads to a genetic selection of abnormal cells, thus experiments were repeated with transient transfection for factor knockdown and results were the same [3]. Collectively these data demonstrate that NMD can proceed via multiple pathways.

Figure 11. NMD is a branched pathway

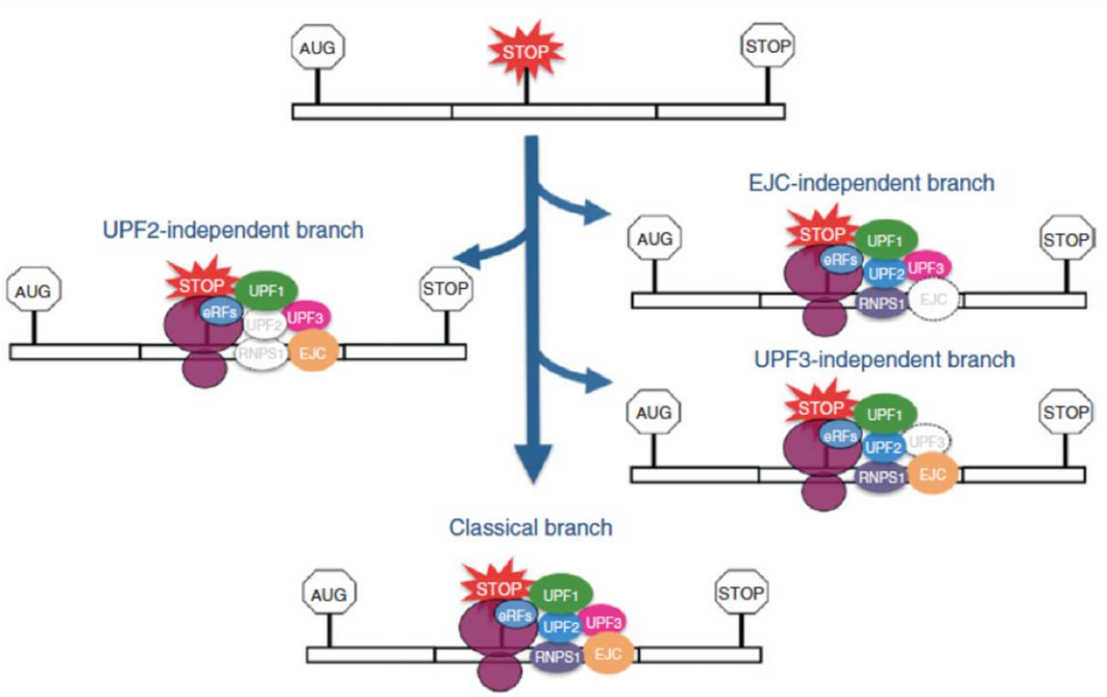

The four branches of the NMD pathway that have been so far identified are depicted[2, 3] and required factors are colored. Reprinted with permission license 3333681320786 from [16].

Premature translation termination

As mentioned earlier, destabilization of nonsense-containing mRNAs depends not only on the recognition of the stop codon by the translational machinery [26, 136-139] but also upon its ability to discern the stop codon as premature. To provide the background required to understand why premature translation termination is unique I have included a brief overview of normal translation termination. Ribosomes translate mRNA sequence one codon at a time as they move through the A, P, and E sites sequentially. Aminoacylated tRNAs enter the ribosome at the A site and are proofread for fidelity. A peptide bond links the incoming amino acid with the growing peptide chain. Translocation of the mRNA shifts the tRNA at the A site to the P site leaving the A site open for another tRNA. The P site tRNA is shifted to the E site during

Figure 12. Normal translation termination.

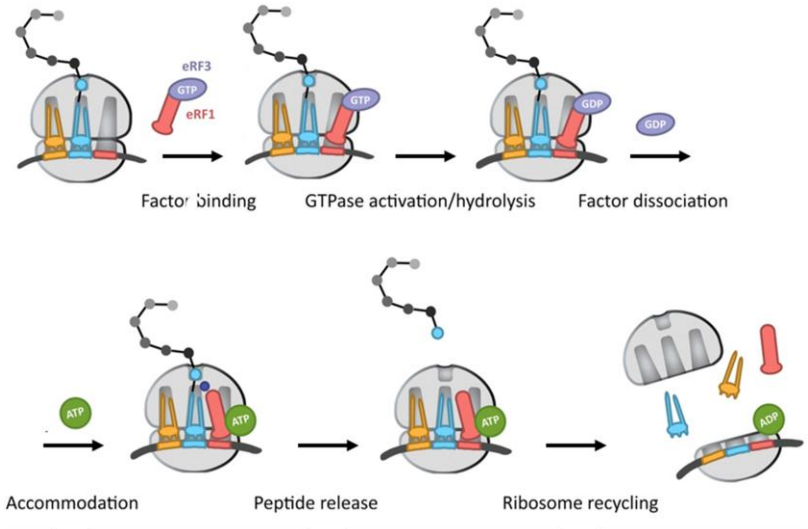

From [1] Copyright 2011 National Acedemy of Sciences, USA. Rrerinted with permission license 3337740921562, Copyright ©2004 Federation of European Biochemical Societies, Published by Elsevier B.V.

translocation and then can exit the ribosome for recycling [140] (Figure 12). This process continues until the ribosome encounters a stop codon. Normal translation termination occurs at the three canonical stop codons - UAA, UAG, and AGU. Translation requires two classes of release factors, in mammals these are eRF1, which is Class I, and eRF3, which is Class II [141, 142]. The stop codon is recognized and bound by eRF1 via a conserved motif [143, 144]. After stop codon recognition, Class II release factors use their GTPase activity to stimulate class I factors [145]. Class I factors act like tRNAs by binding at the A site of the ribosome and elicit hydrolysis of the peptide chain attached to the tRNA bound at the P site [14]. GTP hydrolysis by eRF3 stimulates eRF1, which triggers peptide hydrolysis and release from the ribosome [146]. Next the termination complex must dissociate from the mRNA so it can be recycled for additional termination events. Normal termination is thought to be stimulated by the interaction of PABPC1 with eRF3 [147, 148] based on the observation that deletion of PABPC1 in human cells increases PTC read through [149].

Premature termination is less efficient than normal termination, which is sensed by cells. Encountering an EJC or being positioned far away the poly(A) tail blocks the interaction of eRF3 with PABPC1. In yeast and humans, Upf1 interacts with eRF3 [76, 81, 149, 150] which inhibits Upf1's ATPase activity [81]. This interaction is believed to assemble the SURF (SMG1-Upf1-release factors) complex (Figure 13), comprised of inactive Upf1, SMG1, eRF1 and eRF3, as determined by immunoprecipitation experiments [76]. These findings support the concept that Upf1 is initially recruited to the premature termination complex in an inactive form that must be activated upon binding with the Upf2/Upf3/EJC decay complex [66, 76]. The decay inducing complex (DECID complex) consisting of the ribosome, release factors, Upf1, SMG1, the EJC, Upf2, Upf3, and the PTC-containing mRNA is where SMG1 phosphorylates Upf1 and NMD is induced [151] (Figure 13). Upon activation of Upf1, SMG proteins are recruited and the mRNA is poised to be degraded by the decay machinery.

Figure 13. Premature translation termination

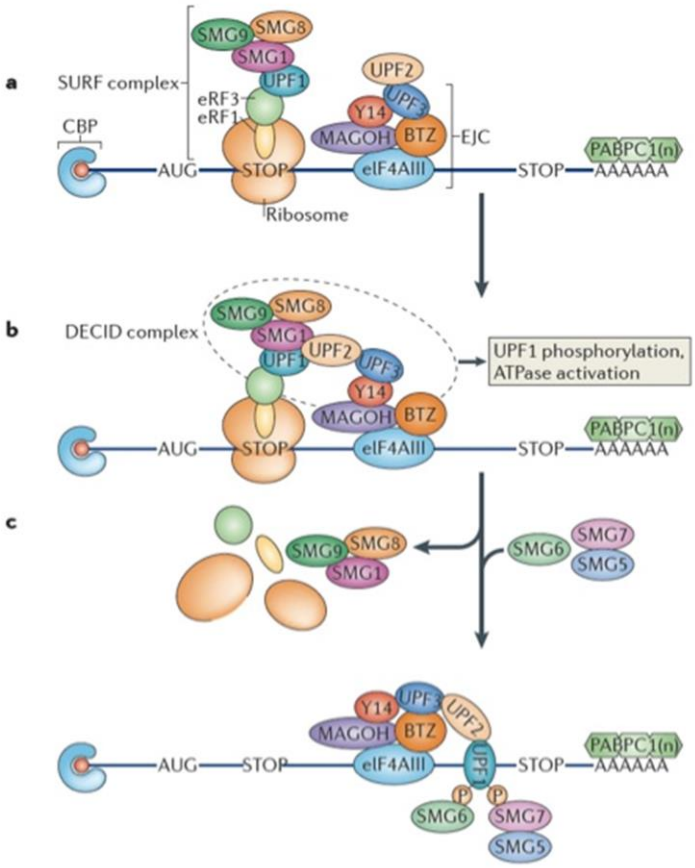

a. The exon junction complex (EJC) is a group of proteins deposited on an mRNA during splicing, 20–24 nucleotides 5′ of an exon–exon boundary. The composition of the EJC is dynamic and includes at least the core proteins Y14, MAGOH, barentsz (BTZ) and eIF4AIII, and one effector of nonsense-mediated decay (NMD), UPF3. In mammalian cells, UPF3 is loaded onto mRNAs during splicing and binds to a composite site comprised of parts of Y14, MAGOH and eIF4AIII[95]. UPF2 is thought to join the complex in the cytoplasm by binding to UPF3 after mRNA export from the nucleus. In parallel, UPF1 associates with eukaryotic release factor 1 (eRF1)-bound eRF3, SMG1, SMG8 and SMG9, collectively forming the SURF (SMG1–UPF1–release factor) complex. RNA cap-binding proteins (CBPs) bind to the cap structure and may include the CBP80–CBP20 complex or eIF4E (not shown). **b** .Premature translational termination leads to retention of the downstream EJC on the transcript, which facilitates interaction of UPF1 with UPF2, leading to the formation of the DECID (decay inducing) complex and to UPF1 phosphorylation and activation of its ATPase activity. Activation of NMD independently of UPF2, UPF3 or some EJC components has been described, suggesting that alternative pathways may also exist. **c.** UPF1 phosphorylation inhibits translation in *cis* and promotes its interaction with SMG6, an endonuclease that can cleave the mRNA, and with the SMG5–SMG7 complex, which seems to promote mRNA deadenylation and decapping. PABPC1, poly(A)-binding protein Reprinted with permission license 3327161320906 from [14].

Target mRNA degradation

Once translation has been terminated at a PTC and Upf1 has been phosphorylated there are 3 major routes to degrade the mRNA (Figure 14). These pathways differ by both the cofactors involved and mechanism of degradation. Two pathways are very similar and are activated by recruitment of SMG5 and/or SMG7 to the target transcript for exonucleolytic decay. The third pathway depends on recruitment of SMG6 to the target transcript for endonucleolytic cleavage. The first pathway occurs via deadenylation-dependent decapping followed by exonucleolytic decay. This is the major mechanism of mRNA decay in yeast and is also used to some extent in humans. This pathway recruits the CCR/NOT4 deadenylation complex via its interaction with SMG7 that was described earlier. Once deadenylation has occurred then the 5' cap is removed by the decapping machinery. The mRNA is then degraded by exonucleolytic cleavage from both ends; in the 5' to 3; direction by Xrn1 and in the 3' to 5' direction by the exosome complex. A second route of degradation is very much similar to the one just described, deadenylation-independent decapping followed by exonucleolytic decay. In this mechanism, the cap is removed from the mRNA without any requirement for a shortening of the poly(A) tail by the deadenylase complex. Degradation occurs from the 5' end by Xrn1 as above. The difference here is that the mRNA may or may not undergo deadenylation and subsequent 3' to 5' decay by the exosome complex. The third route of degradation differs from the first by requiring neither decapping nor deadenylation. In this mechanism, documented in flies and mammals, endonucleolytic cleavage by SMG6 generates fragments for exonucleolytic decay by Xrn1 and the exosome complex. The nature of the factors bound in the mRNA influences which route(s) is(are) used for degradation and also to what extent degradation occurs, but this is a controversial area of NMD. The Kim and Izaurralde labs have conflicting results for the interaction of SMG5 with PNRC2. PNRC2 (proline-rich nuclear receptor coregulatory protein 2) is a small 16kDa coactivator that interacts

Figure 14. Mechanisms of mRNA degradation

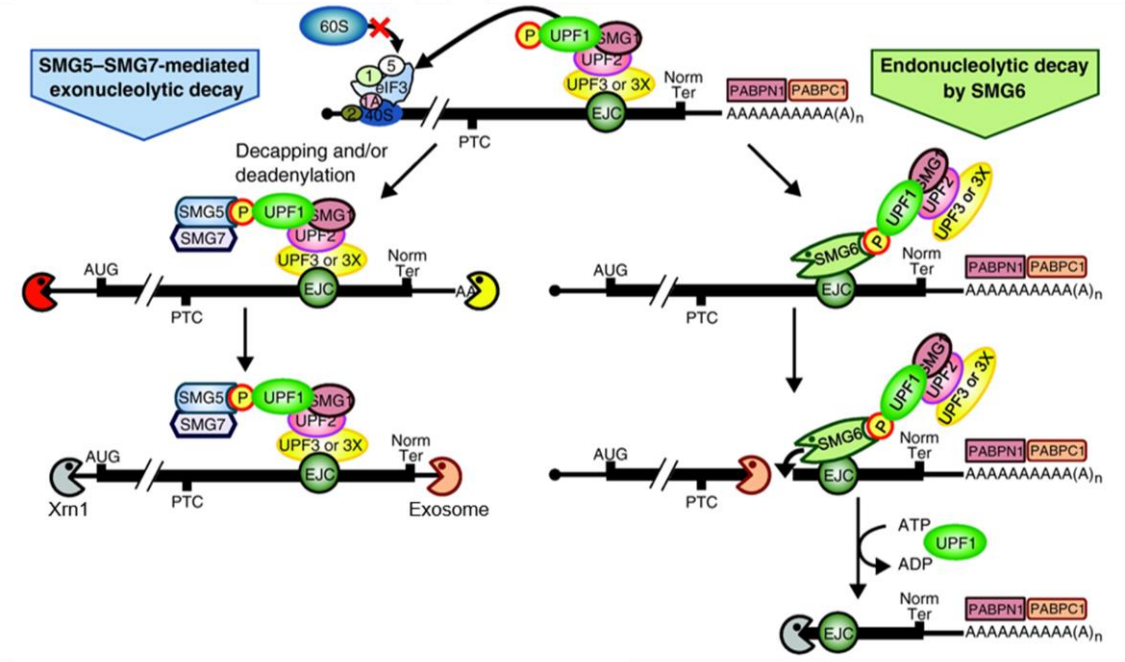

It is uncertain if SMG5–SMG7 and SMG6 bind multiple phosphates on the same UPF1 molecule or, as shown, different phosphorylated UPF1 molecules. In favor of the first possibility, SMG6 co-immunoprecipitates with SMG5 and SMG7 in an RNase A-resistant manner [4]. Since SMG7-mediated mRNA decay occurs independently of SMG6 [8], it is plausible that SMG5–SMG7-mediated NMD leads to deadenylation and/or decapping followed, respectively, by exosome-mediated 3′-to-5′ and XRN1-mediated 5′-to-3′ exonucleolytic activities (reviewed in [19],[22], and [23]). An alternative or additional mRNA degradation pathway involves SMG6, whose binding to hyperphosphorylated UPF1 competes with UPF3X and may replace the interaction of UPF3X with Y14-MAGOH-eIF4AIII EJC constituents [4]. The endonuclease activity of SMG6 cleaves the NMD substrate into a 5′-cleavage product and a 3′-cleavage product. Activation of the RNA-dependent ATPase activity of UPF1 subsequently results in the XRN1-mediated 5′-to-3′ decay of the 3′ fragment, which presumably depends on UPF1 helicase activity [24]. PAPBC1, poly(A)-binding protein C1; PABPN1, poly(A) binding protein N1. Reprinted with permission license 3336061444475 from [25].

interacts with both Upf1 and Dcp1a (mRNA decapping enzyme 1a) [152] linking mRNA surveillance to decapping. Immunoprecipitation with tagged proteins showed PNRC2 preferentially binds to SMG5 over SMG6 or SMG7 [20]. To discern if the composition of the NMD factors on an mRNA are substrate-specific microarray analysis was conducted on total transcripts from HeLa cells depleted for Upf1, SMG5, SMG7, and PNRC2. Upf1 depleted

transcripts represented possible NMD substrates and transcripts common between Upf1 and SMG5, SMG7, and PNRC were compared [153]. Of the 115 transcripts that increased at least 1.5-fold under Upf1 depletion, 68 were common between SMG5 and PNRC2 and only 37 were common between SMG5 and SMG7. Increasing the stringency of analysis to transcripts up-regulated at least 2-fold showed seven were common between SMG5 and PNRC2 and only one was common between SMG5 and SMG7 [20] (Figure 15). The Kim group concluded that these results meant that SMG5 more preferentially interacts with PNRC2 and that interaction is functionally dominant to the SMG5-SMG7 heterodimer [20]. Conversely, the Izaurralde lab investigated the interaction of SMG5 and PNRC2 using their SMG5 mutants that lost SMG7 binding. The interaction site for SMG5 on PNRC2 has not yet been determined and could very well be the same site as SMG7 binding. In contrast to the Kim lab, there was no detectable interaction between the two proteins. Next, they tested binding of tagged PNRC2 with endogenous Upf1, SMG5, and SMG7 but saw only a weak interaction with Upf1.

Figure 15. SMG5, SMG7, and PNRC2 target mRNA overlap

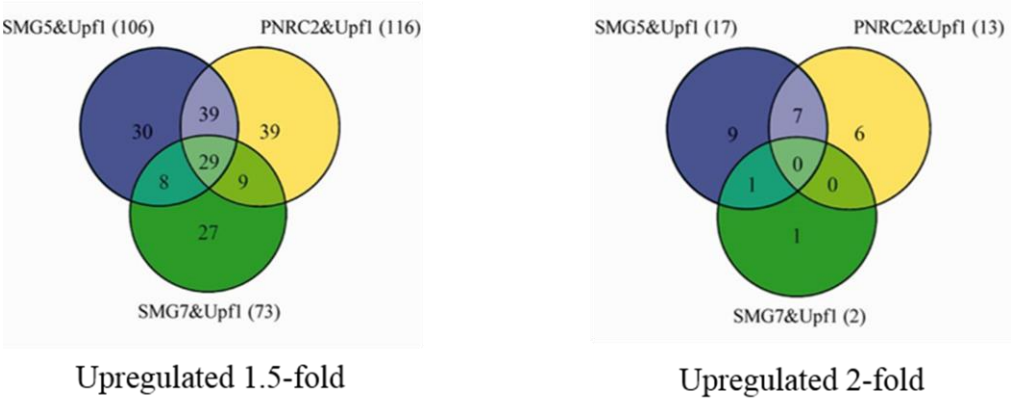

Left:Venn diagrams showing the number of transcripts that were commonly upregulated by at least 1.5-fold upon downregulation of Upf1-interacting factors (SMG5, SMG7 or PNRC2) and upon downregulation of Upf1. The total number of commonly upregulated transcripts after siRNA downregulation is depicted in parentheses. Right: Venn diagrams showing the number of transcripts that were commonly upregulated by at least 2-fold upon downregulation of Upf1-interacting factors (SMG5, SMG7 or PNRC2) and upon downregulation of Upf1. From [20] reprinted with permission license 3340250467311

Tethering of SMG7 to NMD reporter mRNAs in cells depleted of Dcp2 (mRNA decapping enzyme 2) or Xrn1 showed a significant increase in stability of the reporter mRNA. These results indicate that SMG7 may also mediate mRNA degradation via decapping followed by exonucleolytic decay [8]. However, that study did not discern whether decapping was dependent on prior deadenylation. The Izaurralde lab hypothesized that if decapping is inhibited then deadenylated mRNA intermediates should accumulate in the cell. A catalytically inactive dominant negative DCP2 mutant was overexpressed in cells with either full-length or a fragment of SMG7 and accumulation of an NMD reporter was monitored. The extent of deadenylation was assessed by mobility on denaturing gel after oligo(dT)-directed RNase H digestion; which will degrade the RNA complexed with the oligo(dT). Reporter mRNA accumulated in a fast-migrating form corresponding to a completely deadenylated form, thus SMG7 decapping is dependent on deadenylation [113]. Subsequent experiments investigated whether SMG7 binds to a subunit of the deadenylation CCR4-NOT complex consisting of 10 subunits [113]. Individual subunits were expressed along with tagged SMG7 in HEK293 cells and pulldowns were performed. Interestingly, only POP2 interacted with SMG7 in the pull-down assays and was insensitive to RNase treatment [113]. Collectively, these experiments demonstrate that SMG7-mediated mRNA degradation is based on deadenylation-dependent decapping followed by 5' to 3' exonucleolytic decay.

In an alternative pathway, activated SMG6 is bound to RNA; which are then cleaved internally and degraded. This mechanism occurs when SMG6 displaces Upf3b to bind to the EJC, which causes remodeling of the surveillance complex and positions SMG6 to bind phosphorylated Upf1. Activated SMG6 then cleaves the mRNA via its PIN domain. Whether there are multiple or a single cleavage sites remains unresolved. The cleaved mRNA is degraded in the 3'-5' direction by the exosome complex and 5'-3' by Xrn1 [154].

NMD Regulation

Since, NMD serves as both an RNA surveillance and a gene regulatory mechanism, it is a critical process within the cell. As might be expected of any key cellular activity, NMD is tightly regulated. The first evidence of NMD regulation was observed when different transcripts were found to be down-regulated with different efficiencies; PTC-containing mRNAs decreased over a range of 2-100 fold [155]. NMD is regulated by multiple methods, a few examples include developmental regulation, microRNA-mediated regulation, and feedback inhibition. The first evidence of developmental regulation of NMD came in a study in *Drosophila* engineered with a nonsense allele as reporter of NMD strength. As fly embryogenesis proceeded the nonsense gene was stabilized and indicated a decrease in NMD [156]. NMD was found to be very strong three hours after egg laying and gradually declined until 22 hours after egg laying, which coincided with the extent of Upf1 expression analyzed by *in situ* hybridization [156]. This suggests that the level of Upf1 expression controls the magnitude of NMD. Another example is found in vertebrates where NMD is regulated during neuron differentiation and brain development. An *in silico* screen was conducted for conserved miRs that target NMD factors and identified miR128 a as potential regulator of Upf1 and MLN51, an EJC component [157]. Briefly, microRNAs are short, non-coding RNA molecules that function in the regulation of gene expression. The degree of sequence complementarity to the target mRNA induces either degradation or translational repression (Figure 16). Thus, increased expression of a miR leads to decreased expression of its target mRNA. Expression of miR128 is enriched in the brain, represses growth and enhances neural differentiation [158]. To validate Upf1 and MLN51 as miR128 targets, a miR128 or control "mimic" was transfected into human and mouse cell lines with low endogenous expression of miR128. The expression levels of Upf1 and MLN51 were compared to control and found to be downregulated in a miR128-specific manner [157]. Accordingly, by inhibiting NMD miR128 would upregulate expression of mRNAs that otherwise would be degraded. This was confirmed by examination of known NMD substrates whose expression increased under miR128

expression versus control [157]. These results, together with others, support a four step model: (1) miR128 is induced during neuron differentiation, (2) this causes inhibition of the magnitude of NMD, (3) NMD repression leads to upregulation of specific mRNAs, and (4) this triggers a neural program that initiates neural differentiation [16]. Further evidence NMD is important for brain development exists as human Upf3b mutations are associated with mental retardation, autism, and schizophrenia [94, 159, 160].

Figure 16. Biogenesis of miRNAs

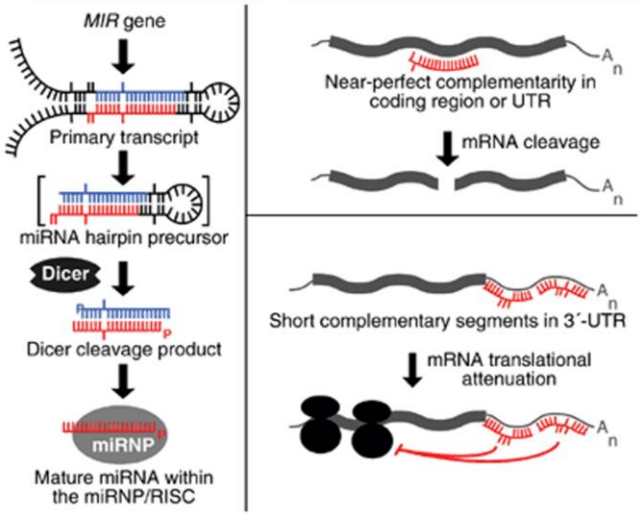

Left: The portion of the primary transcript that contains the miRNA sequence (red) resides on one arm of a predicted stem-loop precursor structure. The transcription start and stop sites for miRNA primary transcripts have not yet been defined. In animals, the hairpin precursor (in brackets) is processed from the primary transcript, but such intermediates have not been detected in plants. Either the primary transcript or this processed hairpin is cleaved by Dicer to yield paired approximately 21-nt RNAs with 2-nt 3′ overhangs, 5′ phosphates, and 3′ hydroxyls. One strand of this short-lived double-stranded intermediate accumulates as the mature miRNA (in red), which acts as a guide RNA within the miRNP/RISC complex. **Right, top**: The near perfect pairing between many plant miRNAs and their mRNA targets directs the RISC to cleave the target near the center of the complementarity site. This is also the classical mode of action for siRNAs during RNAi. **Right, bottom**: Characterized animal miRNAs appear to recognize multiple sites in the 3′-untranslated region (UTR) of target mRNAs. Because they bind to their targets with numerous mismatches, the miRNP/RISC does not cleave the message. Although the message levels remain constant, protein levels decrease, perhaps from translational attenuation. Whether any plant miRNAs act via this mechanism is not known. From [21] www.plantphysiol.org Copyright American Society of Plant Biologists.

Feedback regulation of NMD was first evidenced in microarray analysis of human cell depleted for Upf1. Of the many mRNAs upregulated as a result of NMD inhibition one was the transcript encoding SMG5 [33]. SMG5 mRNA was also upregulated under Upf3b depletion, suggesting it may be regulated by the Upf3b-dependent branch [3]. These results indicate that NMD factors are negatively regulated by NMD, suggesting a simple mechanism of autoregulation. Accordingly, all seven factors have long 3' UTRs greater than 1000 bases; which could account for recognition and NMD targets per the 3'UTR model described earlier. RNA immunoprecipitation experiments determined most of these mRNAs were bound by Upf1 and thus NMD substrates [36, 161]. Such a feedback mechanism allows the NMD pathway to buffer itself against perturbations, such as stress. In addition, NMD feedback acts at the level of protein stability. Depletion of Upf3b causes significant upregulation of Upf3a, its related NMD factor. Experiments showed the increase in Upf3a occurred due to protein stabilization, not mRNA stabilization or increased transcription [3]. Upf3a is normally unstable as it is outcompeted for binding to Upf2 by Upf3b. However, a loss of Upf3B allows more Upf3a to bind Upf2, leading to stabilization, and its weaker stimulation of NMD can partially compensate for Upf3b loss.

NMD and Disease

Nonsense mutations have been estimated to account for 30% of all phenotypically relevant human mutations and thus underlie a multitude of diseases [162]. Cystic fibrosis results from decreased expression of CF transmembrane conductance regulator (CFTR); a chloride channel essential for maintaining ion balance [163]. Cystic fibrosis is caused by many mutations but the PTC-generating W1282X (tryptophan to stop) mutation gives rise to a severe form of the disease [164] due to CFTR mRNA being targeted and degraded by NMD. In a clinical study, patients with the W1282X mutation were treated with aminoglycosides, which cause PTC read-though [165]. Happily, some patients experience production of full-length CFTR and improved function; however, other patients experienced no improvement after treatment [165]. Another

NMD-mediated disease is Duchenne's muscular dystrophy (DMD); which can result from a nonsense mutation in the dystrophin gene. Surprisingly, over 98% of DMD mutations give rise to a PTC at many places along the 11 kilobase transcript [166] and clinical severity differs in patients. PTC-generating mutations are also found in many cancers, as degradation of a tumor suppressor with possible partial function would present a pro-tumor environment. For example, early-onset retinoblastoma is also associated with a PTC causing haploinsufficiency in the tumor-suppressor retinoblastoma gene, predisposing a cancerous state [167]. The role of NMD in disease is complex; NMD can have either a beneficial or detrimental influence depending on the mRNA mutated and the nature of the disease.

PTCs Affect Disease Severity

The impact of PTCs on the pathophysiology of disease was first appreciated in the β-thalassemias. β-thalassemia major affect patients who have either severely limited or no production of β-globin protein. Normal adult hemoglobin is a tetramer consisting of a pair of α-globin chains and a pair of β-globin chains. Synthesis of both chains is highly regulated to maintain an even ratio of α:β [168]. Decreased β-globin mRNA abundance results in decreased levels of β-globin protein, which establishes an imbalance of α/β - a relative excess of α-globin. These excess α-globin chains are unstable and cannot form tetramers causing the unpaired α-globin to precipitate within the red blood cell. The degree of α-chain excess determines the severity of β-thalassemia [169]. The synthesis of β-globin is inhibited the larger this excess of α-globin will be and therefore the more severe the disease. Thalassemic red blood cells fail to achieve the donut-like shape of healthy cells that allow them to properly coordinate oxygen (Figure 17). The bone marrow attempts to compensate for decreased oxygen-carrying by increasing erythropoiesis (red blood cell production).

Figure 17. Phenotype of thalassemic RBCs

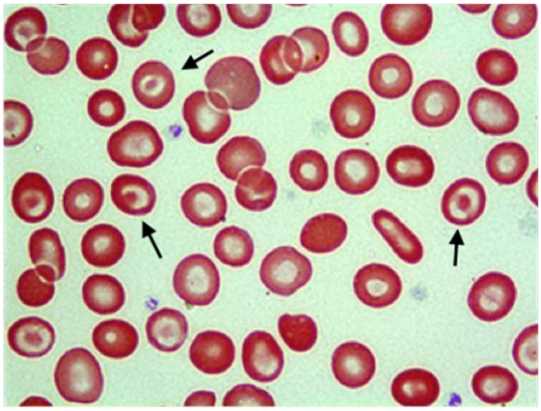

The healthy donut-like phenotype is lost when thalassemic RBCs fail to produce proper hemoglobin tetramers. Arrows indicated diseased cells unable to coordinate Heme and thus bind oxygen. From Wanick, C. 2007 The NIH Catalyst 15:5 [11].

The mRNA encoding β-globin is a relatively short transcript composed of three exons. β-thalassemia often results from a mutation in the first or second exon of the β-globin gene which produces a PTC [170]. The nonsense RNA is then targeted degradation via the NMD pathway. As described above, the location of the PTC along the β-globin mRNA dictates the magnitude of NMD it experiences and influences disease severity. The inheritance of this disorder is usually autosomal recessive with generally asymptomatic heterozygotes. There are notable exceptions as β-globin mRNAs with a nonsense mutation in the last exon evade the NMD pathway and the mRNA is translated into a C-terminally truncated protein [119]. These aberrant proteins act in a dominant negative fashion and result in a rare, heterozygous β-thalassemia with a dominant mode of inheritance [171, 172]. Individuals with nonsense mutations in both alleles suffer severely reduced β-globin protein levels and are characterized as having thalassemia major, also known as Cooley's anemia [173]. Therefore, PTC-containing mRNAs can cause disease and their location along the mRNA affects clinical manifestation.

β-globin decay in erythroid cells

The Ross lab characterized a mutation observed in a Kurdish Jewish family in which a single base deletion in codon 44 of β-globin mRNA results in the introduction of a PTC at codon 60/61. Study of patient cells showed β-globin mRNA levels of less than 1% of normal levels, even though transcription and pre-mRNA processing occur at normal rates [174]. Cloning of this mutation into transgenic mice and cell lines has allowed for in depth study of β-globin mRNA stability. During their study of β-globin mRNA metabolism, the Maquat lab found that three different PTC-generating mutations led to the production of stable, 5' truncated β-globin mRNA species in murine erythroid cells [175]. This is in stark contrast to other nonsense-containing mRNAs that in mammalian cells generally are degraded rapidly and thus abnormally short-lived [176]. The mutations under study included the Kurdish mutation mentioned above, which is the construct used in this project, as well as an Italian and Turkish mutation. The mutations introduced PTCs at different locations along the β-globin mRNA at codons 60/61, 39, and 21-22, respectively (Figure 18). A 5' end-radiolabeled S1 nuclease protection assay (S1 NPA) was used to investigate the identity of the truncated RNAs. S1 NPAs utilize a 5' labeled DNA probe that is

Figure 18 Schematic of PTC locations along -globin mRNA

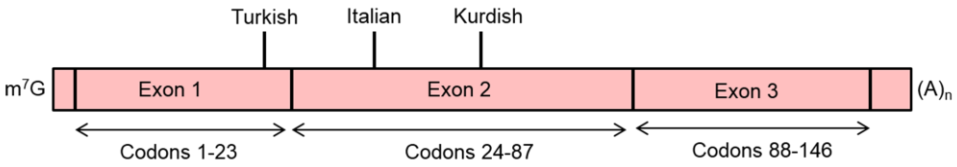

antisense to pre-determined section of the mRNA sequence with additional nonspecific sequence at the 3' end – to differentiate full-length mRNA from undigested probe. The radio-labeled probe

is incubated with mRNA samples and digested with S1 nuclease; which cleaves the unhybridized bases, and leaves he hybridized probe-mRNA intact (Figure 19). The digested RNA is then run on a denaturing PAGE gel against a radio-labeled ladder and species can then be identified by using size to calculate distance from the 5' end. These assays determined that the 3' end of the mRNA was intact and only missing the 5' end [175]. Additional evidence that the 3' end was intact was the retention of the smaller species on oligo(dt) cellulose, indicating the presence of a poly(A) tail. Cellular fractionation localized these truncated mRNAs exclusively to the cytoplasm, pointing to a method of generation occurring after export of the full-length mRNA from the nucleus [177].

Figure 19. S1 nuclease protection assay methodology

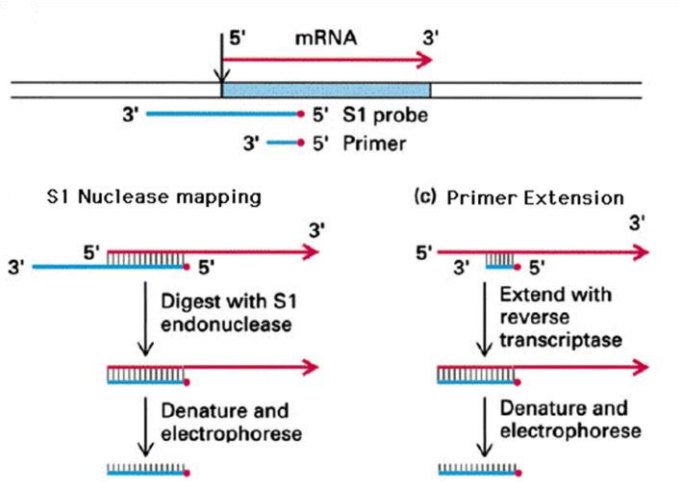

Mapping of band sizes from S1 NPA gel. All bands will start at the same 5' end which is radiolabeled. Band size corresponds to length of RNA as unhybridized probe is digested away with S1 nuclease. From [10] Copyright © BIOS Scientific Publishers Ltd 1999.

Subsequent studies wanted to understand this unexpected stabilization of 5' truncated RNAs, and the intermediates were tested for the presence of a cap structure. The 5' mRNA cap consists of a 7-methylguanosine linked to the first nucleotide via a unique 5'-5' triphosphate linkage [178], all other nucleotides form 5' to 3' linkages to create mRNA polarity. The 5' cap is added co-transcriptionally in the nucleus where it is bound by CBP80 and CBP20; which are then recognized at the nuclear pore and the mRNA is cleared to export to the cytoplasm. RNA lysates from erythroid cells from wildtype transgenic mice and PTC60/61 transgenic mice were analyzed by immunoaffinity chromatography with an anti-cap antibody. Results showed that, as expected the full-length mRNA, and, remarkably, the truncated species were bound by the antibody and were eluted off using synthetic cap analog m^7G only in the PTC60/61 samples [179]. To substantiate these findings, immunoaffinity chromatography was repeated with prior incubation . with tobacco acid pyrophosphatase; which cleaves the pyrophosphate bond present in 5' caps thus removing them. The reacted RNA was loaded onto the affinity columns and was not detected after m^7G elution, thus they were unable to bind the column after loss of the cap [175]. To further corroborate these results RNA from PTC60/61 cells was subjected to 5'to 3' exoribonuclease degradation; which efficiently degrades uncapped but not capped mRNA. The presence of a cap would provide protection from this degradation and capped RNAs will still be detectable post digestion. The results of these experiments were consistent with the PTC 60/61 RNAs have a protected 5' end. Unexpectedly, the wildtype β-globin mRNA yielded the same truncated products as the PTC-containing but to a much lesser extent, indicating that this degradation process is not based solely on the presence of a PTC. Questions remaining were the identity of these 5' ends, how they are generated, and investigate how a cap is added to an mRNA in the cytoplasm and why?

Ensuing collaborative work began the investigation into the mechanism of generation of these truncated RNA species. The 5' truncated RNAs could result from either pausing of a 5' to 3' exonuclease or endonucleoytic cleavage, so their upstream counterparts were sought after.

Poly(A)- RNA from both wildtype and PTC60/61 human β-globin expressing murine erythroleukemic (MEL) cell lines were subjected to S1 NPA. These experiments were similar to the S1 NPA used above but instead utilized a 3' end-radiolabeled probe with excess nonspecific sequence at the 5' end. Results did indeed identify 5' counterparts of the truncated species signifying that they were generated by endonucleolytic cleavage [180]. Next, primer extension was used in order to more accurately map the 5'end of the truncated poly(A)+ RNAs. This protocol involves multiple 5' end-radiolabeled DNA primers complementary to different sequences of β-globin mRNA. These primers were used in a reverse transcription reaction to synthesize first strand cDNA of the various truncated species. The radiolabeled cDNA was then run a gel with sequencing ladders for T or G generated by the Sanger chain termination method. Briefly, ladder preparation uses a 5' radiolabeled primer plus all four DNA bases as normal dNTPs –A,T, C, G – plus one base which is a ddNTP in a reversetranscription reaction with, here, synthetic β-globin RNA of known sequence as template. When this dideoxy base is randomly incorporated into the growing cDNA there is chain termination as the lack of a 3' OH prevents further polymerization. This method creates cDNA of all length of sequence that end in the ddNTP base and the sequence is read from the bottom of the gel upwards. A control primer extension reaction with the synthetic β-globin RNA was included on the gel to identify sites of reverse transcription stalling. Meticulous counting of multiple reactions and comparison with the S1 NPA results the following cleavage sites were identified (given in nt from the 5' end): 67, 92/93, 167, 186/187, 316, and 324 [180]. Surrrounding sequences to the cleavage sites were studied and all but one was close to a UG dinucleotide, leading to the conclusion that an enzyme related to *Xenopus laevis* liver polysome ribonuclease 1 (PMR1), which was characterized as an endoribonuclease with specificity for UG dinucleotides by the Schoenberg lab [181, 182]. This study aims to determine how these truncated RNAs are generated, identify the endonuclease responsible for cleavage, and discern whether a precursor-product relationship exists.

Chapter 2: Quantitative Analysis of Deadenylation-Independent mRNA by Modified MBRACE Assay

Julie A. Dougherty, Roshan Mascarenhas, and Daniel R. Schoenberg

Published in *Polyadenylation: Methods and Protocols*, Methods in Molecular Biology. Rorbach J. and Bobrowicz A.J. (eds) vol 1125, DOI 10.1007/978-1-62703-971-0_28.

JAD wrote foreword, abstract, introduction and methods section. RM helped in writing introduction and document review. DRS reviewed document.

Foreword

A new assay allowing for kinetic analysis of β-globin mRNA was necessary to move forward with the project. The MBRACE assay [183] was identified as a rapid and sensitive assay for studying the 5' ends of RNA. The original protocol was modified to allow for quantitative, rather than qualitative, analysis of data to fit the goals of our study.

Abstract

Endonuclease cleavage is the rate-limiting step in the decay of nonsense-containing human β-globin mRNA in erythroid cells. The 5′-truncated intermediates thus generated are polyadenylated and more stable than the parent mRNA. Northern blotting is commonly used to measure the decay rate of full- length mRNA, and S1 nuclease protection is used to assay the fate of decay intermediates. We have adapted the more sensitive and facile MBRACE assay [183] to quantitatively monitor the decay process by detecting full-length β-globin and its decay intermediates.

Introduction

A premature termination codon (PTC) can arise within an mRNA due to mutation, errors in splicing, or via alternative splicing. Translation of PTC-containing mRNAs can cause deleterious effects in cells by producing C-terminally truncated proteins. A surveillance mechanism termed nonsense-mediated mRNA decay (NMD) recognizes and targets these PTC-containing mRNAs for accelerated degradation via two mechanisms. NMD target mRNAs can be internally cleaved by an endonuclease and then rapidly degraded by exonucleases, with Xrn1 catalyzing 5′–3′ degradation of the down- stream fragment and the exosome complex-associated exonucleases catalyzing 3′–5′ degradation of the upstream fragment. Alternatively, the target mRNAs may undergo deadenylation and decapping followed by exonucleolytic decay from the 5′ and 3′ ends (reviewed in [184]). In erythroid cells, SMG6 catalyzes endonuclease cleavage of PTC-containing human β-globin mRNA (manuscript submitted), but unlike other forms of NMD this uniquely gives rise to stable 5′-truncated products [175, 180].

The conventional approach to studying the decay of nonsense- containing mRNA is to monitor the disappearance of the full- length mRNA; however, this does not fully illustrate the decay process. Stable decay products of PTC-containing β-globin mRNA were originally detected by S1 nuclease protection and primer extension assays [175]. Each of these approaches

is time-consuming, insensitive, difficult to quantify, and impractical for use with large numbers of samples. To monitor changes in both full-length β-globin mRNA and its decay products, we adapted a highly sensitive assay based on molecular beacon rapid amplification of cDNA ends (MBRACE) [183]. MBRACE involves ligation of an RNA linker onto the 5′ end of monophosphorylated mRNA and detection of the resulting product using a probe specific for the linker-mRNA junction. Molecular beacons are single-stranded, dual-labeled fluorescent probes held in a hairpin structure by complementary stem sequences at the ends of the probe with target-specific sequence in the loop region. While in the hairpin configuration the proximity of the quencher blocks fluorescent emission by the reporter. Hybridization of the molecular beacon to the target sequence opens the hairpin structure, separating the reporter dye and quencher and enabling fluorescent emission. Since only one beacon binds per target molecule the fluorescent signal is proportional to the amount of target DNA. Molecular beacons have several advantages over other quantitative PCR-based assays. They do not interfere with primer binding and extension, they fluoresce only when hybridized to the target sequence, and, unlike Taqman probes, they are not dependent on the exonuclease activity of the polymerase [15].

Methods

Erythroid Cell Harvest and Fractionation (See Note 2)

Scrape 1–5 × 10^6 cells into a 15 mL culture tube and centrifuge at 1,000 ×*g* for 5 min then remove media. Wash pellet with 1 mL ice-cold PBS and transfer to 1.7 mL microcentrifuge tube. Centrifuge at 1,000 × *g* for 5 min and remove all PBS. Resuspend cell pellet in 3–5 volumes of erythroid fractionation lysis buffer (EFLB: 100mM NaCl, 10mM Tris HCl pH 8.0, 2mM EDTA, 1% NP-40, 1% β-mercaptoethanol, RNase OUT; see Note 1) by pipetting up and down four to five times, tap the tube, and incubate on ice 5 min. Tap tube and incubate on ice 5 min more, repeat until lysate becomes clear (see Note 3). Centrifuge at 5,000 ×*g* for 10 min at 4 °C to

pellet nuclei and debris. Transfer cytoplasmic supernatant to a new tube pre- chilled on ice (see Note 4).

RNA Extraction

To extract RNA add 1 mL TRIzol® (Life Technologies) to lysate, gently invert to mix, and incubate at room temperature for 5 min. Add 200 µL chloroform and shake vigorously by hand for 15 s, incubate at room temperature 10–15 min. Centrifuge at >12,500 ×*g* for 15 min at 4 °C to separate phases. Transfer upper aqueous phase to new tube. Add 500 µL isopropanol and 20 µg glycogen, invert to mix and incubate on ice for 10 min. Centrifuge at >7,500 ×*g* for 10 min at 4 °C to pellet RNA. Discard supernatant. Wash pellet with 1 mL 80 % ice cold ethanol. Centrifuge at >7,500 ×*g* for 10 min at 4 °C to pellet RNA. Remove ethanol and air-dry for 5–10 min. Resuspend the pellet in an appropriate amount of RNase-free water or 1x TE (10mM TrisHCl, 1mM EDTA, pH 8.0) to keep the RNA concentrated. Incubate at 60 °C for 10 min to fully dissolve pellet, use EDTA at 1 mM final concentration while heating to prevent RNA hydrolysis. Centrifuge briefly to collect and keep on ice (sample may be stored at −80 °C at this point). Quantify RNA using a spectrophotometer, such as the NanoDrop1000.

5´ RLM-RACE to Identify the Sequence at 5´ Ends

Treatment of cytoplasmic RNA with calf intestinal alkaline phosphatase (CIAP) to remove 5´ monophosphates from RNA.

In a 20 µL total reaction volume, combine: 4 µg RNA, 2 µL 10× dephosphorylation buffer (50mM Tris HCl pH 7.6, 0.1mM EDTA; Life Technologies, cat #18009-019) 2 µL (2 U) CIAP (Life Technologies, cat#18009-019), and RNase-free water to 20 µL. Mix gently, centrifuge briefly to collect. Incubate at 37 °C for 1 h. Terminate reaction by adding 115 µL RNase-free water and 15 µL Stop Solution (see Note 5). Extract RNA by adding 150 µL acid phenol–chloroform. Vortex and centrifuge 5 min at 12,500 ×*g* at room temperature. Transfer

upper, aqueous phase to a new microcentrifuge tube. Add 150 µL chloroform. Vortex thoroughly. Centrifuge 5 min at 12,500 ×*g* at room temperature. Transfer upper, aqueous phase to a new microcentrifuge tube. Add 150 µL isopropanol and 20 µg glycogen as carrier. Vortex and incubate on ice 10 min. Centrifuge 20 min at 12,500 ×*g* at room temperature. Rinse the pellet with 500 µL of cold 70 % ethanol. Centrifuge 5 min at 12,500 ×*g* at room temperature. Remove ethanol and air-dry for 10–15 min. Resuspend pellet in 10 µL of RNase-free water. Keep on ice (sample may be stored at −80 °C at this point).

Treatment of CIAP-Reacted RNA with tobacco acid pyrophosphatase (TAP) to remove 5´ Cap and leave a 5´ monophosphate end (See Note 6)

In a 16 µL total reaction volume, combine:

Table 2. TAP reaction master mix

CIAP-reacted RNA	2 µg RNA
10x TAP buffer	1.6 µL
TAP enzyme	0.3 µL
RNase OUT	0.5 µL
RNase-free water	to 16 µL.

TAP enzyme and 10x TAP buffer from Epicentre, cat# T19500
10x TAP buffer: 500mM sodium acetate pH 6.0, 100mM NaCl, 100mM EDTA, 1mM DTT, 0.01% Triton® X-100

Incubate at 37 °C for 2 h, place on ice (sample may be stored at −80 °C at this point)

.

Ligation of RNA Linker to 5´ ends of RNA (See Note 7)

T4 RNA ligase I ligates the 3′ hydroxyl of the RNA linker to the 5′ monophosphate of RNA molecules. The RNA linker should lack a 5' monophosphate to prevent concatamerization of linkers. The 25 nt linker used for 5' RACE (5'-CGAUGGAGCACGAGGACACUGACA-3') was based on the linker from the Invitrogen™ GeneRacer™ protocol (Life Technologies, cat#L150201) .

Heat denature secondary structure of RNA and the RNA linker by combining 8 µL of TAP reaction product (1 µg RNA) and 2 µL 100 µM RNA linker. Heat at 65 °C for 5 min and snap chill on ice.

For a total reaction volume of 16 µL, make a master mix of the following per reaction:

Table 3. RNA linker ligation reaction master mix

10x T4 RNA ligase I buffer	1.6 µL
10mM ATP (if not included in 10x buffer)	1.6 µL
T4 RNA ligase I enzyme	1.0 µL
RNase OUT	0.5 µL
RNase-free water	1.3 µL

T4 RNA ligase I and 10x T4 RNA ligase I from New England Biolabs, cat # M0204S
10x T4 RNA ligase buffer: 500mM Tris Hcl pH 7.4, 100mM $MgCl_2$, 10mM DTT)

Aliquot 6 µL of master mix to each sample, mix gently, and centrifuge briefly to collect. Incubate at 37 °C for 2 h, heat-inactivate enzyme by incubating at 65 °C for 15 min, place on ice (sample may be stored at −80 °C at this point).

First-Strand cDNA Synthesis

cDNA will be synthesized using a gene-specific β-globin reverse primer, 5'-TGATACTTGTGGGCCAGGGCATTA-3', binding at nt 467-490 of the full-length 626 nt transcript. This allows for detection of all β-globin mRNA species (that contain the primer-binding region) and estimation of their 5' ends based on length of PCR products. Invitrogen's SuperScriptIII First Strand cDNA kit was used for all reactions.

Thaw all reagents on ice. For a 20 µL total volume reaction, prepare the RNA/primer master mix including the following per reaction:

Table 4. RT master mix for RNA

5 µM β-globin reverse primer	1 µL
10 mM dNTP	1 µL
Ligation reaction	8 µL

Denature secondary structure by heating at 65 °C for 5 min and snap chilling on ice. Prepare a 2× reaction master mix on ice, containing the following per reaction:

Table 5. 2x RT reaction master mix

10× RT buffer	2 µL
25 mM $MgCl_2$	4 µL
0.1 M DTT	2 µL
SuperScript III reverse transcriptase	1 µL
RNase OUT	1 µL

Add 10 μL 2× reaction master mix to each tube. Incubate at 50 °C 50 min. Heat-inactivate the enzyme at 70 °C for 15 min, place tubes on ice. Add 1 μL RNase H to each reaction, mix gently, and centrifuge briefly to collect. Incubate at 37 °C for 20 min. Place tubes on ice (samples may be stored at −20 °C at this point).

Nested PCR to amplify β-globin species

Perform primary PCR using a forward primer complementary to the 5′ end of the RNA linker, 5'-CGACTGGAGCACGAGGACAG-3', and a reverse primer specific to β-globin, 5'-TGATACTTGTGGGCCAGGGCATTA-3' binding to nt 467-490 . This will amplify all target β-globin cDNA with a ligated adapter, full-length and truncated.

Prepare the primary PCR in 50 μL total reaction volume, under the following conditions: 10 mM Tris–HCl pH 8.3, 50 mM KCl, 1.5 mM $MgCl_2$, 200 μM dNTPs, 400 nM forward primer, 400 nM reverse outer primer, 15 ng cDNA, and 2.5 U Taq DNA poly- merase (Sigma-Aldrich). Thermal cycle conditions: 94 °C 3 min → [94 °C 30 sec → 60 °C 30 sec → 72 °C 1 min] × 35 cycles → 72 °C 5 min.

The secondary PCR reaction utilizes the same forward primer as the primary and a reverse primer, 5'-TAAGGCACCGAGCACTTTCTTGC-3', that binds upstream of that used in the primary reaction at nt 244-267 of full-length β-globin mRNA. Dilute the primary PCR 1:10, 1:100, and 1:1,000 in water for use as template for the secondary reaction. Diluting the primary reaction results in increased detection of the nested product after gel electrophoresis [185].

Perform secondary PCR under the following reaction conditions: 1 μL diluted primary PCR reaction, 10 mM Tris–HCl pH 8.3, 50 mM KCl, 1.5 mM $MgCl_2$, 200 μM dNTPs, 400 nM forward primer, 400 nM reverse nested primer, and 2.5 U Taq DNA polymerase (Sigma) in 50 μL total reaction. Thermal cycle conditions: 94 °C 3 min → [94 °C 30 s → 60 °C 30 s → 72 °C 45 s] × 35 cycles → 72 °C 5 min.

Identification of 5´ Sequence

Electrophorese 8 μL of the secondary PCR reaction on a 3 % low melting point (LMP) agarose gel using 1× TBE buffer. Visualize and document bands with a Bio-Rad GelDoc or similar imager. Size markers allow for identification of products based on size, with full length β-globin product, 292 bp, readily visible (Figure 20). The 3 % LMP agarose gel will resolve <500 bp bands very well.

Excise bands from the gel and purify using a gel extraction kit. Ligate purified bands into pGEM-T cloning vector in a 1.7 mL microcentrifuge tube. For a 10 μL reaction add the following: 20 ng purified DNA, 1 μL pGEM-T vector, 5 μL 2× rapid ligation buffer, 1 μL T4 DNA ligase (3 U), and RNase-free water to 10 μL. Incubate the reaction at 4 °C overnight. Thaw competent E coli cells, such as DH5α, on ice and transform by adding 2 μL of the ligation reaction to 50 μL of cells and keeping on ice for 5 minutes. Heat shock the cells at 42 °C for 45 s and quickly return tubes to ice for another 5 min. Add LB to 1 mL and incubate at 37 °C with shaking for 1 hour. Plate 100 μL of the transformed culture on LB agar plates with 50 μg/mL ampicillin, or appropriate antibiotic, and grow overnight in 37 °C incubator. Choose single colonies, verify ligation of target band with PCR, and sequence multiple positive clones using vector- specific forward and reverse primers (see Note 8).

Identify the RNA linker's 3′ end sequence and following it will be the 5′ sequence of the mRNA of interest. Align sequencing results with mRNA of interest using NCBI's specialized alignment engine bl2seq (http://blast.ncbi.nlm.nih.gov) or other alignment software. Multiple identical sequencing results ensure confidence in the 5′ end of the mRNA of interest. We chose the decay product that amplified well during nested PCR (Figure 20) and determined its 5' most base corresponded to nt 169 of the full-length transcript and will refer to it as Δ169.

Figure 20. Gel electrophoresis of 5' RLM-RACE products

Reprinted with permission license 3367650791786 from [12].

Molecular Beacons

Molecular beacons are single-stranded, dual-labeled fluorescent probes held in a hairpin structure by complementary stem sequences at the ends of the probe (Figure 21). The loop region is complementary to the target sequence; hybridization of the molecular beacon to the target sequence opens the hairpin–loop structure and separates the reporter dye and quencher resulting in fluorescent emission. Since only one beacon binds per target molecule the measured fluorescence is quantitatively proportional to the amount of target cDNA.

Figure 21. Schematic of Molecular Beacon

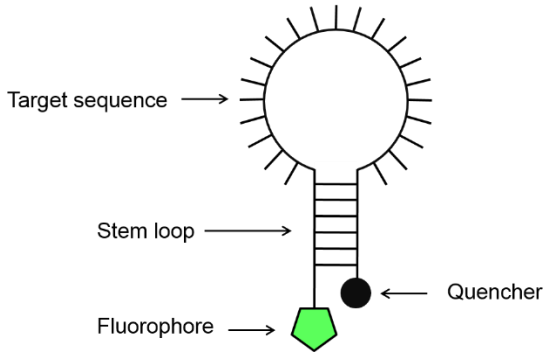

Beacon is held in hairpin when not bound to target. Binding of target sequence separates the fluorophore and quencher, allowing for fluorescent emission.

Molecular Beacon and Primer Design

Most importantly, the beacon needs to be designed to efficiently hybridize to and detect the proper target while reducing nonspecific fluorescence. Beacon design may vary as to the purpose of the assay - standard target detection or allele discrimination (refer to [15] for detailed design tips). A qPCR master mix specific for probes is to be used in these reactions; do not use SYBR green master mix. These experiments utilized PerfeCTa® qPCR FastMix® without ROX (QuantaBiosciences).

Design molecular beacon target sequences to span the junction between the RNA linker and the target product sequence. The full-length beacon's sequence, 5'-6FAM-GGACTGAAGGAGTAGCCAACAT-BHQ1-3', was designed with a majority targeting the linker and the 3' end specific for the full-length 5' end sequence (underlined). The Δ169 beacon sequence, 5'-6FAM-ACTGAAGGAGTAGCCAAGAGG-DABCYL-3', was designed similarly. 6FAM was chosen as the fluorophore since attempts to validate a duplex reaction were not fruitful. Reactions will need to be run separately but the extent of excitation of the fluorophore

will be equal for both products. Forward and reverse primers should have a T_m of 50–65 °C, with 50–60 % GC content. The forward primer needs to be at least 6 nucleotides upstream of the molecular beacon binding site to provide room for the polymerase, our forward primer, 5'-CGACTGGAGCACGAGGACAG-3', bound nt 1-20 of the linker. Our RNA linker was redesigned to increase its length to 44 nt and increase GC content at the 3' end, 5'CGACUGGAGCACGAGGACACUGACAUGGACUGAAGGAGUAGCCA. This means the molecular beacon cannot be designed to the 5′ most end of a target (see Note 9). Design the reverse primer so the resulting amplification product is 75–250 nucleotides in length. We used two different reverse primers here to optimize product length for qPCR and keep the products close to the same size so differences in detection would not depend on product lenth. For full-length detection the reverse primer, 5'-AACTTCATCCACGTTCACCTTGCC-3; binds to nt 99-122 of the full-length transcript and preclude the Δ169 species. The reverse primer for Δ169, 5'-TAAGGCACCGAGCACTTTCTTGC-3', binds to nt 244-267 of the full-length transcript. While it can bind to the full-length cDNA product, detection occurs via binding of the beacon at the junction of linker and mRNA. Optimize molecular beacon conditions empirically by testing varying primer and beacon concentrations. For these experiments, conditions were empirically found to be 250 nM beacon and 500 nM each primer.

Determining the Optimal Beacon Annealing Temperature

The annealing temperature of the reaction should be chosen so that the beacon specifically detects the correct target sequence. The optimal annealing temperature can be determined using a thermal denaturation profile of (1) beacon with correct target, (2) beacon with incorrect target, and (3) beacon alone. Choose the annealing temperature that provides maximal detection of the target sequence and minimal nonspecific detection.

Measure molecular beacon fluorescence in (1) the absence of target, (2) the presence of perfectly complementary target, and (3) the presence of mismatched target. The target

oligonucleotides are created by *in vitro* transcription and subsequent gene-specific cDNA synthesis (see Note 10).

Prepare three reactions containing 200 nM molecular beacon in 1× final qPCR buffer. Add to one reaction a fivefold molar excess of perfectly complementary cDNA, to the next add a fivefold molar excess of mismatched cDNA, and to the last add only buffer (see Note 11).

Using the Illumina Eco Real-Time PCR machine (Eco) choose the "other" detection chemistry and the high-resolution melt option. Select to detect the fluorescence for each preparation while the temperature decreases from 80 to 30 °C. Normalize the data to the buffer control to get the denaturation profiles. The annealing temperature chosen provides the largest window of discrimination between matched and mismatched target detection (Figure 22). This can be completed on other instruments by running the same samples and measuring fluorescence of the sample while decreasing temperature from 80 to 30 °C in 1°C increments for 1 min each and comparing detection curves.

Figure 22. Theoretical thermal denaturation profile for molecular beacon

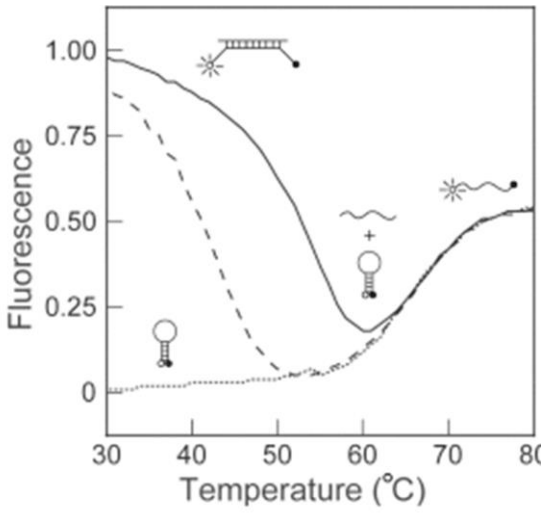

In the presence of either wild-type target (continuous line), mutant target (dashed line), or no target (dotted line). A diagram indicates the state of the molecular beacon over the thermal denaturation profiles. Mismatched hybrids denature 10 to 12°C below the Tm of perfectly matched hybrids. Reprinted with permission 3340450045095 from [15]

Standard curves to ensure efficiency

Standard curves allow for absolute quantification of data and ensure reliable detection by the beacon. Standard curves also determine the efficiency of the qPCR, which is needed to perform relative quantification calculations.

Using the cDNA from the thermal denaturation profiles, create a tenfold dilution series of standards. The dilution series needs to cover a broad range to ensure a proper curve is generated. In the Eco software, choose the "other" detection chemistry and the standardization option. Prepare a master mix of 2× qPCR buffer, primers, and beacon at the optimized conditions and aliquot into wells. Add template, running each standard in triplicate. Be sure to include a no template control for back- ground detection. The Eco software will generate a standard curve graph and provide values for the standard curve line. For tenfold dilutions the ideal slope is −3.32, which indicates an efficiency of 100 %. Acceptable curves will have slopes that range from −3.10 to −3.58, indicating an efficiency from 90 to 110 %, with an R^2 value ≥0.98 [186]. If the standard curve is not acceptable, then try adjusting the reaction conditions. Always use a freshly diluted series of standards and run multiple standard curves on different days.

Determining Beacon Specificity

Determining the degree of nonspecific detection by the beacon is essential to assure confidence in positive readings. To determine the specificity of the molecular beacons, a template containing mutations only at the 3′ binding side of the beacon is needed along with the correct template. For these experiments, full-length beacon was reacted with decay product target and the decay product beacon was reacted with full-length target, as the beacons differ only in their 3′ sequence. Run triplicate qPCR reactions of the tenfold dilution series using a similar molar dilution series. Compare *Ct* values to those for samples of similar molarity, if the *Ct* value for nonspecific template is 7 cycles higher than the *Ct* for correct template, then nonspecific

detection is less than 1%, according to the $2^{-\Delta\Delta Ct}$ method of calculation [187]. In our experiments, nonspecific detection was less than 1%.

Processing Experimental Samples for MBRACE

The workflow for analyzing experimental samples is similar to the 5' RLM-RACE procedure already described. Treatment with CIAP was removed from the protocol due to loss of material during phenol extraction, and experimental samples had limiting RNA amounts. The cDNA synthesis reaction will be performed with an oligo(dT) primer so reverse transcribe all RNAs with an intact poly(A)-tail, which allows for quantification of an internal control RNA during qPCR. The cDNA is used as the template for the modificed MBRACE qPCR followed by quantification and statistical analysis of data.

Figure 23. Workflow of modified MBRACE protocol

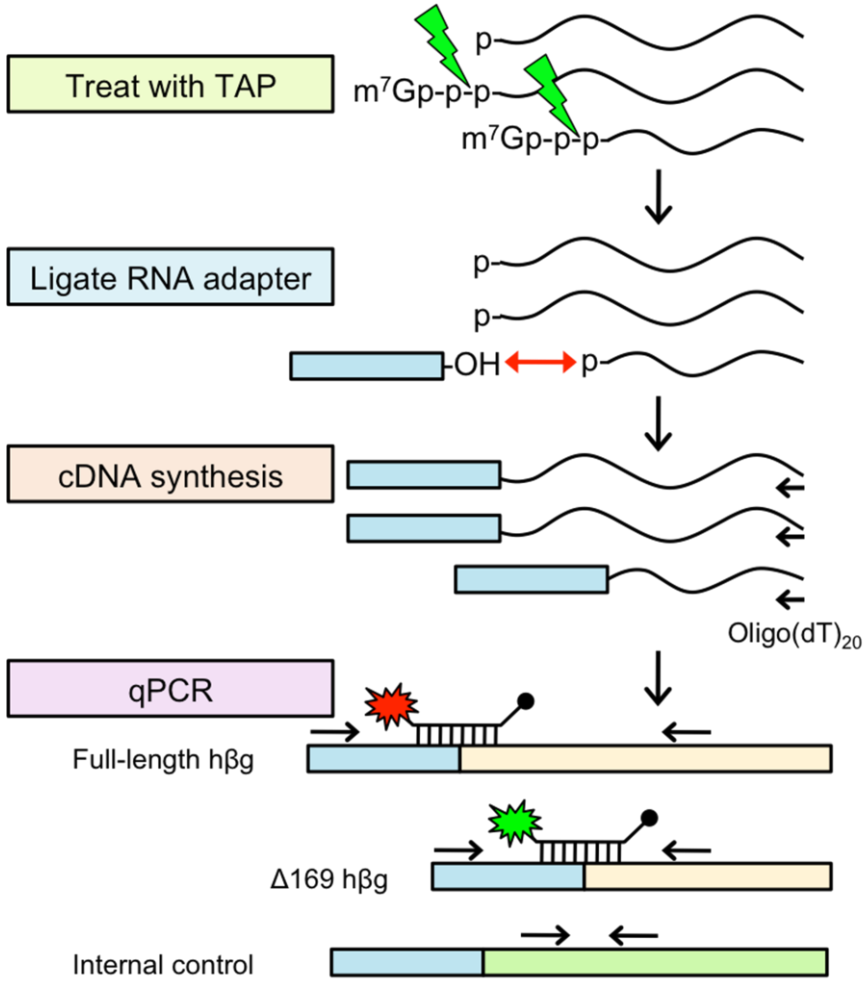

Adapted from [12] with permission license 3367650791786.

TAP Treatment to Remove 5′ Cap

Thaw RNA and 10× TAP buffer on ice. Incubate RNA at 65 °C for 5 min and snap chill on ice to relax secondary structures. Prepare 10 µL total volume reactions as follows: 2 µg RNA, 1 µL 10× TAP buffer, 0.3 µL TAP (3 U), 0.5 µL RNase OUT (20 U), and RNase-free water to 10 µL. Incubate at 37 °C for 1 h. 5. Return tubes to ice (samples may be stored at −80 °C at this point).

RNA Linker Ligation

This step is performed as described earlier. Thaw RNA, 100 μM RNA linker, 10× T4 RNA Ligase I buffer, and 10 mM ATP on ice. Combine 5 μL TAP reaction (1 μg RNA) with 2 μL 100 μM RNA linker and incubate at 65 °C for 5 min then snap chill on ice. Prepare reaction master mix, using the following per reaction: 1.6 μL 10× buffer, 1.6 μL 10 mM ATP (if not in 10×), 1 μL T4 RNA ligase I (10 U), 0.5 μL RNase OUT, and RNase-free water to 16 μL total reaction volume. Add 9 μL reaction mix to tubes and incubate at 37 °C for 1 h. Heat-inactivate enzyme at 65 °C for 15 min. Return tubes to ice.

First-Strand cDNA Synthesis

Perform using SuperScript®III First-Strand Synthesis System for RT-PCR (Life Technologies, cat # 18080-51). For a 20 μL total volume reaction, prepare a RNA/primer master mix including the following per reaction: 1 μL 50 μM oligo$(dT)_{20}$ primer and 1 μL 10 mM dNTP mix per reaction. Aliquot 2 μL master mix into 0.2 mL PCR tubes and add 8 μL ligation reaction (500 ng RNA). The master mix here lowers sample to sample variability for primer and dNTP concentration. Denature secondary structure by heating at 65 °C for 5 min and snap chilling on ice Prepare a 2× reaction master mix on ice, containing the following per reaction:

Table 6. 2x RT reaction mix

10× RT buffer	2 μL
25 mM $MgCl_2$	4 μL
0.1 M DTT	2 μL
SuperScript III reverse transcriptase	1 μL
RNase OUT	1 μL

10x RT buffer : 200mM Tris HCl pH 8,4, 500mM KCl

Add 10 μL 2× reaction master mix to each tube. Incubate at 50 °C 50 min. Heat-inactivate the enzyme at 70 °C for 15 min, place tubes on ice. Add 1 μL RNase H to each reaction, mix gently, and centrifuge briefly to collect. Incubate at 37 °C for 20 min. Place tubes on ice (samples may be stored at −20 °C at this point).

Column Purification of cDNA (See Note 12)

QIAquick PCR purification kit columns (Qiagen, cat #28104) were chosen as they demonstrated the greatest recovery of cDNA [188]. Mix cDNA reaction with 5 volumes (100 μL) of buffer PB. Load onto column and, using a tabletop centrifuge, spin at 12,500 × g for 1 min. Discard the flow through and return columns to collection tubes. Add 750 μL buffer PE to each column. Spin at 12,500 × g for 1 min, discard flow through, and return columns to tubes. Remove residual ethanol by spinning at 12,500 × g for 2 min. Discard collection tubes and place columns in new 1.7 mL elution tubes. Add 52 μL of elution buffer (2 μL will be lost to the column) directly to column and incubate at room temperature for 5 min. Elute by centrifuging at 12,500 × g for 2 min, cDNA concentration at this point is about 10ng/μL. Keep tubes on ice (samples may be stored at −20 °C at this point).

MBRACE qPCR

Thaw purified cDNA, forward and reverse primers, beacons, and qPCR reagent on ice; keep qPCR reagent and beacons under foil to limit light exposure. For a 20 μL total reaction volume, prepare a master mix as follows:

Table 7. Molecular Beacon qPCR master mix

2x PerfeCTa qPCR FastMix	10 µL
10 µM forward primer	1 µL
10 µM reverse primer	1 µL
5 µM beacon	1 µL
RNase-free water	5 µL

The detailed content of 2x PerfeCTa qPCR FastMix is proprietary.

Aliquot 18 µL master mix per well, including wells for a no template control and a positive control, such as a standard from curves generated earlier. Add 2 µL cDNA (20 ng) per well and apply cover to plate. 20ng of cDNA was observed to give reliable and adequate detection while maximizing the number of reactions that could be analyzed by qPCR. Run experimental samples in triplicate for calculation of standard deviation. Agitate plate to mix and centrifuge to collect. Using Eco software, choose "other" detection chemistry. Set the thermal profile: 95 °C 3 min → [95 °C 10 sec → 61 °C 30 sec* → 72 °C 15 sec] × 40 cycles (* denotes fluorescence detection). Remember to set the fluorescent detection for the annealing step as this is when the beacons fluoresce. Once the run is completed, set the threshold and base line to "Auto." Export the data for analysis. Set a separate qPCR reaction for an internal control mRNA, such as β-actin or GAPDH, using SYBR green chemistry. Run each sample in triplicate for the control mRNA. Again, set the Eco software to automatically determine baseline and threshold. Export the data for analysis.

Analyzing qPCR Data

Absolute Quantification

Absolute quantification calculates the input amount of the target by relating the qRT-PCR signal to a standard curve of known quantity. The quantity of the gene of interest is interpolated

along the linear regression line generated by the standard curve. The range of standards must be broad enough to generate a curve containing amounts relevant to the experiment - quantity may NOT be extrapolated from the standard curve, as the relationship may no longer be linear outside of the standard curve range. The equation for the linear regression line will allow for absolute quantification of unknowns. The equation will be given in $y = mx + b$ format - where *y* is the Ct, *x* is the quantity, *m* is the slope, and *b* is the *y*-intercept. The unknown Ct values substitute in for *y* and the equation $x = (y - b)/m$ is solved to determine the quantity. Absolute quantification assumes the qPCR reactions for each target have equal amplification efficiencies. If efficiencies are not equal then relative quantification should be used. Additionally, absolute quantification may not be effective when small changes in mRNA are observed, thus relative quantification may prove more fruitful.

Relative Quantification

Relative quantification reports the fold change between the target transcript of one sample versus another. Changes in fold expression across treatments or groups may prove more useful in some studies. An internal reference transcript, a housekeeping gene, is to be used to account for experimental variation. A proper internal reference must not be affected by the treatment; in our study we used β-actin. If a housekeeping gene is not the desired normalization control then an exogenous RNA, such as luciferase, may be spiked into the cell lysate prior to RNA extraction to act as a calibrator. If the amplification efficiencies of the target and reference gene are similar then the Livak method is used for calculations [189]. In this method of calculation the relative expression ratio, *R*, is given as

$$R = 2^{-\Delta\Delta Ct}$$

To determine the value of $\Delta\Delta Ct$, ΔCt values are first calculated for both the target and reference mRNA using

$$\Delta Ct = Ct_{sample} - Ct_{control}$$

where control refers to the housekeeping gene. This step is also called normalization of the data as the reference control may differ due to experimental variations. Calculate the standard deviation for ΔCt using the equation

$$s = \sqrt{s_1^2 + s_2^2}$$

where s_1 and s_2 represent the standard deviations of the Ct values. The reference sample needs to be chosen, to which the other samples will be compared -untreated control or wildtype is a good choice for the reference sample. Next, $\Delta\Delta Ct$ is calculated by the equation

$$\Delta\Delta Ct = \Delta Ct_{sample} - \Delta Ct_{ref}$$

The resulting values are substituted into the relative expression ration equation. Note that the reference sample fold expression, $2^{-\Delta\Delta Ct}$, equal to 1. The standard deviation for $\Delta\Delta Ct$ is the same as the standard deviation of the corresponding ΔCt value. In our experiments, β-actin acted as the control and the wildtype cell line acted as the reference (see Figure 24). If the amplification efficiencies differ, then the Pfaffl efficiency-corrected calculation model based on multiple samples is used [190]. This model states the relative expression ratio, R, is calculated by the equation

$$R = \frac{(E_{ref})^{Ct_{sample}}}{(E_{tar})^{Ct_{sample}}} \div \frac{(E_{ref})^{Ct_{control}}}{(E_{tar})^{Ct_{control}}}$$

Control refers to the housekeeping gene or a calibrator. E refers to the efficiency of amplification of a standard curve for those particular qPCR reaction conditions; the slope of the linear regression line determines the amplification efficiency as:

$$E = 10^{(-1/slope)}$$

E_{ref} refers to the qPCR efficiency of the reference sample. Likewise, E_{tar} refers to the qPCR efficiency of the target sample. $Ct_{control}$ refers to the Ct value of the internal normalization control mRNA, the housekeeping gene or calibrator. See Figure 24 for an example of relative quantification.

.

Figure 24. Calculation and results of MBRACE validation experiments

Sample	full-length β-globin Average Ct	β-actin Average Ct	ΔCt full-length - β-actin	ΔΔCt ΔCt(sample) -ΔCt(WT)	Fold expression relative to WT 2^-ΔΔCt
WT β-globin	23.79±0.21	18.60±0.22	5.19±0.30	0.00±0.30	1.00 (0.81-1.23)
PTC β-globin	26.32±0.21	19.04±0.21	7.27±0.30	2.08±0.30	0.24 (0.19-0.29)

Sample	β-globin decay product Average Ct	β-actin Average Ct	ΔCt decay product - β-actin	ΔΔCt ΔCt(sample) -ΔCt(WT)	Fold expression relative to WT 2^-ΔΔCt
WT β-globin	26.09±0.13	18.60±0.22	7.49±0.26	0.00±0.26	1.00 (0.84-1.20)
PTC β-globin	22.26±0.07	19.04±0.21	3.21±0.22	-4.28±0.22	19.38 (16.68-22.63)

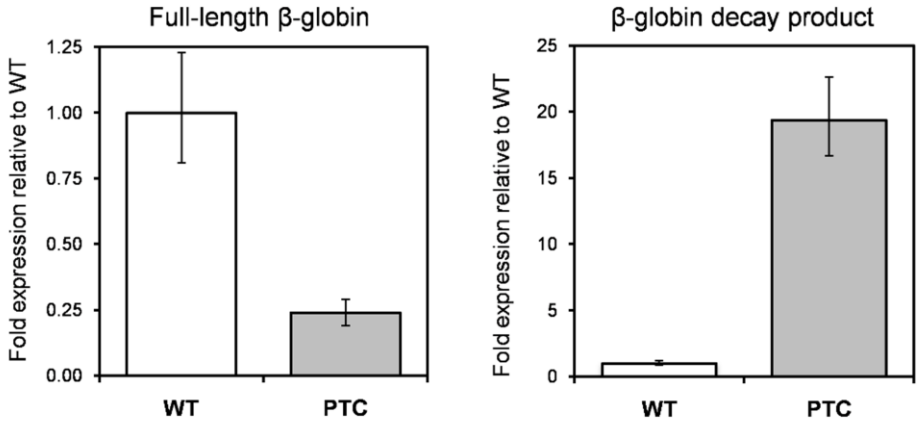

Values shown are +/- standard deviation.

Notes

1. Prepare an incomplete stock of EFLB composed of all components except DTT and RNase OUT (Life Technologies, cat # 10777-019); this can be stored at −20 °C. Prior to use, thaw on ice and complete buffer by adding DTT and RNase OUT, then keep it on ice. Discard any remaining unused completed buffer.

2. Erythroid cells are difficult to lyse so this method will not be appropriate for all cell types. Use an established fractionation protocol for the cell type being used.
3. The lysate should become clear but not viscous as this denotes lysis of the nuclear membrane. Three cycles of tapping/ incubation have been adequate for erythroid cells. RNA can be assessed for proper cyto-nuclear fractionation by denaturing gel electrophoresis and observation of the mature 18S and 28S rRNAs highly concentrated in the cytoplasm and two larger pre-cursor rRNA bands only seen in the nucleus.
4. To lyse the nucleus, resuspend the pellet in 3–5 volumes of EFLB and process as with cytoplasm -tapping and incubating on ice. Centrifuge at 5,000 × g to pellet cell debris. Transfer nuclear supernatant to a new tube pre-chilled on ice.
5. CIAP must be inactivated/removed or it will continue to dephosphorylate RNA after subsequent TAP-mediated cleavage of the 5′ cap, which would leave all the RNA without a 5′ monophosphate.
6. As of this writing, TAP is exclusively sold by Epicentre and is quite expensive. To economize costs, scale up the reactions and use an aliquot of the TAP reaction for subsequent work. Save the remainder of the TAP reaction at −80 °C.
7. Order an RNA linker without a 5′ monophosphate, the lack of a 5′ monophosphate will prevent concatamerization of the linker molecules. Excess adapter needs to be used in the reaction to ensure as many molecules as possible are ligated. Aliquot the RNA linker for storage at −80 °C to avoid freeze-thaw cycles. The RNA linker sequence was adapted from GeneRacer® protocol by Invitrogen. To complete the 5′ RACE experiments, a 25mer RNA linker was used, which was later changed for the MBRACE qPCR to a 44mer RNA linker to provide room for hybridization of the forward primer and the beacon.
8. Use of vector-specific forward and reverse primers will allow for sequencing the entire insert. Using forward and reverse sequencing primers also lends greater assurance of junction

sequence as it is determined by two separate reactions. Sequencing several independent colonies provides verification of junction sequence.

9. Avoid selecting a molecular beacon target sequence in an area of strong secondary structure.
10. Specific target cDNAs are needed to perform the denaturation profiles, standard curves, and verify specificity of the beacons since the linker-specific sequence is shared. Synthetic 90mer DNA oligonucleotides of reverse complementarity to T7 promoter sequence-RNA linker-5′ end mRNA sequence were ordered through Sigma-Aldrich. 1 μg of 90 nt DNA was combined with 2 μL of 50 μM T7 promoter-specific primer in a 0.65 mL tube. This tube was placed in a 1.7 mL tube filled with RNase-free water and the set was heated to 95 °C on a heat block for 10 min. The set of tubes was then removed and placed at room temperature to cool slowly and allow the primer to properly hybridize to the 90mer and form a double-stranded T7 promoter. T7-directed in vitro transcription was completed using the Ambion MAXIscript T7/SP6 kit in a 30 μL reaction volume per manufacturer's instructions. The reaction was then treated with Turbo DNase to degrade the DNA template. Resulting RNA was stored at −80 °C. The full-length mRNA product served as proper target for the full-length beacon and improper target for the decay product beacon. Alternatively the decay product served as proper target for the decay beacon and improper target for the full-length beacon.
11. For detection with the beacons, the original RNA linker sequence needed to be altered to increase the annealing temperature for the beacon. Additionally, the RNA linker length was increased to 44 bp to accommodate binding of the forward primer and beacon.
12. cDNA column purification was necessary in our experiments to yield proper detection amplification curves with the molecular beacons.
13. The conditions for these particular constructs and experiments and may not be the optimal conditions for other constructs. These conditions could be used as a starting point for optimization. Parameters to optimize include primer concentration, beacon concentration, template concentration (sometimes less is better), annealing temperature, and qPCR reagent.

Also, due to the sensitivity of the MBRACE assay, use well-maintained and calibrated pipettes, as small deviations can become large differences.

14. An alternative to using molecular beacons would be to use SYBR green chemistry—if it can be proven to be highly specific. Designing the forward primer to hybridize to the RNA linker–mRNA junction sequence would serve to differentiate the products. Standard curves and specificity testing would be necessary to guarantee-specific detection. qPCR products should be electrophoresed on an agarose gel and the 5′ end sequences of the resulting product(s) verified by 5′ RACE as above to additionally ensure specificity. Bioline's SensiFAST SYBR reagents have shown superior sensitivity.

Acknowledgements

We wish to thank members of the Schoenberg lab for their helpful comments in developing this methodology. This work was supported by the National Institute of General Medical Science of the National Institutes of Health under award number GM079707.

Chapter 3: SMG6 Cleavages Generates Metastable Decay Intermediates from Nonsense-Containing β-globin mRNA

Mascarenhas*, R., Dougherty*, J.A., and Schoenberg, D.R. (2013) *PLoS ONE*. **8**(9): e74791. Doi:10.1371/journal.pone.0074791. * These authors contributed equally to this work.

*Disclaimer: RM performed Upf1 KD (Figure 27), pre-cursor-product experiments (Figure 28), SMG6KD (Figure 29) and experiments involving PMR1 (Figure 33). JAD designed and validated MBRACE assay (Figure 26), performed TAP-treatment analysis (Figure 26), SMG6 complementations (Figure 30), and analysis of Upf1 phosphorylation status (Figure 31). DRS generated figure 25.

INTRODUCTION

Endonuclease decay was thought to play a minor role in mRNA turnover before results from deep sequencing showed widespread evidence for endonuclease cleavage throughout the mammalian mRNA transcriptome [184, 191]. Despite this relatively little is known about the enzymes that generate these cleavages, and only a few bona fide mRNA endoribonucleases have been identified and characterized [192]. A major complication to the study of endonuclease-mediated mRNA decay is the rapidity with which cleavage products are cleared by 5'-3' and 3'-5' exonucleases [192]. For the most part decay intermediates are only detected by knocking down Xrn1 to stabilize the downstream fragment [103] or by PCR amplification after ligating a

primer to the newly formed 3' ends of cleavage products [193]. A possible exception to this is the decay of nonsense-containing β-globin mRNA in erythroid cells.

In 1989 Lim and Maquat [177] showed that 5'-truncated forms of human β-globin mRNA accumulate in erythroid cells of mice that are transgenic for several nonsense containing alleles. The same 5'-truncated RNAs accumulate in murine erythroleukemia cells that are stably transfected with wild type and nonsense-containing human β-globin genes [180, 194]. We showed previously that these shortened RNAs were generated by endonuclease cleavage [180], but because they were only seen in erythroid cells it was unclear if these are intermediates in the decay process or the products of a cell type-specific processing that is unique to β-globin mRNA in its native cell environment. Complicating matters further, the same 5'-truncated RNAs were also seen in cells expressing wild type β-globin mRNA, albeit at a much lower level [180], and their quantity is increased by coexpressing *Xenopus* PMR1 in these cells [194]. This was originally interpreted as evidence that erythroid cells employ a PMR1-like endonuclease to degrade β-globin mRNA, but that finding preceded the identification of SMG6 as an endonuclease that catalyzes the degradation of nonsense-containing mRNA [104, 116].

Progress in studying endonuclease decay has been limited by the challenges inherent in quantifying short-lived decay intermediates. Thus, if the shortened forms of β-globin mRNA are indeed decay intermediates we could take advantage of their appearance to address several questions about the decay process. To address this we developed an inducible line of erythroid cells which were used to monitor the cytoplasmic appearance of full-length normal (WT-hβG) and PTC-containing (PTC-hβG) human β-globin mRNA after treating cells with doxycycline to induce transcription of their respective genes. Changes in full-length mRNA and one of the 5'-truncated RNAs were determined using a modification of Molecular Beacon Rapid Amplification of cDNA Ends (MBRACE) [183], a qRT-PCR-based assay for quantifying products after ligation of a common primer to uncapped 5' ends.

MATERIALS AND METHODS

Plasmid constructs

A wild type (WT) human β-globin gene and a gene with a nonsense codon at position 60/61 (PTC60/61, [180]) were cloned into a modified form of pcDNA3 (pcDNA3/TO) with a tetracycline operator element upstream of the multiple cloning site. Destabilized forms of each of these were generated by insertional mutagenesis of the nucleolin/α-CP binding site (H124 insertion) [9]. Plasmids expressing wild type and PTC-containing T-cell receptor –β (TCRβ) mRNA (pAc/IF-TCRβ) [195] were provided by Miles Wilkinson. pcDNA3-HA-SMG6 and SMG6-m4 provided by Oliver Mühlemann were used for complementation experiments. All of the primers described here and below are listed in Table 8.

Cell culture

Murine erythroleukemia (MEL) cells that were stably transfected with wild type (Norm2) or nonsense-containing (Thal10) β-globin genes were described previously [180]. Thal10 cells express a form of β-globin mRNA with a single base deletion that results in a nonsense codon at position 60/61 in the mature transcript. Norm2 and Thal10 cells were cultured in Minimal Essential Medium alpha (alpha MEM) supplemented with 10% FBS, and β-globin gene transcription was induced by treating for 48 hr with 1.5% DMSO. K562 cell lines were obtained from the American Type Culture Collection and cultured in the same medium as Norm2 and Thal10 cells. A line of tetracycline inducible K562 cells was generated by transduction with a tetracycline repressor-expressing lentivirus (pLenti6/TR, Invitrogen). Transduction was performed by adding viral supernatant to cells in a 24-well culture plate and centrifuging at 300 x g for 2 hr, 25°C using a JS5.3 rotor in a Beckman Avanti J-20 XPI centrifuge. 100 individual colonies were selected by growth for 14 days in medium containing 10 μg/ml blasticidin (Invitrogen) and tested for tetracycline-regulated inducibility by electroporation with pcDNA4/TO/LacZ and with inducible β-globin plasmids and the one showing highest inducibility

and tightest regulation was selected for use in this study. Electroporation was performed using a Neon® (Invitrogen) electroporator. $1x10^6$ cells were centrifuged at 100 x g for 4 min, the cell pellet was washed with PBS and resuspended in 100 µl of resuspension buffer 'T' (Invitrogen, MPK10025Tb, proprietary composition) as per manufacturer's protocol. 3 µg of plasmid DNA was added and electroporation was performed with a 100 µl tip using 2 x 20 millisecond pulses of 1300 volts.

siRNA knockdowns

For the experiments in Figure 27 and Figure 29, 1 x 10^6 tet-inducible K562 cells electroporated with plasmids expressing inducible forms of β-globin mRNA (WT or PTC60/61) or constitutively expressed forms of T cell receptor (TCR) β (WT or PTC) plasmids were cultured for 16 hr in antibiotic-free medium. The recovered cells were resuspended in 750 µl Accell siRNA delivery media (Thermo, Cat# B-005000). 100 µM solutions of control (Thermo, D-001950-01), Upf1 (Thermo, E-011763-00-0005) or SMG6 (Thermo, E-017845-00-0005) SMARTpool siRNAs were prepared in 1X siRNA buffer (Cat# B-002000-UB-100). 7.5 µl of the 100 µM siRNA solution was added to cells in siRNA delivery media and 100 µl aliquots were placed into individual wells in a 96-well plate. The next day cells were transferred to individual wells of a 24-well plate, and β-globin was induced 48 hr after knockdown by treating for 6 hr with 1 µg/ml doxycycline. A SMG6 siRNA (5' GCUGCAGGUUACUUACAAG 3', with 3' UU overhangs) was generated that corresponds to the shRNA target in [104]. In the experiment in Figure 30 $2x10^6$ tetracycline-inducible K562 cells were electroporated with 10 nM of control or SMG6 siRNA in 100 µl of buffer 'R'. The same cells were electroporated 24 hr later with 10 nM of each siRNA, 0 µg of WT- or PTC-hβG-expressing plasmid, and 20 µg of empty vector, SMG6-expressing plasmid pcDNA3-HA-SMG6 or SMG6 plasmid with the 3 catalytic aspartate residues in the PIN domain changed to asparagine (SMG6-m4, [104]). β-globin gene transcription was induced 16 hr later by adding 1 µg/ml doxycycline to the medium and cytoplasmic RNA was

isolated 6 hr after induction. Western blotting was used to determine the effectiveness of knockdown, modified MBRACE assay was used to monitor full-length and Δ169 RNA, and TCRβ mRNA was assayed by qRT- PCR.

Isolation of cytoplasmic RNA and protein

Cell were harvested by centrifugation and washed twice with ice cold PBS. Norm2 and Thal10 cells were resuspended in lysis buffer containing 0.1 M NaCl, 10 mM Tris-HCl pH 8.0, 2 mM EDTA, 1% NP-40, 1% 2-mercaptoethanol, 1 mM dithiothreitol, and 80 units/ml RNaseOUT. K562 cells were resuspended in modified lysis buffer containing 0.15 M NaCl, 50 mM Tris-HCl pH 7.5, 10 mM KCl, 10 mM $MgCl_2$, 0.2% NP-40, 2 mM dithiothreitol and 80 units/ml RNaseOUT. These were placed on ice for 5 min, the tubes were gently flicked and incubated on ice for an additional 5 min. The lysates were centrifuged at 5000 x *g* at 4°C for 10 min to pellet the nuclei, supernatant (cytoplasmic) fractions were transferred to chilled microcentrifuge tubes and RNA was extracted using Trizol Reagent (Life Technologies) as recommended by the manufacturer's protocol. Cell lysate was used directly for protein quantification and visualization by western blot analysis.

Antibodies

Affinity-purified rabbit polyclonal antibody to the tetracycline repressor protein was obtained from MoBiTec. Rabbit polyclonal antibodies to hUpf1 and hSMG6 were provided by Jens Lykke-Andersen, and rabbit polyclonal anti-phosphoUpf1 was obtained from Millipore, Inc. Horseradish peroxidase (HRP)-coupled goat anti-rabbit IgG and goat anti-mouse IgG were obtained from Santa Cruz Biotechnology.

Western blot analysis

Samples were denatured in 2x Laemmli sample buffer (Bio-Rad Laboratories) with β-mercaptoethanol. 10 μg of cytoplasmic protein was separated on 10% Mini-PROTEAN® TGX™ precast gels (Bio-Rad Laboratories) and transferred onto Immobilon®-P PVDF membrane (EMD Millipore). Membranes were blocked with 5% nonfat dry milk in Tris-buffered saline containing 0.05% Tween-20 (TBS-T), incubated with primary antibody (1:1000 dilution) in the same solution, washed with TBS-T, then incubated with horseradish peroxidase-coupled secondary antibody (1:10000 dilution). For experiments with anti-phospho-Upf1 antibody blots were blocked with 1x TBS + 3% BSA for 2 hr at 25°C. They were incubated overnight at 4°C in the same solution with a 1:250 dilution of anti-phospho-Upf1 antibody and secondary antibody incubation was performed in 1X TBS + 3% BSA. Membranes were developed with ECL-plus or for phospho-Upf1 Western blotting a 1:1 mixture of ECL-prime solutions A and B, and visualized on X-ray film (GeneMate).

S1 nuclease protection assay

S1 nuclease protection assay was performed as described in [196]. RNA was dissolved in S1 hybridization buffer (80% formamide, 40 mM PIPES, pH6.4, 0.4 M NaCl, 1 mM EDTA) and incubated overnight at 52°C with 3-5 x 10^4 dpm of [^{32}P]-end-labeled antisense DNA probe. The antisense probe was obtained by asymmetric PCR using the human β-globin cDNA plasmid pSPkβC or the mouse β-actin cDNA plasmid pBSβactin as templates. T4 polynucleotide kinase was used to label the 5' end of the antisense β-globin primer HBB-AS: beginning at position 250, primer 1249: beginning at position 346 and the antisense β-actin primer YO-41 with γ-[^{32}P] ATP (3,000 Ci/mmol). The unlabeled β-globin sense primer (HBB-S) and β-actin sense primer (ACT-S) correspond to sequences just upstream of the β-globin or β-actin cDNA in the expression plasmid. The [^{32}P] labeled probe generated by this reaction was purified by electrophoresis on a 6% polyacrylamide/urea gel. After hybridization, S1 nuclease solution (0.28 M NaCl, 0.05 M

sodium acetate, pH 5.2, 4.5 mM $ZnSO_4$, 20 μg/ml sheared salmon sperm DNA, 100 units S1 nuclease, Invitrogen) was added to each reaction and the mixture was incubated at 28°C for 2 h. Samples were precipitated with ethanol and electrophoresed on denaturing 6% polyacrylamide/urea gels. Protected fragments were visualized and quantified by PhosphorImager.

MBRACE, modified MBRACE and qRT-PCR assays

1 μg of DNase I-treated cytoplasmic RNA was incubated with 3 units of tobacco acid pyrophosphatase (TAP, Epicentre) at 37°C for 2 hr in 1X TAP buffer. An RNA adapter (RNA ADP) was ligated to this using T4 RNA ligase I (New England Biolabs) in T4 RNA ligase reaction buffer supplemented with 1mM ATP at 37°C for 2 hr. cDNA was prepared using SuperScript® III first-strand synthesis system (Life Technologies) and the product was purified using QIAquick® PCR purification columns (Qiagen). Approximately 20 ng of cDNA was used per qPCR reaction containing 500 nM forward (MBRACE-F) and reverse primers (HBB-FL-R1, HBB-Δ169-R1), 250 nM molecular beacon (HBB-FL-MB, HBB-Δ169-MB) in 1X PerfeCTa qPCR FASTmix (Quanta Biosciences). PCR was performed using an Eco Real-Time PCR system (Illumina®) and the following thermal profile: 95°C for 3 min, [95°C 10 sec, 61°C 30 sec with signal detection, 72°C 15 sec] for 40 cycles. Ct baseline and threshold were automatically determined by Eco software. Molecular beacons were designed to the junction sequence between the RNA adapter and full-length or Δ169 β-globin mRNA. HEX-BHQ1 and 6FAM-Dabcyl fluorophore-quencher pairs were used to label the full-length and decay product beacons respectively. HPLC purified beacons were resuspended in 1x TE (10 mM Tris-HCl pH 8.0, 1 mM EDTA) buffer and stored in aliquots at -80°C. Modified MBRACE assay used primers designed to the junction between the ligated adapter RNA and full-length (HBB-JS-F) and Δ169 (HBB-Δ169 -JS-F) RNA. β-globin specific primers (HBB-FL-R1, HBB-Δ169-R1 in MEL, HBB-FL-R2,

HBB-Δ169-R2 in K562) were designed to generate similar length products that could be verified by gel electrophoresis. The locations of these primers on hβG mRNA are shown in Figure 32. S1. Reaction conditions to detect full-length β-globin and its decay product were as follows: 20 ng cDNA, 375 nM junction-specific and reverse primers in 1X SYBR Green PCR Master Mix (Applied Biosystems/ Life Technologies) in 10 μl reaction volume. The control mRNA TCRβ (TCRβ-F, TCRβ-R), GFP (emGFP-F, emGFP-R), and β-actin (MA-F, MA-R) levels were also quantified by similar method using indicated primers. qPCR was performed on the Eco Real Time PCR system with thermal profiles for all SYBR Green reactions as follows: 95°C for 10 min, [95°C for 10 sec, 60°C 30 sec with signal detection] for 40 cycles followed by a melt curve. ROX present in master mix acted as well-to-well normalization control. The Eco software automatically determined Ct baseline and threshold. To determine the fold change in transfection experiments, β-globin mRNA levels were normalized to the levels of co-transfection control GFP mRNA. In MEL cells β-globin mRNA levels were normalized to β-actin mRNA.

Data analysis

Experiments were conducted in biological triplicate and qPCR reactions were performed in sample triplicate. Ct values for each replicate were averaged, ΔCt was calculated by subtracting the control (β-actin or GFP) Ct from the sample Ct. ΔCt values were averaged over the replicates and the average ΔCt for WT β-globin acted as the reference value. The ΔΔCt value was calculated by subtracting the ΔCt of WT from the sample ΔCt value. Fold expression was calculated using the $2^{-\Delta\Delta Ct}$ method [189]. Statistical analysis was performed using JMP9 (SAS, North Carolina) software. Data distribution and variance determined the appropriate method of analysis, all of which were performed 2-tailed with an α=0.05. Graphs were generated using GraphPad Prism 5 (GraphPad Software, Inc.) and bars represent standard deviation.

RESULTS

Actinomycin D chase shows prolonged presence of 5' truncated RNAs in the erythroid cell cytoplasm

Our previous work used murine erythroleukemia cells that were stably transfected with WT-hβG (Norm2) or PTC-hβG (Thal10) transgenes to study β-globin mRNA decay [180, 194]. Using Actinomycin D and Northern blotting we showed that full-length wild type mRNA has a half-life of 12 hr in Norm2 cells and PTC-containing mRNA decays with biphasic kinetics and a half-life of 100 min [194]. Neither of the earlier studies looked at the fate of the 5'-truncated RNAs, and because these are more abundant in Thal10 cell,s we repeated Actinomycin D chase to analyze mRNA stability. However, this time we used S1 nuclease protection to monitor changes in full-length and 5'-truncated RNAs (Figure 25). Again, full-length PTC-hβG mRNA showed a biphasic curve similar our previous results and to PTC-hβG mRNA in non-erythroid cells [197]. Although they appeared to be more stable than full-length mRNA there were differences in the patterns seen for each of the 5'-truncated RNAs. The transcripts whose 5' ends were closest to that of full-length mRNA disappeared at a faster rate than those whose 5' ends were further away. Although it does not constitute proof, this is consistent with multiple endonuclease cleavage events happening over time until a limit digest is reached.

Figure 25. Prolonged cytoplasmic residence of 5' truncated forms of PTC-hBg mRNA.

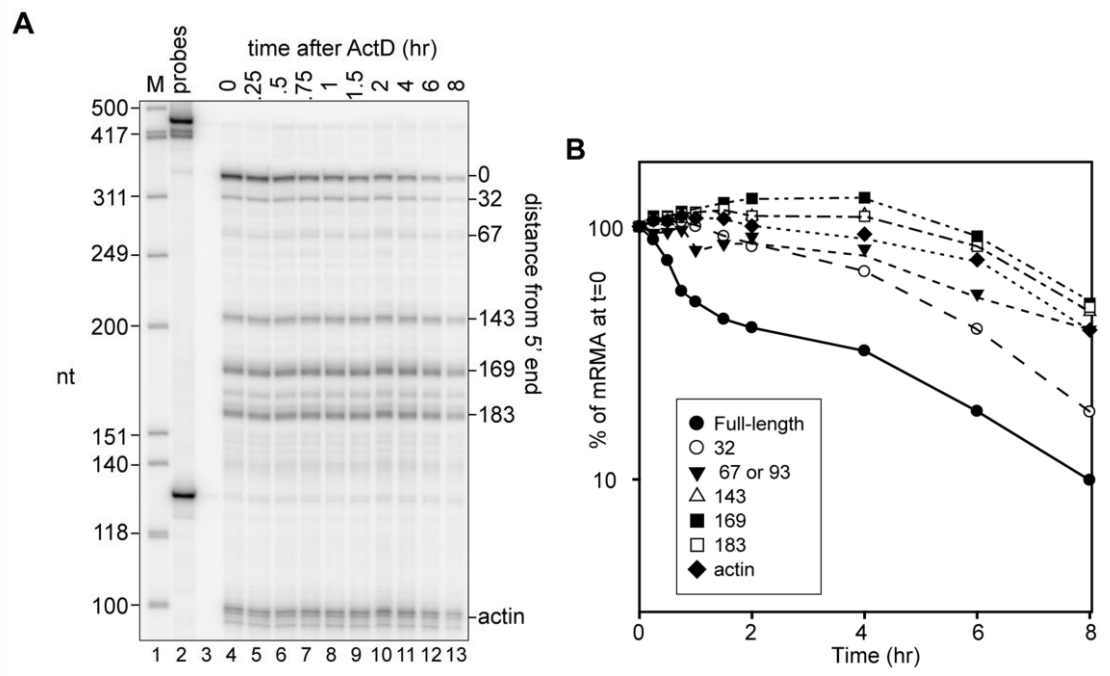

A. Actinomycin D (6 μg/ml) was added to DMSO-induced Thal10 cells at time 0 and cytoplasmic RNA recovered at the indicated times was assayed by S1 nuclease protection using a probe for the first 354 nt of β-globin mRNA. Hinf I restriction fragments of φX174 DNA were used as size markers (M, lane 1) and the location of each of the products relative to the 5' end of β-globin mRNA is indicated on the right side of the autoradiogram. **B.** The amount of each species was quantified by phosphorimager analysis and plotted on the right as a function of time after addition of Actinomycin D.

A quantitative assay for full-length and 5'-truncated β-globin RNAs

Given the challenge presented by the prolonged presence of 5'-truncated RNAs we sought an alternative approach for studying hβG mRNA decay in erythroid cells. The first step involved the development of a method for quantifying full-length mRNA and one of the truncated transcripts, and for this we selected Molecular Beacon Rapid Amplification of cDNA Ends (MBRACE) [183] (Figure 26A). In this assay, cytoplasmic RNA is first treated with a phosphatase to prevent primer ligation to uncapped ends. The cap is removed with tobacco acid yrophosphatase (TAP), an RNA adapter is ligated onto the newly created 5'-monophosphate ends

and the products are quantified using junction-specific molecular beacons as indicated in the figure or by qRT-PCR. Results in the left and middle panels of Figure 26B comparing untreated with TAP-treated RNA demonstrate the importance of removing the cap for MBRACE assay of full-length WT- and PTC-hβG mRNAs.

A similar approach was then developed for quantifying one of the 5'-truncated RNAs shown in the right panel of Figure 26C. 5'-RACE that was performed using TAP-treated RNA from PTC-hβG-expressing Thal10 cells and individual cloned products were sequenced to confirm that the junction with the ligated primer matched each of the 5' ends identified in [180] by primer extension and S1 nuclease protection. The transcript lacking 169 from the 5' end (Δ169) was then selected for assay development. Our discovery of cytoplasmic capping [198] was the result of following an earlier report describing the 5' ends of the truncated RNAs as having a cap or cap-like structure [179]. The presence of a cap on 5'-truncated RNAs is evident in the right panel of Figure 26B, where TAP treatment of RNA from PTC-hβG-expressing cells resulted in an almost 800-fold increase in signal for Δ169 RNA. Finally, the applicability of MBRACE assay for quantifying changes in full-length and Δ169 RNA was confirmed by the comparable results obtained by MBRACE assay (Figure 26D) and S1 nuclease protection (Figure 26C) performed with RNA from MEL cells expressing WT- and PTC-hβG mRNA.

Figure 26. Development of a modified MBRACE assay for quantifying full-length and one of the 5' truncated B-globin mRNAs

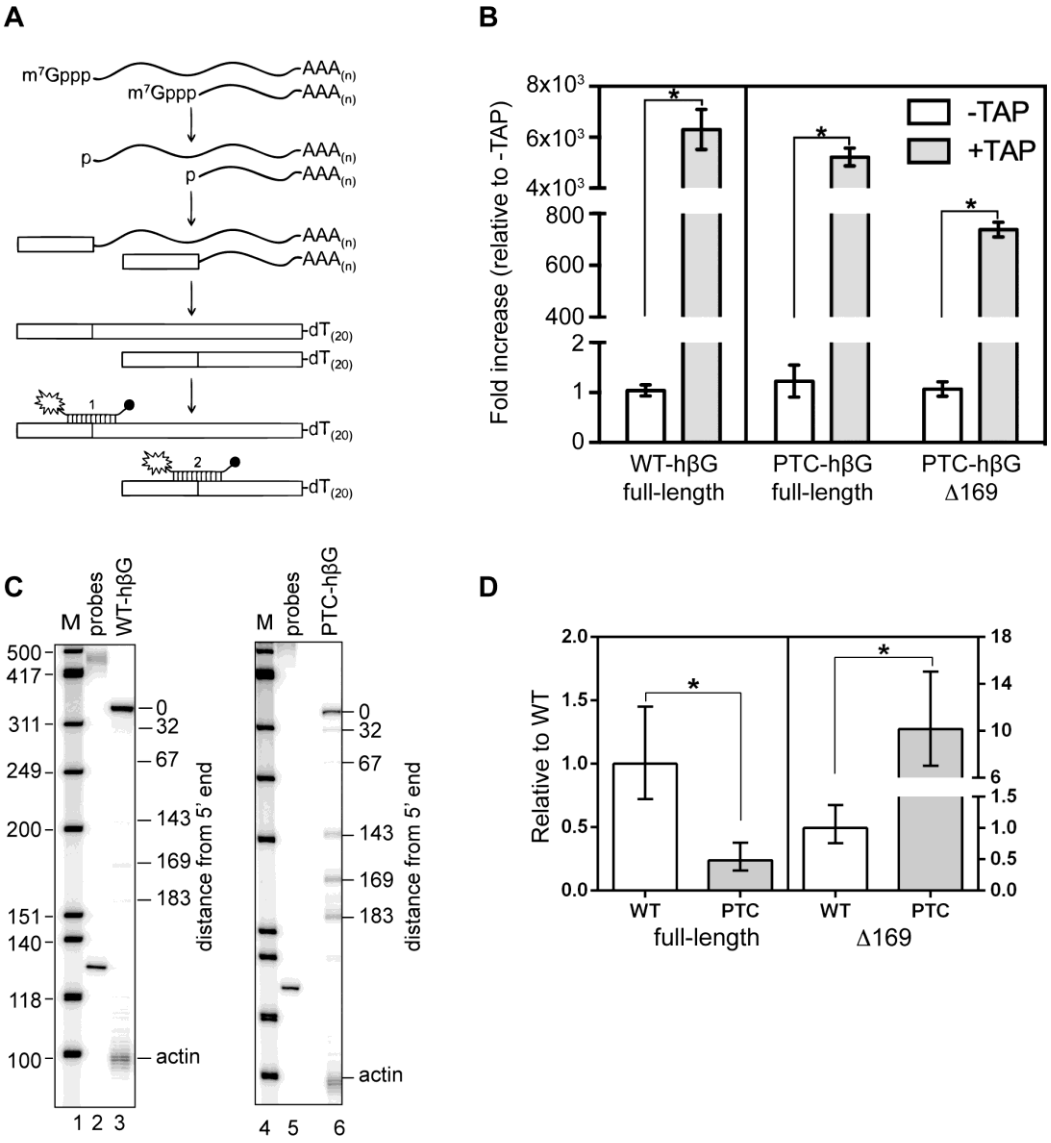

Development of a modified MBRACE assay for quantifying full-length and one of the 5'-truncated β-globin mRNAs. **A.** A schematic of the modified MBRACE assay is shown, and the locations of each of the primers are presented in Table 8. **B.** RNA from triplicate cultures of MEL cells expressing WT-hβG or PTC-hβG mRNA was added directly to the ligation reaction with the 5' RNA adapter (-TAP, open bars) or treated with tobacco acid pyrophosphatase (+TAP, grey bars) before ligation. Results obtained without TAP treatment were arbitrarily set to 1 and results obtained with TAP-treated RNA were normalized to the -TAP samples. The results represent the mean ± standard deviation for triplicate samples. * indicates $p<0.01$ by Student's two-tailed T-test. **C.** S1 nuclease protection assay was used to demonstrate the increased accumulation of 5'-truncated RNAs in cells expressing PTC-hβG mRNA (lane 6) compared to WT-hβG mRNA (lane 3). The locations of each of the 5'-truncated RNAs with respect to the cap site are indicated to the right of each autoradiogram. **D.** The transcript missing 169 nt (169) was selected as a representative truncated RNA. Cytoplasmic RNA from MEL cells expressing WT- or PTC-hβG mRNA was used to demonstrate applicability of the modified MBRACE assay for quantifying changes in full-length mRNA and Δ169 RNA. In each graph the amount of RNA from each cell line was first normalized to β-actin. Shown is the mean ± standard deviation for biological triplicates, * indicates $p<0.001$ by two-tailed t-test.

NMD is responsible for the increase in 5' truncated RNAs from PTC-hβG mRNA

Although K562 cells are an erythroid cell line they do not express hβG mRNA. We developed a line of tetracycline inducible K562 cells to circumvent complications resulting from the prolonged cytoplasmic lifetime of 5'-truncated RNAs. In each of the following experiments these cells were electroporated with plasmids expressing tetracycline inducible full-length WT- and PTC-hβG genes, and changes in full-length and Δ169 RNA were quantified by MBRACE assay after inducing their transcription with doxycycline. In the experiment in Figure 27 electroporated K562 cells were treated with Accell® control or Upf1 siRNAs before inducing WT- or PTC-hβG mRNA. This reduced Upf1 to 10% of control (Figure 27A), and the stabilization of nonsense-containing TCRβ mRNA (Figure 27B) demonstrated its effectiveness in inactivating NMD. Knocking down Upf1 had little impact on WT-hβG mRNA or the amount of Δ169 RNA in cells expressing WT-hβG mRNA; however, the stabilization of full-length PTC-hβG mRNA and reduction in the level of Δ169 RNA to that observed with WT-hβG (Figure 27C and D) confirm that NMD is responsible for the increased appearance of 5'-truncated transcripts from PTC-hβG mRNA.

Figure 27. Evidence that NMD is responsible for the accumulation of Δ169 RNA from PTC-hβg mRNA

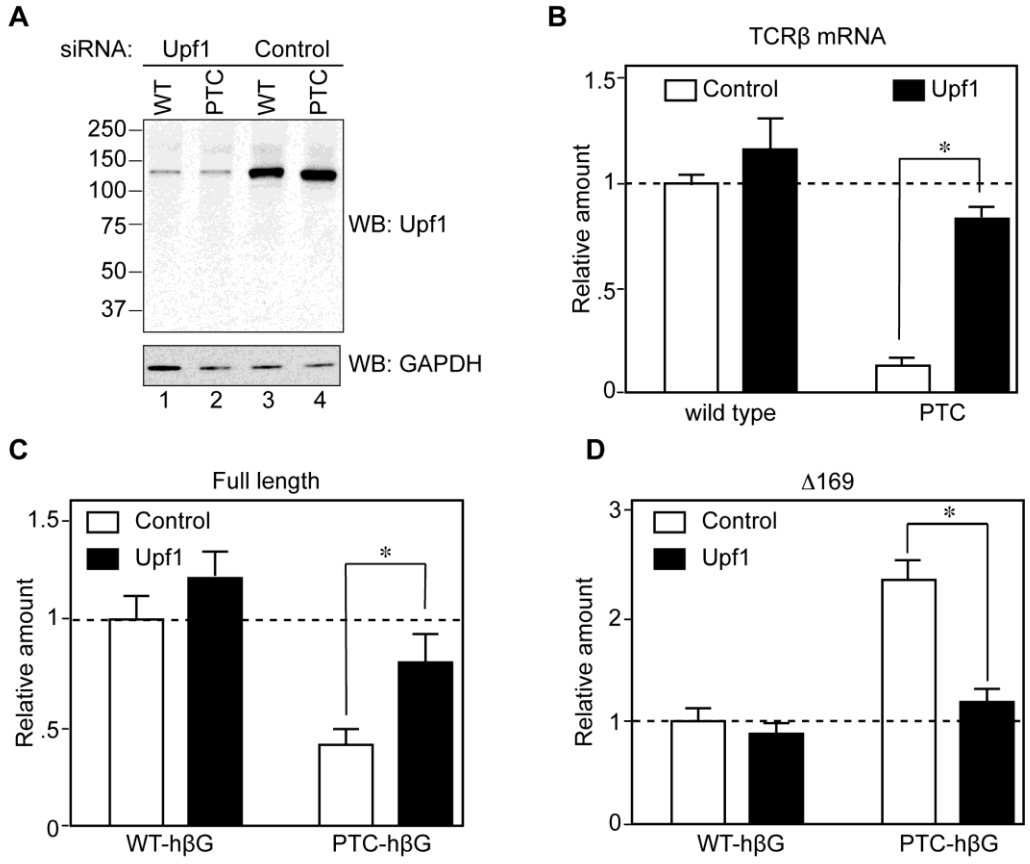

Tet-inducible K562 cells in antibiotic-free medium were electroporated with plasmids expressing constitutive wild type or nonsense-containing TCRβ genes, or each of the inducible β-globin genes, and a GFP control. Sixteen hr later they were transfected with Accell SmartPool® Upf1 or control siRNAs, cultured for an additional 48 hr, then induced with doxycycline for 6 hr. **A**. Cytoplasmic extracts from WT- and PTC-hβG expressing cells were assayed by Western blotting for efficiency of Upf1 knockdown. **B.** The effectiveness of Upf1 knockdown in inhibiting NMD was determined by qRT-PCR analysis of changes in WT- versus PTC-TCRβ mRNA. **C.** The modified MBRACE assay was used to quantify the impact of Upf1 knockdown full-length WT- and PTC-hβG mRNA. **D.** Modified MBRACE assay was used to monitor the impact of Upf1 knockdown on the production of Δ169 RNA. The results represent the mean ± standard deviation of triplicate cultures,
* indicates $p<0.05$ by two-tailed Student's T-test.

The 5' truncated RNAs are metastable decay intermediates

The prolonged cytoplasmic residence of 5'-truncated RNAs after Actinomycin D (Figure 25) ruled out the use of transcription inhibitors in determining whether these are intermediates of PTC-hβG decay. Instead we monitored the appearance of both forms of hβG mRNA over time after inducing transcription of their respective WT- and PTC-hβG genes (Figure 28). If the truncated RNAs are decay intermediates the expectation is their appearance in the cytoplasm should follow that of full-length mRNA. Changes in each transcript over 12 hr after induction are shown in Figure 28A, and the first 3 hr after induction, where initial differences are more evident, are shown enlarged in (Figure 28B). The appearance of Δ169 RNA after full-length WT- and PTC-hβG mRNA is consistent with assignment of the shortened RNAs as intermediates in the decay process.

To obtain more definitive evidence of this we looked for a way to accentuate the differences in time of appearance of full-length and Δ169 RNA that was compatible with the inducible cell system. To address this we took advantage of the fact that given the same degree of induction an mRNA that turns over rapidly will reach a new steady state sooner than one with a slower rate of decay [199]. The prolonged stability of hβG mRNA (and possibly the 5' truncated transcripts) is due in part from the binding of nucleolin to a site in the 3'-UTR [9]. In the experiment in Figure 28C the time course appearance of the different RNAs was repeated using WT- and PTC-βG genes with inactivated nucleolin binding sites (H124, [9]). As anticipated, this reduced the degree to which of each mRNA accumulated; however, it provided clear and convincing evidence of differences in the time of appearance of full-length and Δ169 RNAs. Addditionally, the absence of the stable 5' truncated RNAs in the nucleus but presence in the cytoplasm excludes alternative transcription start site selection as the mechanism of generation. The observation that PTCs at different locations along the β-globin mRNA were generating identical 5' truncated products dismissed alternative splicing as a plausible mechanism. The hypothesis that an endonuclease was responsible for cleavage came from earlier

studies with PMR1 [180, 194] Collectively, these data confirm that the 5’-truncated RNAs are endonuclease-generated decay intermediates.

Figure 28. Evidence that 5' truncated RNAs are decay intermediates.

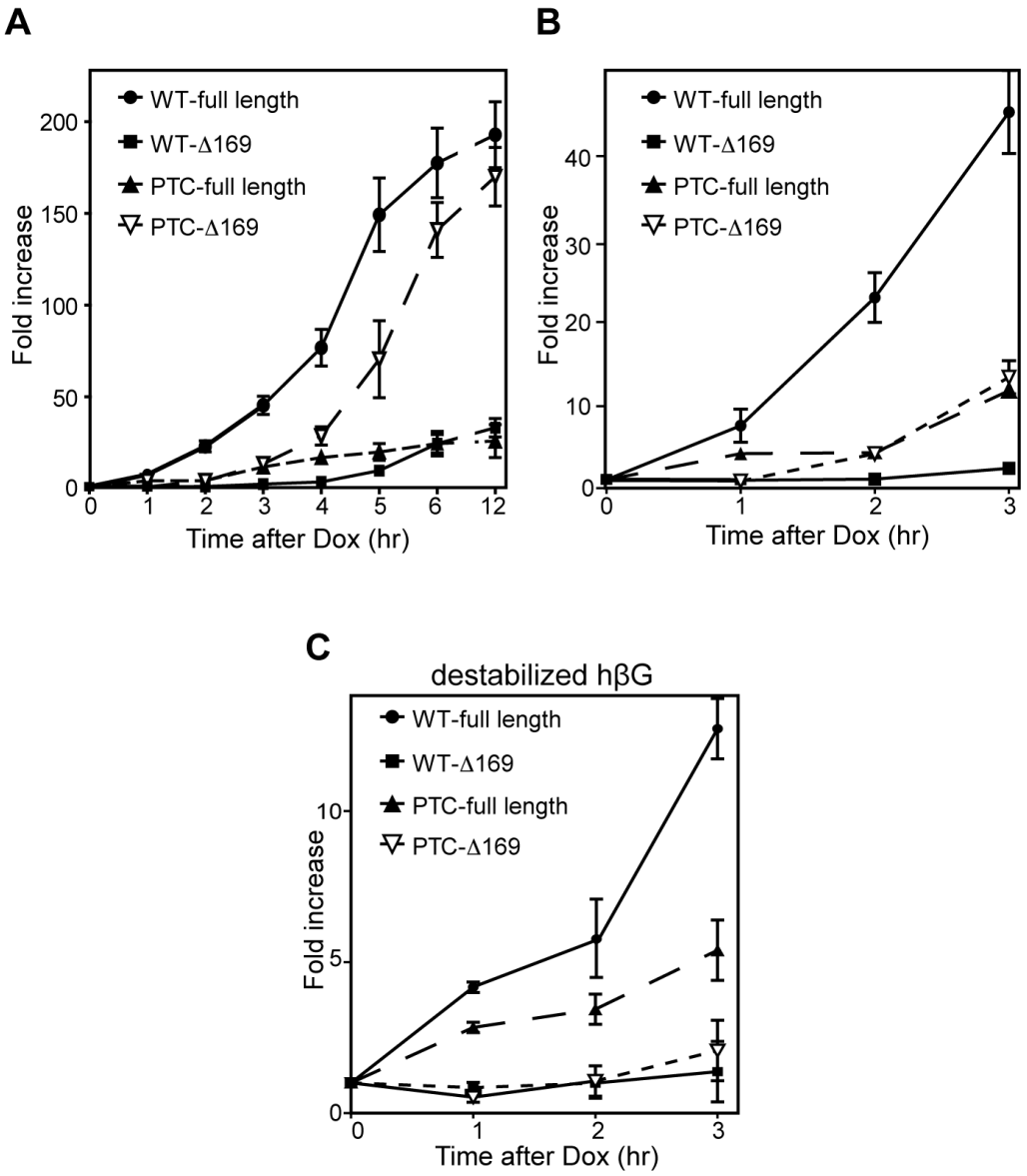

A. Doxycycline was added at time 0 to tet-inducible K562 cells that were electroporated 16 hr earlier with plasmids bearing inducible WT- or PTC-hβG genes and a GFP control. Cytoplasmic RNA isolated at intervals over 12 hr of induction was analyzed by modified MBRACE assay for changes in full-length and Δ169 forms of hβG mRNA. **B.** The first 3 hr of induction is shown enlarged. **C.** The experiment was repeated except that the plasmids that were electroporated into tet-inducible K562 cells expressed a destabilized form of β-globin mRNA (H124 mutation) as a result of disruption of the 3'-UTR nucleolin binding site [9]. Each point represents the mean ± standard deviation for triplicate determinations.

SMG6 is the endonuclease that generates 5'-truncated forms of PTC-hβG mRNA

We next sought to determine the identity of the endonuclease responsible for generating the 5'-truncated decay intermediates. Our previous work suggested this was PMR1 or a PMR1-like endonuclease [180, 194]. However this was ruled out by the lack of any impact on WT- or PTC-hβG mRNA of inhibiting PMR1 activation or overexpressing human PMR1 (Figure 33). SMG6 is a PIN-domain containing endonuclease that participates in the degradation of nonsense-containing mRNAs [104, 116]. It lacks sequence selectivity, and specificity for nonsense-containing mRNAs results from its binding to the exon junction at the same site as Upf3b [4]. In the experiment in Figure 29 K562 cells electroporated with plasmids expressing WT- and PTC-hβG mRNA were knocked down for SMG6 before adding doxycycline to induce WT- and PTC-hβG mRNA. Knockdown depleted ~90% of SMG6 (A) and this had the anticipated effect of stabilizing PTC-containing TCRβ mRNA (Figure 29B). SMG6 knockdown had no impact on WT full-length or Δ169 RNA, increased full-length PTC-hβG mRNA and returned the amount Δ169 RNA to the level generated from WT-hβg mRNA (Figure 29A and B)

Although these data are consistent with SMG6 generating Δ169 RNA it was formally possible that the observed effects were secondary to changes in Upf1 phosphorylation [151]. This was first addressed by a complementation experiment similar to that performed in [104]. In the experiment in Figure 30, tetracycline-inducible K562 cells were electroporated with control or SMG6 siRNAs, then a second time with the same siRNAs together with empty vector or plasmids expressing siRNA-resistant SMG6 or an inactive form of SMG6 with the 3 active site aspartic acid residues changed to asparagine (SMG6-m4). The second round of transfection included tetracycline-inducible plasmids expressing WT- and PTC-hβG mRNA, and cells recovered 6 hr after induction were analyzed by Western blotting for changes in SMG6 and by modified MBRACE assay.

Figure 29. SMG6-knockdown increases full-length PTC hβg mRNA and decreases Δ169 RNA

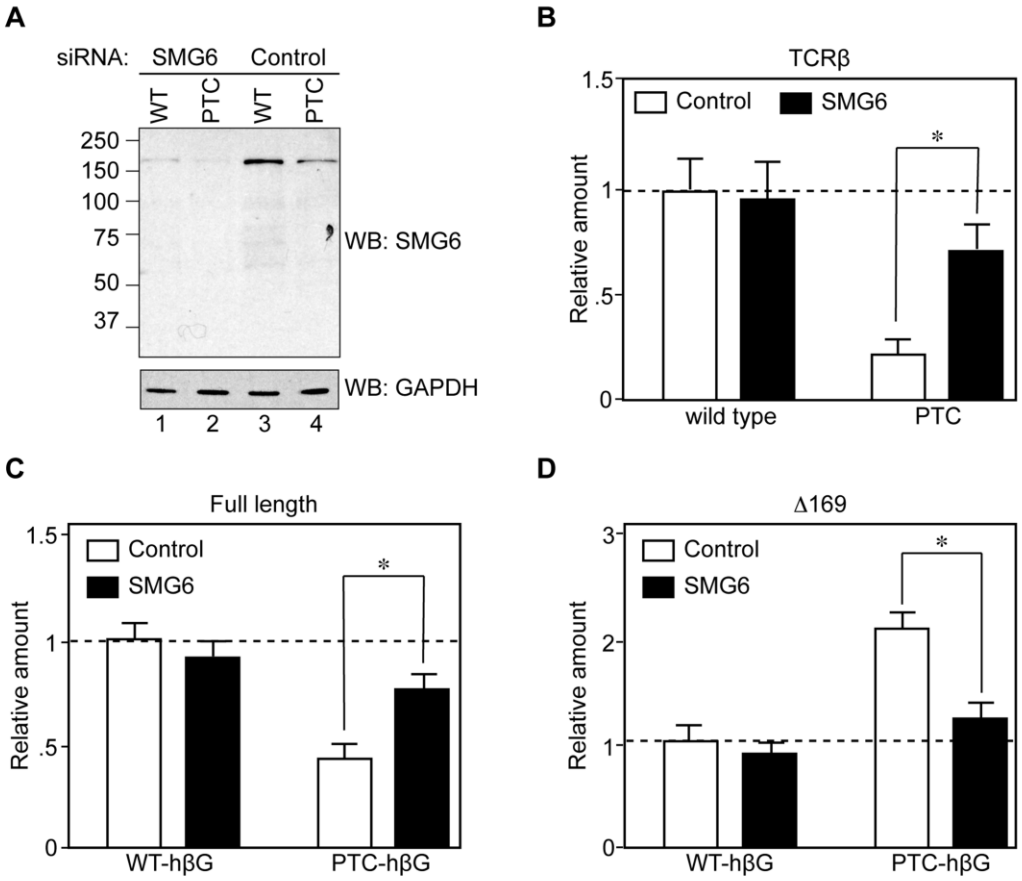

Tet-inducible K562 cells in antibiotic-free medium were electroporated as in Fig. 3, with plasmids expressing constitutive WT- or PTC-TCRβ genes, or each of the inducible hβG genes, and a GFP control. Sixteen hr later they were transfected with Accell SmartPool® SMG6 or control siRNAs, cultured for an additional 48 hr, then induced with doxycycline for 6 hr. **A.** Cytoplasmic extracts from cells expressing each form of β-globin mRNA were assayed by Western blotting for efficiency of SMG6 knockdown. **B.** The effectiveness of SMG6 knockdown in inhibiting NMD was determined by qRT-PCR analysis of changes in WT- versus PTC-TCRβ mRNA. **C.** The modified MBRACE assay was used to quantify the impact of SMG6 knockdown full-length WT- and PTC-hβG mRNA. **D.** Modified MBRACE assay was used to monitor the impact of SMG6 knockdown on the production of Δ169 RNA. The results represent the mean ± standard deviation of triplicate cultures, * indicates $p<0.05$ by two-tailed Student's t-test.

SMG6 knockdown reduced levels of the endogenous protein to ~30% of control (Figure 30A, compare lane 3 with lanes 4 and 5), and in each transfected siRNA-resistant SMG6 was overexpressed compared to endogenous protein (Figure 30A, compare lanes 1,2,6-9 with lane 3). The similar expression of each form of recombinant SMG6 confirmed that each of these is resistant to SMG6 siRNA and therefore capable of complementing the impact of SMG6 knockdown on PTC-hβG NMD. Results in Figure 30B show that neither SMG6 knockdown nor its complementation with exogenous SMG6 had any impact on wild-type full-length or Δ169 RNA (grey bars). As in Figure 29, SMG6 knockdown increased the amount of full-length PTC-hβG mRNA and decreased the amount of Δ169 RNA (SMG6 siRNA + vector). This was reversed by co-expression of siRNA-resistant SMG6, but not by co-expression of catalytically-inactive SMG6-m4, thus confirming the identity of SMG6 as the enzyme that is responsible for generating stable decay products from PTC-hβG mRNA.

Altering SMG6 has no impact on the phosphorylation state of Upf1

In Okada-Katsuhata et al. [151] NMD was inhibited by SMG6 knockdown or by overexpression of an inactive form of SMG6. SMG6 functions in the dephosphorylation of Upf1, and in each case this was reported to result from interference with the cycling of Upf1 between phosphorylation states. The absence of an inhibitory effect of SMG6m4 on PTC-hβG mRNA decay in Figure 30B argued against this. Nevertheless, to be certain that the results in Figure 29 and Figure 30 indeed demonstrate a direct role for SMG6 endonuclease activity in generating stable decay intermediates we looked at the impact of each of these changes on the phosphorylation state of Upf1. In the experiment in Figure 31, K562 cells were electroporated as in Figure 30 with control or SMG6 siRNAs, and with empty vector or with plasmids

Figure 30. Complementataion identifies SMG6 is the endonuclease responsible for generating Δ169 RNA from PTC hβg mRNA

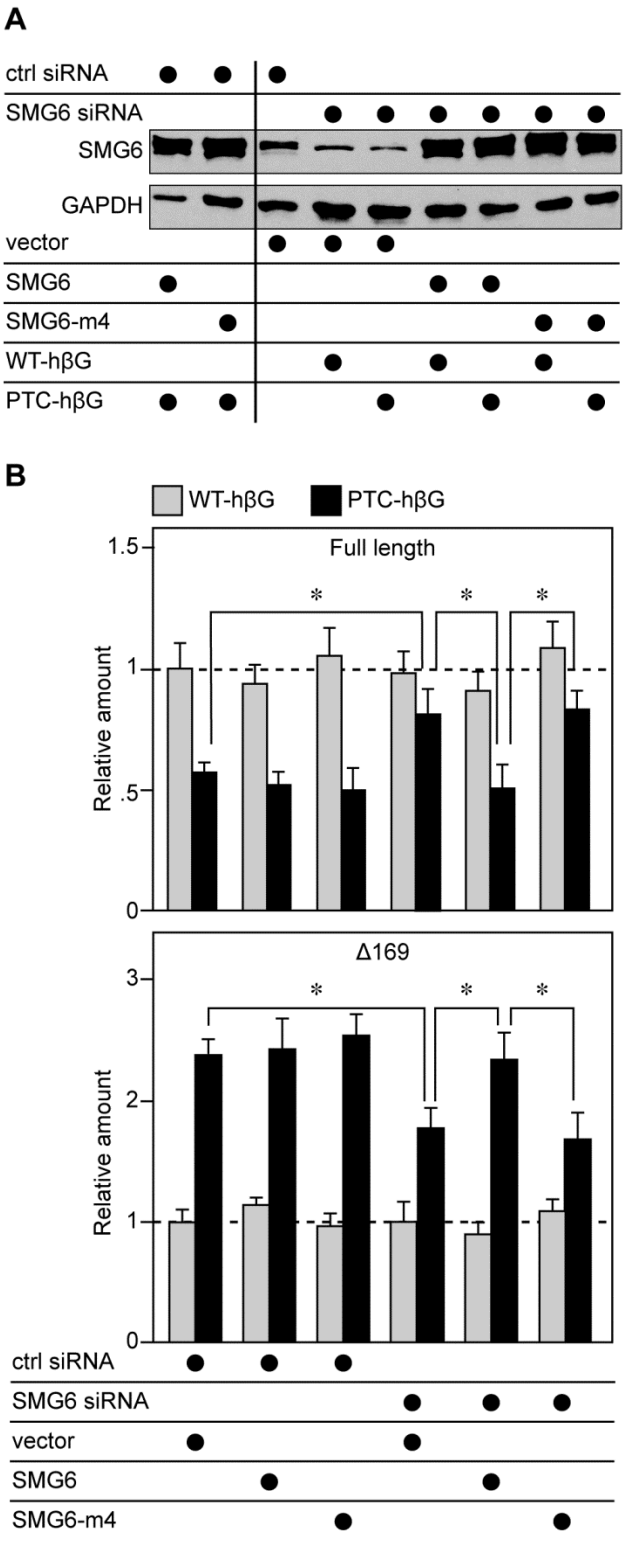

Tet-inducible K562 cells in antibiotic-free medium were electroporated as in Figure 27, with control or SMG6 siRNAs. Twenty-four hr later they were electroporated again with the same siRNAs plus empty vector or plasmids expressing siRNA resistant SMG6 or a catalytically-inactive form of SMG6 (SMG6-m4) and plasmids expressing each of the inducible hβG genes. Doxycycline was added 16 hr later to induce each of the hβG genes. **A.** Cytoplasmic extracts from triplicate cultures were pooled and analyzed by Western blotting with anti-SMG6 antibody or with antibody to GAPDH. **B.** Cytoplasmic RNA from individual cultures was analyzed by modified MBRACE assay for full-length (upper panel) and Δ169 (lower panel) forms of hβG mRNA. The results represent the mean ± standard deviation of triplicate cultures, * indicates $p<0.05$ by two-tailed Student's t-test.

expressing SMG6 or SMG6-m4. Western blotting with anti-SMG6 antibody (Figure 31top panel) confirmed the effectiveness of each of these steps in reducing or increasing each form of SMG6. Importantly, Western blotting with an anti-phosphoUpf1 antibody showed that none of these treatments had any impact on the phosphorylation state of Upf1(Figure 31).

Figure 31. Upf1 phosphorylation status is unaffected by SMG6 knockdown or overexpression of inactive SMG6

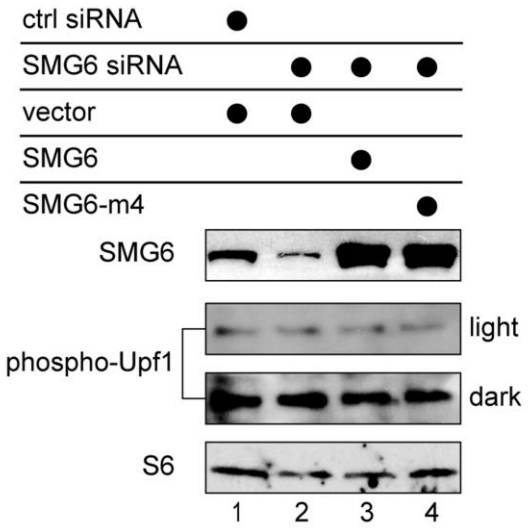

Tet-inducible K562 cells were electroporated as in Figure 30 with control or SMG6 siRNAs and empty vector, or plasmids expressing SMG6 or inactive SMG6-m4. Cytoplasmic extracts recovered 16 hr after the second round of electroporation were analyzed by Western blotting with antibodies to SMG6 (top panel) or to phospho-Upf1 (middle and lower panels). Both light and dark exposures are shown.

DISCUSSION

To the best of our knowledge the 5'-truncated forms of PTC-hβG mRNA examined here are the only example of metastable products of nonsense-mediated mRNA decay. They were first identified in erythroid cells of mice expressing a nonsense-containing transgene [177], and to date have only been detected in erythroid cells. Like the parent mRNA the 5' ends of these RNAs are

capped [179, 198] and they have an intact 3'-poly(A) tail [180]. S1 nuclease protection assays performed on cytoplasmic RNA recovered over 8 hr of actinomycin D treatment showed full-length PTC-hβG mRNA decayed with biphasic kinetics (Figure 25) that resemble the decay of PTC-hβG mRNA in non-erythroid cells [197]. The decay curves in Figure 25B indicated that the 5'-truncated RNAs disappear more slowly than full-length PTC-hβG mRNA. However, the transcripts with 5' ends closer to the cap appear to decay more quickly than transcripts whose 5' ends are further from the cap, the result one might expect for RNA undergoing multiple cleavage events until reaching some limit digest. The complexity of this precluded the use transcriptional inhibition to study the relationship of the 5'-truncated transcripts to PTC-hβG mRNA decay. This was instead addressed through the use of an inducible erythroid cell line and a modification of the MBRACE assay for quantifying changes in full-length mRNA and one of the truncated RNAs (Δ169). In the course of qualifying this assay we reaffirmed results in [198] showing the 5'-truncated RNAs are capped (Figure 26B).

Nonsense-containing mRNAs have been reported to undergo deadenylation, decapping, 5'-exonucleolytic decay, 3'-exonucleolytic decay and endonucleolytic decay [14, 184]. The rules by which any given mRNA selected for a particular degradation pathway have not been determined. Results presented here confirm that NMD is responsible for the decay of full-length PTC-hβG mRNA and identify the 5'-truncated RNAs as decay intermediates. Three different experiments demonstrated that SMG6 is the endonuclease that generates these intermediates. The first (Figure 29) looked at the impact of SMG6 knockdown alone, and the most straightforward interpretation of these data identifies SMG6 is the enzyme that cleaves PTC-hβG mRNA to generate the stable Δ169 intermediate. However, SMG6 has been reported to function in the dephosphorylation of Upf1, and its knock down in HeLa cells was reported to inhibit NMD secondary to the accumulation of phospho-Upf1 [151]. To address this we performed a complementation experiment in which we knocked down SMG6 and expressed siRNA-resistant forms of SMG6 or SMG6 with the 3 aspartic acid residues in the PIN domain catalytic core

changed to asparagine (SMG6-m4). Results in Figure 30show that expression of siRNA resistant SMG6 reversed the effect of SMG6 knockdown on the generation of Δ169 RNA from PTC-hβG mRNA, but expression of SMG6-m4 did not, thus supporting the identification of SMG6 as the responsible endonuclease.

Results in Figure 31 also brought to light a difference between our results and those in [151] regarding the impact of overexpressing inactive forms of SMG6. In that study NMD was inhibited by overexpression of SMG6 with a single aspartate-to-alanine PIN domain mutation (D1251A). We saw no evidence for inhibition of NMD with overexpression of SMG6-m4 in K562 cells. In Figure 30 each form of SMG6 was clearly overexpressed (Figure 30A); however, as evident in the first 3 datasets in Figure 30B neither of these had any impact on full-length or Δ169 RNA. We do not know why these results differ from those in [151], but this may be due to differences in the form of inactive SMG6 used in our study, or to the fact that our experiments examined hβG mRNA in its native cell context.

Still it remained formally possible that SMG6 knockdown still resulted in the accumulation of phosho-Upf1 and expression of SMG6-m4 just helped to keep Upf1 in the phosphorylated state. This was ruled out by the results of Figure 31, where we saw no evidence for changes in the phosphorylation state of Upf1 regardless of whether SMG6 was knocked down or an inactive form of SMG6 was expressed in these cells. Together with the preceding experiments these data provide proof that metastable decay intermediates are generated by SMG6 cleavage of PTC-hβG mRNA.

Finally, K562 cells do not natively express β-globin mRNA but they do express detectable levels of δ-globin mRNA [200]. In the course of this work we identified a form of δ-globin mRNA whose 5' end matched that of Δ169 RNA. This raised a question that was not answered by this study; to wit, why are the same 5'-truncated RNAs also detectable in cells expressing WT-hβG mRNA? These were seen in [180] and [194], and again here by both S1 nuclease protection and by the modified MBRACE assay (Figure 26). Although the

endonuclease responsible for generating these fragments has yet to be identified, the fact that both WT- and PTC-hβG mRNA are cleaved at the same sites suggests features of the mRNP play a major role in determining the location of endonuclease cleavage sites.

ACKNOWLEDGMENTS

We thank Miles Wilkinson for providing the TCRβ plasmids, Jens Lykke-Andersen for antibodies to Upf1 and SMG6, Oliver Mühlemann for SMG6-expressing plasmids, Yuichi Otsuka and Jennifer Stanich for help with assays and members of the Schoenberg lab for their helpful comments and discussion. The research reported in this publication was supported by the National Institute of General Medical Sciences of the National Institutes of Health under award numbers R01GM079707, R01GM084177 and R01GM038277. The content is solely the responsibility of the authors and does not necessarily represent the official views of the National Institutes of Health. J.A.D. was supported by an RNA fellowship from the Ohio State University Center for RNA Biology.

Figure 32. Sequence alignment of human beta- and delta-globin mRNA and locations of MBRACE primers.

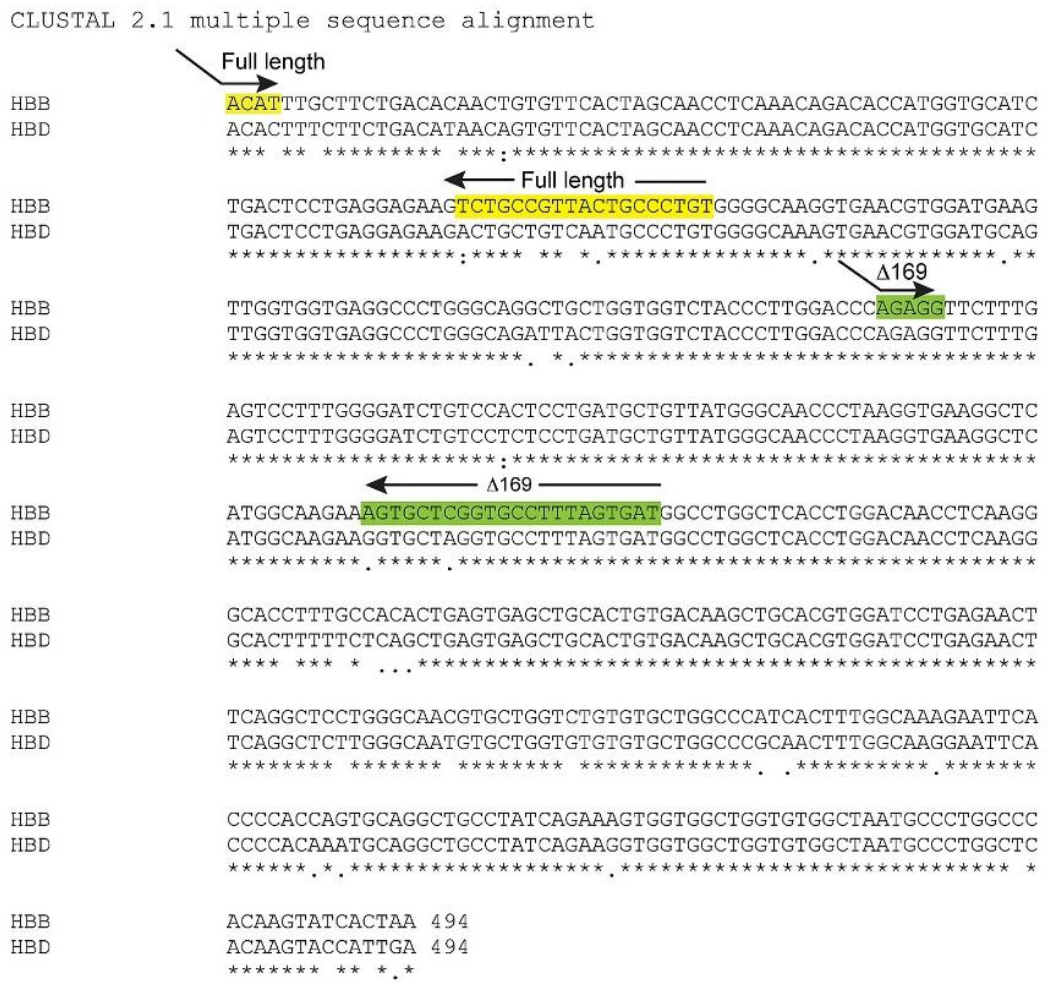

Human beta-globin (HBB) and delta-globin (HBD) mRNAs are shown aligned. The yellow highlights identify the locations of primers used to quantify full-length mRNA and the green highlights identify the locations of primers used to quantify D169 RNA. Note that the sequence at the 5′ D169 primer binding site is identical for beta- and delta-globin mRNA.

Figure 33. Impact of changes in PMR1 on full-length and Δ169 hβG mRNA.

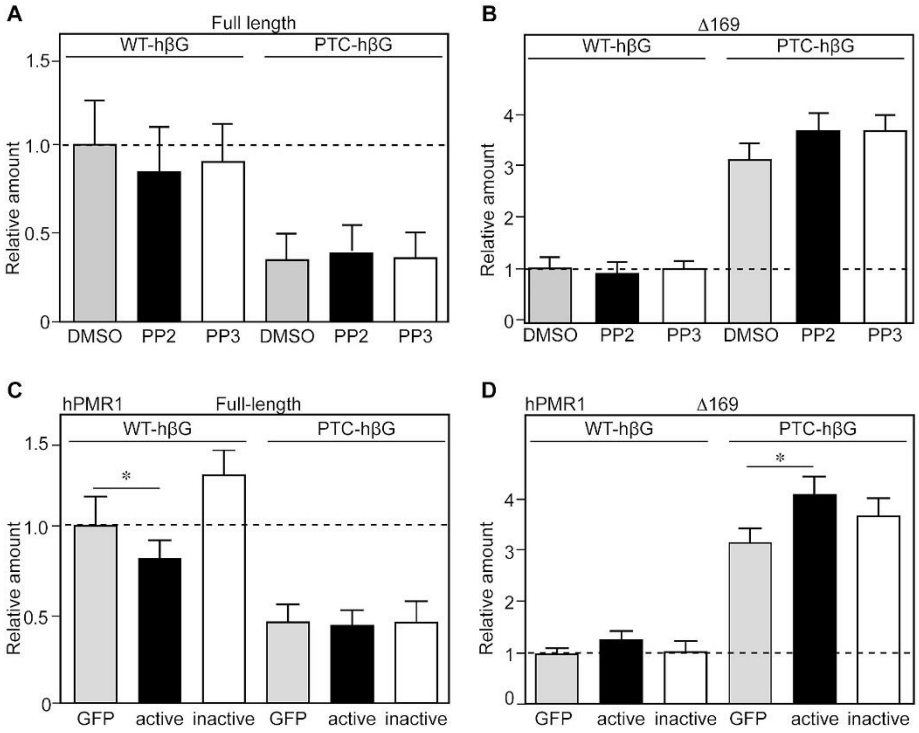

A and **B.** Tet-inducible K562 cells electroporated with inducible WT- and PTC-hβG genes were treated with DMSO (vehicle), PP3 (an inactive analog of PP2), or PP2 c-Src inhibitor to inactivate PMR1 targeting to polysomes [6, 7]. Cytoplasmic RNA recovered 6 hr after induction was assayed by modified MBRACE for changes in full-length (**A**) and Δ169 RNA (**B**). **C** and **D**. Tet-inducible K562 cells were electroporated with WT- and PTC-hβG expressing plasmids together with plasmids expressing GFP, active hPMR1 or inactive hPMR1. Cytoplasmic RNA recovered 6 hr after induction was analyzed by modified MBRACE for changes in full-length (**C**) and Δ169 RNA (**D**). The results represent the mean ± standard deviation of triplicate cultures, *indicates $p<0.05$ by two-tailed Student's t-test.

Table 8. Oligonucleotides and Primers

Oligonucleotide name	Sequence
HBB-AS	5'-TTTCTTGCCATGAGCCTTCACCTTA-3'
1249	5'-ACGTGCAGCTTGTCACAGTG-3'
YO-41	5'-TTGCCAATAGTGATGACCTG-3'
HBB-S	5'-CATACGATTTAGGTGACACTATAG-3'
ACT-S	5'-ACAAAAGCTGGAGCTCCAC-3'
RNA ADA (adapter)	5’-CGACUGGAGCACGAGGACACUGACAUGGACUGAAGGAGUAGCCA-3’
MBRACE-F	5’-CGACTGGAGCACGAGGACAC-3’
HBB-FL-MB	5’-6FAM-GGACTGAAGGAGTAGCCAACAT-BHQ1-3’
HBB-Δ169-MB	5’-6FAM-ACTGAAGGAGTAGCCAAGAGG-DABCYL-3’
HBB-JS-F	5'-GGACTGAAGGAGTAGCCAACAT-3'
HBB-Δ169-JS-F	5'-ACTGAAGGAGTAGCCAAGAGG-3'
HBB-FL-R1	5’-AACTTCATCCACGTTCACCTTGCC-3’
HBB-Δ169-R1	5’-TAAAGGCACCGAGCACTTTCTTGC-3’
HBB-FL-R2	5'-ACAGGGCAGTAACGGCAGA-3'
HBB-Δ169-R2	5'-ATCACTAAAGGCACCGAGCACT-3'
TCRβ-F	5'-GGGCTGAGGCTGATCCATTA-3'
TCRβ-R	5'-TGGAGTCACATTTCTCAGAT-3'
emGFP-F	5'-TCAAGGAGGACGGCAACATC-3'
emGFP-R	5'-TGTGGCGGGTCTTGAAGTTC-3'
MA-F (mouse β-actin)	5’-TGTGATGGTGGGAATGGGTCAGAA-3’
MA-R (mouse β-actin)	5’-TGTGGTGCCAGATCTTCTCCATGT-3’

Chapter 4: Discussion

Overall, this study had three main goals. First, I needed to establish the identity of the full-length and 5' truncated β-globin RNAs to design a detection regimen. Previous work in the Maquat lab [177] and later in collaboration with the Schoenberg [180] lab used S1 nuclease protection assays (S1 NPA), primer extension analysis, and electrophoretic mobility to map the 5' ends of the truncated RNAs. While these assays are accurate in their determination of 5' ends they may not be precise. Thus, I sought to precisely identify the 5' ends of full-length β-globin mRNA and the 5' truncated species by 5'-RLM-RACE and sequencing of PCR products. This approach would identify the 5' most nucleotide and whether that nucleotide (nt) varies or not. Completing this goal was necessary to provide a sequence template upon which a detection method was designed. Secondly, I set out to determine whether a precursor-product relationship existed between the parent, full-length β-globin transcript and the 5' truncated RNAs existed, as this was important because it had not yet been shown in the over 20 years since the truncated RNAs were first observed [177]. Lastly, I sought to determine how the 5' truncated β-globin products were generated and identify the responsible enzyme. After the discovery of the truncated RNAs in 1989, the Maquat lab [177] hypothesized the shortened species were generated either by decapping and 5'to 3' exonucleolytic decay or by endonuclease cleavage. Work done by the Schoenberg lab pointed towards PMR1, or an enzyme like it, as the endonuclease responsible for cleavage. Later discovery of SMG6 and its role in degradation of nonsense-containing mRNAs made their method of generation less clear. Therefore, both enzymes, and a third, were studied for their role in the generation of the 5' truncated mRNAs. After discussing

the findings associated with each of these goals I will elaborate on some alternative uses for the systems I have developed and results I have observed.

Establishing the identity of and a detection regimen for 5' truncated β-globin RNAs

In 1989, the Maquat lab observed three truncated RNA species by S1 NPA and determined they lacked 70, 85, or 185 nt from the mRNA 5' end [177]. Later collaborative work observed 12 truncated species by observation in at least 2 out of 3 techniques. Ends were identified as lacking 67, 77, 92/93, 143, 167, 186/187, 214, 259, 269, 276, 316 and 324 nt from the 5' end of full-length β-globin transcript [180]. However, these determinations may be subjective depending on whether the gel ran straight, how well the ladder ran, and estimating the sizes by comparing migration of the ladder to the observed band. These methods are accurate in nature but may or may not be precise. I wanted to precisely identify the 5' end sequences to determine which bases are involved and if the 5' ends remained constant. Determining the precise identity of the 5' ends was integral to designing a sensitive and quantitative detection system.

5' RLM-RACE to identify 5' ends

The first step in establishing how the 5' truncated β-globin RNAs arise is to determine the 5' ends of the full-length and shortened species. I chose to use 5' RNA-linker-mediated rapid amplification of cDNA ends (5'RLM-RACE) for this task as it is an established protocol for sequencing the very 5' ends of RNAs. The ligation of a RNA linker to the 5' end of mRNA provides a region of known sequence which allows for subsequent amplification of the following unknown sequence. I exploited the fact that RNA ligase 1 will ligate an RNA linker onto all mRNAs with a 5' monophosphate end, thus providing me with a common sequence to target by PCR. Since previous reports showed that the 5' truncated RNAs were capped [179], I needed to specifically target capped RNAs while excluding uncapped ones. To do this, RNA from MEL cells expressing wild type and PTC60/61 β-globin was treated with alkaline phosphatase to

remove the 5' monophosphate from RNAs. Next, the RNA was treated with TAP to cleave the cap and create a 5' monophosphate end on the remaining RNAs. This left two populations of RNA, those with a 5' monophosphate, which are substrates for RNA ligase 1, and those with a 5' hydroxyl, which are not. The RNA linker was ligated to the substrate RNAs and then gene-specific reverse transcription was used to generate β-globin cDNA, any and all forms containing the primer binding site. Nested PCR with adapter and gene-specific primers allowed for visualization of the β-globin species with gel electrophoresis. Full-length product was observed at its expected size and numerous smaller bands, assumed to be the 5' truncated species, were also observed. The bands were excised, purified, and cloned into a vector for sequencing of their 5' ends. Full-length product sequencing confirmed the 5' end was indeed base 1 of the mRNA sequence. We chose the truncated RNA with the highest amplification and determined its 5' end to be at base 169 of the full-length mRNA, thus naming it Δ169. Sequencing of multiple colonies showed that the 5' base did not vary across colonies. This 5' end was consistent with S1 NPA mapping and primer extension assays mentioned earlier that predicted a 5' truncated β-globin RNA lacking 167 nt from the 5' end. These findings offered me a way to further analyze the truncated β-globin mRNAs by designing a detection method.

Designing a sensitive and quantitative detection method - MBRACE

A highly sensitive, quantitative assay to measure RNA decay had been established in the lab. Unfortunately, the company that manufactured the proprietary reagents was bought out and academic sales were discontinued. This meant a new technology needed to be developed to quantitatively study the decay of β-globin mRNA, sensitively and reliably. S1 NPA was used previously but was not practical for the purpose of this study. MEL cells are difficult to transfect, which meant knockdown and other experimental manipulations needed to be performed on a small scale and S1 NPA requires a large amount of input RNA. The MBRACE assay was identified in a literature search as an alternative approach for quantifying the decay products

[183]. The original protocol utilized amplification of cDNA prior to performing gene-specific nested PCR and detection by qPCR. Because we wanted to perform kinetic analysis of β-globin mRNA decay we needed to modify the assay to be more conducive to quantitative analysis. We modified the original protocol by removing the nested PCR after cDNA synthesis to minimize possible detection differences due to PCR bias. So CIAP-TAP-treated RNA would be synthesized into cDNA followed by detection with qPCR. Since MBRACE qPCR is based on binding of the fluorescent molecular beacons to the linker-target junctions, their design and validation needed to be completed next.

Molecular beacons

The molecular beacons were designed to span the junction across the 3' end of the RNA linker to the 5' β-globin RNA sequence. Molecular beacons were chosen over Taqman probes as they are not dependent on the nuclease activity of the polymerase and fluoresce only when bound to their target. The beacons were designed with a majority of their 5' ends binding the adaptor and 4-5 bases of the 3' end complementary to the very 5' end of the targeted β-globin sequences. This would prevent non-specific detection of β-globin since most of the beacon binding was mediated by the adaptor. Although the sequences of the two beacons only differed by a few bases, detection using molecular beacons is very specific, non-specific detection was less than 1%. The beacons were originally designed with different fluorophores so that full-length and Δ169 β-globin could be detected in a single duplex reaction. Much time was spent attempting to optimize the duplex reaction but this probed to be unsuccessful as results were inconsistent. Additionally, the level of excitation of the two fluorophores by their respective lasers was not equal. That of the Δ169 beacon was maximal and excitation of the full-length beacon was less than maximal. Thus, the full-length beacon was altered to have the same fluorophore as Δ169 and the two targets would be analyzed in separate reactions. Using the same fluorophore provides equal excitation and emission in the reactions so that differences in detection are not due

to the fluorophore used. With that final change beacon specificity, sensitivity, and reaction efficiency were all optimized and validated. Therefore, I designed and verified a reliable, quantitative and sensitive assay for study of full-length and Δ169 β-globin on the small scale necessitated by erythroid cells. However, we still needed a tightly regulated erythroid expression system in order to conduct our experiments.

Erythroid cells

I established a new system to surmount some of the difficulties that remained from previous experiments. One of the complications was that β-globin mRNA was constantly expressed in the MEL cell system. This made analyzing the levels of full-length and 5' truncated β-globin RNA difficult due to a high background of the 5' truncated species. To overcome this I established and used an inducible erythroid cell line that tightly regulated β-globin mRNA expression, which made kinetic and knockdown experiments possible.

In order to perform kinetic and knockdown experiments we needed erythroid cells with closely regulated expression of β-globin mRNA. The MEL cells used in the past showed an increase in β-globin mRNA transcription upon inducing differentiation with DMSO, but they had very leaky expression and a readily detectable level of background expression. That combined with the difficulty of performing transfections led us to seek out a new erythroid model cell line. K562 cells are human erythroleukemic cells that presented such an opportunity since they do not express β-globin. While still difficult to transfect, the efficiency was much better than with the MEL cells. I established tetracycline-regulated stable cell lines, which would express β-globin mRNA only when induced. During pilot experiments to verify regulated expression and MBRACE detection of full-length and Δ169 β-globin in transfected K562 cells the Δ169 truncated RNA was detected in the parental cell line. This unexpected result lead me to PCR amplify the parental β-globin cDNA reaction and clone it into vector to determine the identity of the resulting band. Sequencing results revealed I was detecting δ-globin, a globin family member

with 85% sequence homology to β-globin. Detection of an identical truncated 5' end in a related protein suggests that the mechanism of decay that β-globin undergoes is conserved. While this finding was very, it meant that the Δ169 beacon I designed could not be used for detection with these cells, as the junction sequence was not unique to β-globin. Consequently, the modified MBRACE assay was redesigned to one that used SYBR green-based qPCR detection, which emits fluorescenece when bound to double-stranded DNA . The primer sets for detection utilized a forward primer complementary to the junction sequence and a β-globin-specific reverse primer. I tested the new detection design with the regulated K562 cells and no longer saw detection of δ-globinRNA in the parental cells. With regulated expression and specific detection we now had a system to induce expression of β-globin mRNA and quantitatively detect the full-length and Δ169 β-globin RNA species.

Establishing a precursor-product relationship between full-length and 5' truncated β-globin RNA

Previous work in the Maquat lab [175], suggested there was a precursor-product relationship between full-length β-globin and the 5' truncated species. To summarize their work briefly, cells expressing wild type and PTC-containing β-globin mRNA were treated with transcription inhibitors and the fate of full-length and truncated RNAs was determined over time. The Maquat lab observed a decrease in full-length β-globin mRNA, which coincided with an increase in the shortened species. While this behavior hinted at a precursor-product relationship, it was not conclusive proof. Due to the limitations of the system, a precursor-product relationship cannot be determined when the product is more stable than the precursor. In the regulated K562 cell system, transcription of β-globin mRNA is induced at time zero and monitored for appearance of the different mRNA species would reveal whether a precursor-product relationship existed. If it did then full-length β-globin would accumulate prior to the appearance of the Δ169 species.

At time zero, β-globin mRNA expression was induced in the regulated K562 cells and RNA was harvested over a time course. Full-length and Δ169 β-globin levels were monitored with our modified SYBR green MBRACE assay. Results showed an accumulation of full-length mRNA prior to the appearance of the Δ169 species (Figure 28). This gave a clear picture of a precursor-product relationship as more rapidly degraded mRNAs will accumulate to a steady state level faster than more slowly degraded mRNAS. Even more distinct results were seen using the destabilized constructs (Figure 28C) and we concluded that the Δ169 species is a decay product of the full-length β-globin transcript.

Determining the method of generation of the Δ169 decay product

Experiments in the Maquat lab ruled out generation of the stable 5' truncated RNA via alternative transcription start sites or aberrant alternative splicing. Observations that the shortened RNAs were not seen in the nuclear fraction and the determination that 3 different PTC-generating mutations present at 3 different locations produced the same pattern of 5' truncated RNAs ruled out alternative transcription start site usage [177]. Aberrant alternative splicing was doubtful as the mechanism of generation since it is highly unlikely that the 3 different PTCs studied would create or destroy the same splice donor and/or acceptor sites. Additionally, if they arose from missplicing then the S1 NPA would not detect the same pattern of truncated mRNA as their inclusion of sequences would vary [177]. Therefore it was hypothesized that due to the presence of a PTC and lack of detection of truncated RNAs in wild type β-globin samples that NMD was involved in their generation [177].

Conversely, experiments in Schoenberg lab demonstrated PMR1, or an enzyme like it, was the endonuclease responsible for cleavage. Further, the same pattern of truncated RNAs were observed in wild type β-globin samples, albeit to a lesser extent, pointed towards an already in place mechanism that was augmented by the presence of a PTC. It was unknown at the time that NMD also regulated physiological mRNAs not just nonsense-containing mRNAs, which

complicated whether the NMD pathway was involved. The subsequent determination that SMG6 generated NMD decay intermediates added to the mystery of the mechanism of generation. Using the regulated K562 cell system I investigated the involvement of NMD in generation of the stable decay intermediates and further investigated 3 candidate endonucleases for their involvement.

The role of NMD in β-globin decay

Preliminary experiments using MEL cells were consistent with involvement of the NMD pathway in the generation of the decay products. MEL cells expressing wild type or PTC60/61 β-globin mRNAs were treated with and without cycloheximide. Cycloheximide causes freezing of translating ribosomes on mRNAs, acting as a general translation inhibitor. As NMD is dependent on active translation, if it were involved in β-globin mRNA decay then inhibiting translation would inhibit generation of Δ169. I observed a stabilization of full-length β-globin and decreased detection of Δ169 RNA during translation inhibition (unpublished data). Since cycloheximide only inhibits NMD indirectly, additional NMD-targeted experiments needed to be conducted to further determine NMD's involvement. As Upf1 is the master regulator of the NMD pathway, I used siRNAs to knockdown Upf1 expression in the inducible K562 cell system. Under my level of Upf1 knockdown our most robust NMD reporter, PTC-containing TCRβ, we observed stabilization of full-length mRNA, indicating that my knockdown was sufficient to inhibit NMD. Subsequent experiments were conducted with the wild type and PTC60/61 β-globin constructs under Upf1 knockdown conditions. Full-length PTC-60/61 β-globin was significantly stabilized and accumulation of Δ169 decreased significantly under Upf1 knockdown (Figure 27). This specific inhibition of NMD via Upf1 knockdown is strong evidence that the Δ169 decay intermediate is generated by the NMD machinery. These were the first results that convincingly attributed a stable decay product to NMD.

Determine the nuclease responsible for cleavage

Several possibilities still remained for how the decay fragments were generated. PMR1-mediated cleavage had been proposed in 2002 [180]. The discovery of SMG6 in 2008 [116] implicated it as the endonuclease. Zc3h12a was also a candidate enzyme, as mice deficient for it were severely anemic [201], like thalassemic mice. All three endonuclease active sites have at least some homology to a PIN domain and have demonstrated RNA cleavage. To be thorough, all three enzymes were tested for their involvement in generation of the Δ169 stable β-globin decay product.

PMR1 and Zc3h12a

One attractive possibility was that PMR1 generated the decay intermediates as evidenced by previous work in the Schoenberg lab [194], which occurred prior to SMG6 discovery. I performed experiments in my inducible K562 cell system to verify if this was true. PMR1 was expressed in its active or inactive form in the regulated K562, with GFP-expressing plasmid serving as empty vector control. Experiments were also conducted using c-Src inhibitors to block activation of PMR1, as phosphorylation via c-Src activates the enzyme, prior to expression of PTC60/61 β-globin. Both sets of experiments showed no increase in Δ169 with active PMR1 or without c-Src inhibition (Figure 33). Additionally, a decrease in full-length β-globin was not seen. Furthermore, conditions with inactive PMR1 and c-SRC inhibition did not stabilize full-length b-globin and decrease Δ169 detection. Therefore, PMR1 was ruled out as the endonucleolytic generator of the decay intermediates. To be thorough we tested another endonuclease encoded by the Zc3h12a gene. Zc3h12a was recently identified as an RNase involved in the regulation of the inflammatory response [201]. Yet again, we expressed catalytically active or inactive mutant protein with GFP-expressing plasmid serving as empty vector control. We observed no significant changes in detection of full-length or Δ169 β-globin under expression of either form of Zc3h12a (unpublished data). Therefore, Zc3h12a was also

determined to not be the endonuclease responsible for decay intermediate generation. The involvement of NMD in decay product generation and the presence of a PTC indicated that NMD-associated endonuclease SMG6 might be responsible for generation of the decay products.

SMG6

Since involvement of the NMD pathway had been demonstrated, it naturally followed that experiments focused on SMG6 would be conducted. SMG6 knockdown experiments were performed in the inducible K562 cells with similar results to Upf1 knockdown. Again, we verified that knockdown of SMG6 was sufficient to inhibit NMD by monitoring the PTC-containing TCRβ reporter, which confirmed that it was. Briefly, full-length PTC60/61 β-globin was stabilized under SMG6 knockdown and the Δ169 fragment was significantly diminished when compared to control knockdown (Figure 29). These results offered an supportive data that NMD is involved in β-globin mRNA decay intermediate generation. However, this was not clear proof that the catalytic activity of SMG6 was responsible for cleavage. To test this hypothesis, knockdown of endogenous SMG6 was complemented with expression of either wild type SMG6 or a mutant form with inactive endonuclease activity. Equal expression of the two forms, endogenous and tagged-exogenous, of SMG6 was shown by Western blot. Then I used the modified MBRACE to analyze RNA harvested from the same cells. I once again saw significant stabilization of the full-length transcript and a significant decrease accumulation of the Δ169 decay intermediate (Figure 30). These data offered solid support that SMG6 is an endonuclease responsible for cleaving full-length β-globin and therefore generating the stable decay intermediates.

As far as we know, this is the only case where stable decay intermediates of the NMD pathway have been observed. Other experiments studying NMD in nonerythroid cells have only detected 3' decay intermediates with concomitant knockdown of Xrn1. It is very interesting that these stable decay intermediates are also observed in erythroid cells expressing wildtype β-globin,

although to a much lesser extent. Since SMG6 has of yet to demonstrate sequence specificity, it stands to reason that the mRNP is dictating cleavage site selection. The reasons as to why erythroid cells generate these stable intermediates is still unknown. Because cells are not wasteful with resources it would be reasonable to hypothesize that the stable intermediates serve a purpose. An N-terminally truncated protein translated from one of these intermediates may have different activity, localization, folding, or regulation - depending on the truncation - as compared to wild type protein.

Future directions

The study of these stable decay intermediates led to the discovery of the cytoplasmic capping enzyme compex (cCE) by the Schoenberg laboratory [198] with the β-globin decay intermediates being the first documented targets. The results of this project identify SMG6 cleavage as the first documented enzymatic process to create cytoplasmic capping substrates. Recapping of mRNAs gives rise to many interesting questions. Work is ongoing to determine the role of the cCE in the stability of the β-globin decay intermediates. Is the presence of a 5' cap the cause or consequence of their stability? I will be testing this in K562 cells with tetracycline inducible expression of WT and an inactive form of cCE that acts as a dominant negative. The destabilized form of PTC-60/61 β-globin will be studied alongside normal PTC60/61 β-globin when cytoplasmic capping is ongoing and when it is inhibited. Additionally, Δ169 has a 5' cap and an intact poly(A) making it translation competent and I want to determine its translation status in the cell. Cytoplasmic capping target mRNAs were found to shift from polysomes to the mRNP fraction when capping was inhibited [202]. Based on those results and that active translation is required for NMD, Δ169 may very well be found on polysomes. In preparation of that possible outcome, the β-globin mRNA was analyzed for a downstream AUG with proper Kozak consensus sequence for translation initiation. Serendipitously, I located one at base 216, which lies within the Δ169 product. I am planning to perform polysome fractionation to

determine translation status of the mRNA and also assess fractions for β-globin protein expression by Western blot. A C-terminally 6xHis-tagged construct will allow for detection of any forms of β-globin with an intact C-terminal. Studies have shown that C-terminally truncated β-globin protein acts as a dominant negative and exacerbates thalassemia symptoms [171, 172]. Whether we detect N-terminally truncated β-globin protein remains to be seen.

Implications

While these experiments are the only known case of stable decay intermediates it is very likely that other cases exist. Additional stable decay products of other mRNAs may exist and could be verified using the methods I established for this project. Validation analysis could be done by 5' RLM-RACE and subsequent modified MBRACE, but only if candidate RNAs are already identified. Recently, at the 2013 Cold Spring Harbor Laboratories Meeting on Eukaryotic mRNA processing, work was presented that encompassed identifying any and all nonsense-containing mRNAs in HEK293 cells by deep sequencing. Cells were treated with Xrn1-targeted siRNAs to stabilize 3' decay fragments and mRNA was harvested and sent for deep sequencing. Subsequent experiments were conducted with co-depletion of Xrn1 and SMG6 or Upf1 to identify NMD-targeted decay fragments. Results of this study may identify some stabilized 5' truncated decay intermediates, and publication is eagerly awaited. I could expand on their work by mining their sequencing data for candidate RNAs.

I would first analyze the deep sequencing data for mRNAs where there is a differential in mapping of reads for the 5' ends versus the 3' ends of RNAs. To narrow down potential candidates, mRNAs that have a 5' to 3' read ratio of about one will be excluded, but mRNAs with a 5' to 3' read ratio of 0.5 or lower will represent candidate RNAs. These candidates could be verified by Upf1 and/or SMG6 knockdown and additional deep sequencing. The knockdown conditions will eliminate the imbalance of read distribution and define the data set. The identified

candidates will be validated using the 5'-RLM-RACE by my modified MBRACE detection method.

Alternatively, a 5' end-biased library could be constructed by hybridizing an RNA linker with 15 nt of known sequence followed by 6Ns (random combination of A,U,C,G for 6 bases) to the 5' ends of poly(A)-enriched and ribosomal RNA-depleted mRNA (as in [202]). Aligning sequences detected by paired-end sequencing of such a library to the human genome could identify possible stable decay intermediates as they map 5' ends. Analyzing mapping of reads for those downstream of the normal transcription start site would identify potential mRNA candidates. Validation of candidate mRNAs could again be assessed with Upf1 and/or SMG6 knockdown, followed by modified MBRACE protocol. If the decay products were generated similarly to the β-globin decay intermediates then the detection of the candidate decay intermediates would decrease under knockdown conditions.

However, it is possible that stable 5' truncated mRNAs are generated in a manner that differs from that of β-globin mRNA. Other possible experiments to determine their method of generation would include knockdown of Xrn1 to block 5' to 3' exonucleolytic decay. Alternatively, Dcp2, a decapping enzyme, could be knocked down in concert with Xrn1 to determine whether they are generated by decapping followed by exonucleolytic decay. Another possible method of generation is differential transcription start site usage, which could be determined by examining nuclear mRNAs. It is also possible that the stable decay intermediates are generated by an endonuclease other than SMG6. The mode of generation would need to determines for each candidate mRNA multiple methods may exist.

Furthermore, NMD-targeted mRNAs may need to be studied in the cell type where they are normally expressed. If they serve a special purpose then it would likely occur where they are natively found; the stable β-globin intermediates are only observed in erythroid tissue and cells. If these 5' truncated β-globin decay intermediates are found on polysomes and a corresponding truncated protein is detected then the reason behind their generation gets more interesting. Cap

analysis of gene expression (CAGE) studies have already identified RNAs with capped 5' ends downstream of the wild type 5' end [203]. Endonuclease-mediated cleavage of full-length mRNAs to generate 5' truncated RNA that are recapped by cCE could be a mechanism by which the cell expands or regulates its transcriptome and/or proteome. Since cells are not careless with resources, it would be reasonable to hypothesize that the stable intermediates serve a purpose. An N-terminally truncated protein translated from one of these intermediates may have different activity, localization, folding, or regulation as compared to wild type protein.

These results present many questions to be addressed in the field and whose answers could prove to be very interesting. Recapping of 5' ends is a mechanism by which a cell could have altered protein functions that are not due to DNA mutations. Depending on which amino acids are included in the truncated protein form could be beneficial or detrimental to the cell. Endonuclease cleavage of mRNA could be occurring more frequently than previously thought and could be generating cytoplasmic capping targets. The methods developed and results observed in this project could serve as a jumping off point for future studies.

List of References

1. Shoemaker, C.J. and R. Green, *Kinetic analysis reveals the ordered coupling of translation termination and ribosome recycling in yeast.* Proc Natl Acad Sci U S A, 2011. **108**(51): p. E1392-8.
2. Gehring, N.H., et al., *Exon-junction complex components specify distinct routes of nonsense-mediated mRNA decay with differential cofactor requirements.* Mol Cell, 2005. **20**(1): p. 65-75.
3. Chan, W.K., et al., *An alternative branch of the nonsense-mediated decay pathway.* EMBO J, 2007. **26**(7): p. 1820-30.
4. Kashima, I., et al., *SMG6 interacts with the exon junction complex via two conserved EJC-binding motifs (EBMs) required for nonsense-mediated mRNA decay.* Genes Dev, 2010. **24**(21): p. 2440-50.
5. Cheng, J., et al., *Introns are cis effectors of the nonsense-codon-mediated reduction in nuclear mRNA abundance.* Mol Cell Biol, 1994. **14**(9): p. 6317-25.
6. Yang, F., Y. Peng, and D.R. Schoenberg, *Endonuclease-mediated mRNA decay requires tyrosine phosphorylation of polysomal ribonuclease 1 (PMR1) for the targeting and degradation of polyribosome-bound substrate mRNA.* J Biol Chem, 2004. **279**(47): p. 48993-9002.
7. Peng, Y. and D.R. Schoenberg, *c-Src activates endonuclease-mediated mRNA decay.* Mol Cell, 2007. **25**(5): p. 779-87.
8. Unterholzner, L. and E. Izaurralde, *SMG7 acts as a molecular link between mRNA surveillance and mRNA decay.* Mol Cell, 2004. **16**(4): p. 587-596.
9. Jiang, Y., X.S. Xu, and J.E. Russell, *A nucleolin-binding 3' untranslated region element stabilizes beta-globin mRNA in vivo.* Mol Cell Biol, 2006. **26**(6): p. 2419-29.
10. Brown, T.A., *Genomes*. 1999, Oxford, United Kingdom: BIOS Scientific Publishers Ltd.
11. Wanjek, C., *Signal Discovery Opens Pathway to Therapies for Iron-Overload Ills.* The NIH Catalyst, 2007. **15**(5).
12. Dougherty, J.A., R. Mascarenhas, and D.R. Schoenberg, *Quantitative Analysis of Deadenylation-Independent mRNA Decay by a Modified MBRACE Assay.* Methods Mol Biol, 2014. **1125**: p. 353-71.
13. Glavan, F.B.-A., I. Izaurralde E. Conti, E, *Structures of the PIN domains of SMG6 and SMG5 reveal a nuclease within the mRNA surveillance complex.* EMBO J, 2006. **25**(21): p. 5117-5125.
14. Kervestin, S. and A. Jacobson, *NMD: a multifaceted response to premature translational termination.* Nat Rev Mol Cell Biol, 2012. **13**(11): p. 700-12.

15. Vet, J.A. and S.A. Marras, *Design and optimization of molecular beacon real-time polymerase chain reaction assays.* Methods in Molecular Biology, 2005. **288**: p. 273-90.
16. Huang, L. and M.F. Wilkinson, *Regulation of nonsense-mediated mRNA decay.* Wiley Interdiscip Rev RNA, 2012. **3**(6): p. 807-28.
17. Nicholson, P. and O. Muhlemann, *Cutting the nonsense: the degradation of PTC-containing mRNAs.* Biochem Soc Trans, 2010. **38**(6): p. 1615-1620.
18. Isken, O. and L.E. Maquat, *The multiple lives of NMD factors: balancing roles in gene and genome regulation.* Nat Rev Genet, 2008. **9**(9): p. 699-712.
19. Franks, T.M. and J. Lykke-Andersen, *The control of mRNA decapping and P-body formation.* Mol Cell, 2008. **32**(5): p. 605-15.
20. Cho, H., et al., *SMG5-PNRC2 is functionally dominant compared with SMG5-SMG7 in mammalian nonsense-mediated mRNA decay.* Nucleic Acids Res, 2013. **41**(2): p. 1319-28.
21. Bartel, B. and D.P. Bartel, *MicroRNAs: at the root of plant development?* Plant Physiol, 2003. **132**(2): p. 709-17.
22. Parker, R. and H. Song, *The enzymes and control of eukaryotic mRNA turnover.* Nat Struct Mol Biol, 2004. **11**(2): p. 121-7.
23. Schmid, M. and T.H. Jensen, *The exosome: a multipurpose RNA-decay machine.* Trends Biochem Sci, 2008. **33**(10): p. 501-10.
24. Franks, T.M., G. Singh, and J. Lykke-Andersen, *Upf1 ATPase-dependent mRNP disassembly is required for completion of nonsense- mediated mRNA decay.* Cell, 2010. **143**(6): p. 938-950.
25. Hwang, J. and L.E. Maquat, *Nonsense-mediated mRNA decay (NMD) in animal embryogenesis: to die or not to die, that is the question.* Curr Opin Genet Dev, 2011. **21**(4): p. 422-30.
26. Losson, R. and F. Lacroute, *Interference of nonsense mutations with eukaryotic messenger RNA stability.* Proc Natl Acad Sci U S A, 1979. **76**(10): p. 5134-7.
27. Maquat, L.E., et al., *Unstable beta-globin mRNA in mRNA-deficient beta o thalassemia.* Cell, 1981. **27**(3 Pt 2): p. 543-53.
28. Guan, Q., et al., *Impact of nonsense-mediated mRNA decay on the global expression profile of budding yeast.* PLoS Genet, 2006. **2**(11): p. e203.
29. He, F., et al., *Genome-wide analysis of mRNAs regulated by the nonsense-mediated and 5' to 3' mRNA decay pathways in yeast.* Mol Cell, 2003. **12**(6): p. 1439-52.
30. Lelivelt, M.J. and M.R. Culbertson, *Yeast Upf proteins required for RNA surveillance affect global expression of the yeast transcriptome.* Mol Cell Biol, 1999. **19**(10): p. 6710-9.
31. Ramani, A.K., et al., *High resolution transcriptome maps for wild-type and nonsense-mediated decay-defective Caenorhabditis elegans.* Genome Biol, 2009. **10**(9): p. R101.
32. Rehwinkel, J., et al., *Nonsense-mediated mRNA decay factors act in concert to regulate common mRNA targets.* RNA, 2005. **11**(10): p. 1530-44.
33. Mendell, J.T., et al., *Nonsense surveillance regulates expression of diverse classes of mammalian transcripts and mutes genomic noise.* Nat Genet, 2004. **36**(10): p. 1073-8.

34. Viegas, M.H., et al., *The abundance of RNPS1, a protein component of the exon junction complex, can determine the variability in efficiency of the Nonsense Mediated Decay pathway.* Nucleic Acids Res, 2007. **35**(13): p. 4542-51.
35. Wittmann, J., E.M. Hol, and H.M. Jack, *hUPF2 silencing identifies physiologic substrates of mammalian nonsense-mediated mRNA decay.* Mol Cell Biol, 2006. **26**(4): p. 1272-87.
36. Yepiskoposyan, H., et al., *Autoregulation of the nonsense-mediated mRNA decay pathway in human cells.* RNA, 2011. **17**(12): p. 2108-18.
37. Amrani, N., M.S. Sachs, and A. Jacobson, *Early nonsense: mRNA decay solves a translational problem.* Nat Rev Mol Cell Biol, 2006. **7**(6): p. 415-25.
38. Anderson, P., *NMD in Caenorhabditis elegans*, in *Nonsense-mediated mRNA decay*, L.E. Maquat, Editor. 2006, Landes Biosciences, Texas. p. 139-150.
39. Pulak, R. and P. Anderson, *mRNA surveillance by the Caenorhabditis elegans smg genes.* Genes Dev, 1993. **7**(10): p. 1885-97.
40. Hodgkin, J., et al., *A new kind of informational suppression in the nematode Caenorhabditis elegans.* Genetics, 1989. **123**(2): p. 301-13.
41. Domeier, M.E., et al., *A link between RNA interference and nonsense-mediated decay in Caenorhabditis elegans.* Science, 2000. **289**(5486): p. 1928-31.
42. Maniatis, T. and B. Tasic, *Alternative pre-mRNA splicing and proteome expansion in metazoans.* Nature, 2002. **418**(6894): p. 236-43.
43. Schmucker, D., et al., *Drosophila Dscam is an axon guidance receptor exhibiting extraordinary molecular diversity.* Cell, 2000. **101**(6): p. 671-84.
44. Garcia, J., et al., *A conformational switch in the Piccolo C2A domain regulated by alternative splicing.* Nat Struct Mol Biol, 2004. **11**(1): p. 45-53.
45. Resch, A., et al., *Assessing the impact of alternative splicing on domain interactions in the human proteome.* J Proteome Res, 2004. **3**(1): p. 76-83.
46. Xing, Y., Q. Xu, and C. Lee, *Widespread production of novel soluble protein isoforms by alternative splicing removal of transmembrane anchoring domains.* FEBS Lett, 2003. **555**(3): p. 572-8.
47. Stamm, S., et al., *An alternative-exon database and its statistical analysis.* DNA Cell Biol, 2000. **19**(12): p. 739-56.
48. Lewis, B.P., R.E. Green, and S.E. Brenner, *Evidence for the widespread coupling of alternative splicing and nonsense-mediated mRNA decay in humans.* Proc Natl Acad Sci U S A, 2003. **100**(1): p. 189-92.
49. Wittkopp, N., et al., *Nonsense-mediated mRNA decay effectors are essential for zebrafish embryonic development and survival.* Mol Cell Biol, 2009. **29**(13): p. 3517-28.
50. Metzstein, M.M. and M.A. Krasnow, *Functions of the nonsense-mediated mRNA decay pathway in Drosophila development.* PLoS Genet, 2006. **2**(12): p. e180.
51. Avery, P., et al., *Drosophila Upf1 and Upf2 loss of function inhibits cell growth and causes animal death in a Upf3-independent manner.* RNA, 2011. **17**(4): p. 624-38.
52. Medghalchi, S.M., et al., *Rent1, a trans-effector of nonsense-mediated mRNA decay, is essential for mammalian embryonic viability.* Hum Mol Genet, 2001. **10**(2): p. 99-105.

53. Weischenfeldt, J., et al., *NMD is essential for hematopoietic stem and progenitor cells and for eliminating by-products of programmed DNA rearrangements.* Genes Dev, 2008. **22**(10): p. 1381-96.
54. McIlwain, D.R., et al., *Smg1 is required for embryogenesis and regulates diverse genes via alternative splicing coupled to nonsense-mediated mRNA decay.* Proc Natl Acad Sci U S A, 2010. **107**(27): p. 12186-91.
55. Azzalin, C.M. and J. Lingner, *The human RNA surveillance factor UPF1 is required for S phase progression and genome stability.* Curr Biol, 2006. **16**(4): p. 433-9.
56. Azzalin, C.M., et al., *Telomeric repeat containing RNA and RNA surveillance factors at mammalian chromosome ends.* Science, 2007. **318**(5851): p. 798-801.
57. Brumbaugh, K.M., et al., *The mRNA surveillance protein hSMG-1 functions in genotoxic stress response pathways in mammalian cells.* Mol Cell, 2004. **14**(5): p. 585-98.
58. Reichenbach, P., et al., *A human homolog of yeast Est1 associates with telomerase and uncaps chromosome ends when overexpressed.* Curr Biol, 2003. **13**(7): p. 568-74.
59. Culbertson, M.R., K.M. Underbrink, and G.R. Fink, *Frameshift suppression Saccharomyces cerevisiae. II. Genetic properties of group II suppressors.* Genetics, 1980. **95**(4): p. 833-53.
60. Leeds, P., et al., *The product of the yeast UPF1 gene is required for rapid turnover of mRNAs containing a premature translational termination codon.* Genes Dev, 1991. **5**(12A): p. 2303-14.
61. He, F. and A. Jacobson, *Identification of a novel component of the nonsense-mediated mRNA decay pathway by use of an interacting protein screen.* Genes Dev, 1995. **9**(4): p. 437-54.
62. Perlick, H.A., et al., *Mammalian orthologues of a yeast regulator of nonsense transcript stability.* Proc Natl Acad Sci U S A, 1996. **93**(20): p. 10928-32.
63. Conti, E. and E. Izaurralde, *Nonsense-mediated mRNA decay: molecular insights and mechanistic variations across species.* Curr Opin Cell Biol, 2005. **17**(3): p. 316-25.
64. Cui, Y., et al., *Identification and characterization of genes that are required for the accelerated degradation of mRNAs containing a premature translational termination codon.* Genes Dev, 1995. **9**(4): p. 423-36.
65. Czaplinski, K., et al., *Purification and characterization of the Upf1 protein: a factor involved in translation and mRNA degradation.* RNA, 1995. **1**(6): p. 610-23.
66. Chamieh, H., et al., *NMD factors UPF2 and UPF3 bridge UPF1 to the exon junction complex and stimulate its RNA helicase activity.* Nat Struct Mol Biol, 2008. **15**(1): p. 85-93.
67. Bhattacharya, A., et al., *Characterization of the biochemical properties of the human Upf1 gene product that is involved in nonsense-mediated mRNA decay.* RNA, 2000. **6**(9): p. 1226-35.
68. Weng, Y., K. Czaplinski, and S.W. Peltz, *Genetic and biochemical characterization of mutations in the ATPase and helicase regions of the Upf1 protein.* Mol Cell Biol, 1996. **16**(10): p. 5477-90.

69. Jacobson, A. and E. Izaurralde, in *Translational Control in Biology and Medicine*, M.B. Mathews, N. Sonenberg, and J.W.B. Hershey, Editors. 2007, Cold Spring Harbor Laboratory Press: Cold Spring Harbor, NY. p. 659-691.
70. Leeds, P., et al., *Gene products that promote mRNA turnover in Saccharomyces cerevisiae.* Mol Cell Biol, 1992. **12**(5): p. 2165-77.
71. Altamura, N., et al., *NAM7 nuclear gene encodes a novel member of a family of helicases with a Zn-ligand motif and is involved in mitochondrial functions in Saccharomyces cerevisiae.* J Mol Biol, 1992. **224**(3): p. 575-87.
72. Cheng, Z., et al., *Structural and functional insights into the human Upf1 helicase core.* EMBO J, 2007. **26**(1): p. 253-64.
73. Weng, Y., K. Czaplinski, and S.W. Peltz, *ATP is a cofactor of the Upf1 protein that modulates its translation termination and RNA binding activities.* RNA, 1998. **4**(2): p. 205-14.
74. Chakrabarti, S., et al., *Molecular mechanisms for the RNA-dependent ATPase activity of Upf1 and its regulation by Upf2.* Mol Cell, 2011. **41**(6): p. 693-703.
75. Clerici, M., et al., *Unusual bipartite mode of interaction between the nonsense-mediated decay factors, UPF1 and UPF2.* EMBO J, 2009. **28**(15): p. 2293-306.
76. Kashima, I., et al., *Binding of a novel SMG-1-Upf1-eRF1-eRF3 complex (SURF) to the exon junction complex triggers Upf1 phosphorylation and nonsense-mediated mRNA decay.* Genes Dev, 2006. **20**(3): p. 355-67.
77. Ohnishi, T., et al., *Phosphorylation of hUPF1 induces formation of mRNA surveillance complexes containing hSMG-5 and hSMG-7.* Mol Cell, 2003. **12**(5): p. 1187-200.
78. Yamashita, A., et al., *Human SMG-1, a novel phosphatidylinositol 3-kinase-related protein kinase, associates with components of the mRNA surveillance complex and is involved in the regulation of nonsense-mediated mRNA decay.* Genes Dev, 2001. **15**(17): p. 2215-28.
79. Lykke-Andersen, J., M.D. Shu, and J.A. Steitz, *Human Upf proteins target an mRNA for nonsense-mediated decay when bound downstream of a termination codon.* Cell, 2000. **103**(7): p. 1121-31.
80. Mendell, J.T., C.M. ap Rhys, and H.C. Dietz, *Separable roles for rent1/hUpf1 in altered splicing and decay of nonsense transcripts.* Science, 2002. **298**(5592): p. 419-22.
81. Czaplinski, K., et al., *The surveillance complex interacts with the translation release factors to enhance termination and degrade aberrant mRNAs.* Genes Dev, 1998. **12**(11): p. 1665-77.
82. Kaygun, H. and W. Marzluff, *Regulated degradation of replication-dependent histone mRNAs requires both ATR and Upf1.* Nat Struct Mol Biol, 2005. **12**(9): p. 794-800.
83. Nott, A., H. Le Hir, and M.J. Moore, *Splicing enhances translation in mammalian cells: an additional function of the exon junction complex.* Genes Dev, 2004. **18**(2): p. 210-22.
84. Applequist, S.E., et al., *Cloning and characterization of HUPF1, a human homolog of the Saccharomyces cerevisiae nonsense mRNA-reducing UPF1 protein.* Nucleic Acids Res, 1997. **25**(4): p. 814-21.

85. Carastro, L.M., et al., *Identification of delta helicase as the bovine homolog of HUPF1: demonstration of an interaction with the third subunit of DNA polymerase delta.* Nucleic Acids Res, 2002. **30**(10): p. 2232-43.
86. Sittman, D.B., R.A. Graves, and W.F. Marzluff, *Histone mRNA concentrations are regulated at the level of transcription and mRNA degradation.* Proc Natl Acad Sci U S A, 1983. **80**(7): p. 1849-53.
87. Mendell, J.T., et al., *Novel Upf2p orthologues suggest a functional link between translation initiation and nonsense surveillance complexes.* Mol Cell Biol, 2000. **20**(23): p. 8944-57.
88. Serin, G., et al., *Identification and characterization of human orthologues to Saccharomyces cerevisiae Upf2 protein and Upf3 protein (Caenorhabditis elegans SMG-4).* Mol Cell Biol, 2001. **21**(1): p. 209-23.
89. He, F., A.H. Brown, and A. Jacobson, *Interaction between Nmd2p and Upf1p is required for activity but not for dominant-negative inhibition of the nonsense-mediated mRNA decay pathway in yeast.* RNA, 1996. **2**(2): p. 153-70.
90. Kadlec, J., E. Izaurralde, and S. Cusack, *The structural basis for the interaction between nonsense-mediated mRNA decay factors UPF2 and UPF3.* Nat Struct Mol Biol, 2004. **11**(4): p. 330-7.
91. Kunz, J.B., et al., *Functions of hUpf3a and hUpf3b in nonsense-mediated mRNA decay and translation.* RNA, 2006. **12**(6): p. 1015-22.
92. Chan, W.K., et al., *A UPF3-mediated regulatory switch that maintains RNA surveillance.* Nat Struct Mol Biol, 2009. **16**(7): p. 747-53.
93. Gehring, N.H., et al., *Y14 and hUpf3b Form an NMD-Activating Complex.* Mol Cell, 2003. **11**: p. 939-949.
94. Tarpey, P.S., et al., *Mutations in UPF3B, a member of the nonsense-mediated mRNA decay complex, cause syndromic and nonsyndromic mental retardation.* Nat Genet, 2007. **39**(9): p. 1127-33.
95. Denning, G., et al., *Cloning of a novel phosphatidylinositol kinase-related kinase: characterization of the human SMG-1 RNA surveillance protein.* J Biol Chem, 2001. **276**(25): p. 22709-14.
96. Oliveira, V., et al., *A protective role for the human SMG-1 kinase against tumor necrosis factor-alpha-induced apoptosis.* J Biol Chem, 2008. **283**(19): p. 13174-84.
97. Grimson, A., et al., *SMG-1 is a phosphatidylinositol kinase-related protein kinase required for nonsense-mediated mRNA Decay in Caenorhabditis elegans.* Mol Cell Biol, 2004. **24**(17): p. 7483-90.
98. Yamashita, A., I. Kashima, and S. Ohno, *The role of SMG-1 in nonsense-mediated mRNA decay.* Biochim Biophys Acta, 2005. **1754**(1-2): p. 305-15.
99. Gehen, S.C., et al., *hSMG-1 and ATM sequentially and independently regulate the G1 checkpoint during oxidative stress.* Oncogene, 2008. **27**(29): p. 4065-74.
100. Chiu, S.Y., et al., *Characterization of human Smg5/7a: a protein with similarities to Caenorhabditis elegans SMG5 and SMG7 that functions in the dephosphorylation of Upf1.* RNA, 2003. **9**(1): p. 77-87.
101. Anders, K.R., A. Grimson, and P. Anderson, *SMG-5, required for C. elegans nonsense-mediated mRNA decay, associates with SMG-2 and protein phosphatase 2A.* EMBO J, 2003. **22**(3): p. 641-650.

102. Clissold, P.M. and C.P. Ponting, *PIN domains in nonsense-mediated mRNA decay and RNAi.* Curr Biol, 2000. **10**(24): p. R888-90.
103. Gatfield, D. and E. Izaurralde, *Nonsense-mediated messenger RNA decay is initiated by endonucleolytic cleavage in Drosophila.* Nature, 2004. **429**(6991): p. 575-578.
104. Eberle, A.B., et al., *SMG6 promotes endonucleolytic cleavage of nonsense mRNA in human cells.* Nat Struct Mol Biol, 2009. **16**(1): p. 49-55.
105. Fukuhara, N.E., J. Unterholzner, L. Lindner, D. Izaurralde, E. Conti, E., *SMG7 is a 14-3-3-like adaptor in the nonsense-mediated mRNA decay pathway.* Molecular Cell, 2005. **17**(4): p. 537-547.
106. Bhuvanagiri, M., et al., *NMD: RNA biology meets human genetic medicine.* Biochem J, 2010. **430**(3): p. 365-77.
107. Lykke-Andersen, J., M.D. Shu, and J.A. Steitz, *Communication of the position of exon-exon junctions to the mRNA surveillance machinery by the protein RNPS1*. Science, 2001. **293**(5536): p. 1836-9.
108. Page, M.F., et al., *SMG-2 is a phosphorylated protein required for mRNA surveillance in Caenorhabditis elegans and related to Upf1p of yeast.* Mol Cell Biol, 1999. **19**(9): p. 5943-51.
109. Aronoff, R., R. Baran, and J. Hodkin, *Molecular identi®cation of smg-4, required for mRNA surveillance in C. elegans.* Gene, 2001. **268**: p. 153-164.
110. Pal, M., et al., *Evidence that phosphorylation of human Upfl protein varies with intracellular location and is mediated by a wortmannin-sensitive and rapamycin-sensitive PI 3-kinase-related kinase signaling pathway.* RNA, 2001. **7**(1): p. 5-15.
111. Lempiainen, H. and T.D. Halazonetis, *Emerging common themes in regulation of PIKKs and PI3Ks.* EMBO J, 2009. **28**(20): p. 3067-73.
112. Yamashita, A., et al., *SMG-8 and SMG-9, two novel subunits of the SMG-1 complex, regulate remodeling of the mRNA surveillance complex during nonsense-mediated mRNA decay.* Genes Dev, 2009. **23**(9): p. 1091-105.
113. Loh, B., S. Jonas, and E. Izaurralde, *The SMG5-SMG7 heterodimer directly recruits the CCR4-NOT deadenylase complex to mRNAs containing nonsense codons via interaction with POP2.* Genes Dev, 2013. **27**(19): p. 2125-38.
114. Forest, K.T., et al., *The pilus-retraction protein PilT: ultrastructure of the biological assembly.* Acta Crystallogr D Biol Crystallogr, 2004. **60**(Pt 5): p. 978-82.
115. Marchler-Bauer, A., et al., *CDD: conserved domains and protein three-dimensional structure.* Nucleic Acids Res, 2013. **41**(Database issue): p. D348-52.
116. Huntzinger, E., et al., *SMG6 is the catalytic endonuclease that cleaves mRNAs containing nonsense codons in metazoan.* RNA, 2008. **14**(12): p. 2609-2617.
117. Buchwald, G., et al., *Insights into the recruitment of the NMD machinery from the crystal structure of a core EJC-UPF3b complex.* Proc Natl Acad Sci U S A, 2010. **107**(22): p. 10050-5.
118. Le Hir, H., et al., *The exon-exon junction complex provides a binding platform for factors involved in mRNA export and nonsense-mediated mRNA decay.* EMBO J, 2001. **20**(17): p. 4987-97.

119. Nagy, E. and L.E. Maquat, *A rule for termination-codon position within intron-containing genes: when nonsense affects RNA abundance.* Trends Biochem Sci, 1998. **23**(6): p. 198-199.
120. Thermann, R., et al., *Binary specification of nonsense codons by splicing and cytoplasmic translation.* EMBO J, 1998. **17**(12): p. 3484-94.
121. Neu-Yilik, G., et al., *Mechanism of escape from nonsense-mediated mRNA decay of human beta-globin transcripts with nonsense mutations in the first exon.* RNA, 2011. **17**(5): p. 843-54.
122. Amrani, N., et al., *A faux 3'-UTR promotes aberrant termination and triggers nonsense-mediated mRNA decay.* Nature, 2004. **432**(7013): p. 112-8.
123. Behm-Ansmant, I., et al., *A conserved role for cytoplasmic poly(A)-binding protein 1 (PABPC1) in nonsense-mediated mRNA decay.* EMBO J, 2007. **26**(6): p. 1591-601.
124. Silva, A.L., et al., *Proximity of the poly(A)-binding protein to a premature termination codon inhibits mammalian nonsense-mediated mRNA decay.* RNA, 2008. **14**(3): p. 563-76.
125. Ishigaki, Y., et al., *Evidence for a pioneer round of mRNA translation: mRNAs subject to nonsense-mediated decay in mammalian cells are bound by CBP80 and CBP20.* Cell, 2001. **106**(5): p. 607-17.
126. Maquat, L.E., et al., *CBP80-promoted mRNP rearrangements during the pioneer round of translation, nonsense-mediated mRNA decay, and thereafter.* Cold Spring Harb Symp Quant Biol, 2010. **75**: p. 127-34.
127. Lejeune, F., et al., *The exon junction complex is detected on CBP80-bound but not eIF4E-bound mRNA in mammalian cells: dynamics of mRNP remodeling.* EMBO J, 2002. **21**(13): p. 3536-45.
128. Hosoda, N., et al., *CBP80 promotes interaction of Upf1 with Upf2 during nonsense-mediated mRNA decay in mammalian cells.* Nat Struct Mol Biol, 2005. **12**(10): p. 893-901.
129. Lejeune, F., A.C. Ranganathan, and L.E. Maquat, *eIF4G is required for the pioneer round of translation in mammalian cells.* Nat Struct Mol Biol, 2004. **11**(10): p. 992-1000.
130. Chiu, S.Y., et al., *The pioneer translation initiation complex is functionally distinct from but structurally overlaps with the steady-state translation initiation complex.* Genes Dev, 2004. **18**(7): p. 745-54.
131. Gorlich, D., et al., *Importin provides a link between nuclear protein import and U snRNA export.* Cell, 1996. **87**(1): p. 21-32.
132. Sato, H. and L.E. Maquat, *Remodeling of the pioneer translation initiation complex involves translation and the karyopherin importin beta.* Genes Dev, 2009. **23**(21): p. 2537-50.
133. Moerke, N.J., et al., *Small-molecule inhibition of the interaction between the translation initiation factors eIF4E and eIF4G.* Cell, 2007. **128**(2): p. 257-67.
134. Durand, S. and J. Lykke-Andersen, *Nonsense-mediated mRNA decay occurs during eIF4F-dependent translation in human cells.* Nat Struct Mol Biol, 2013. **20**(6): p. 702-9.

135. Rufener, S.C. and O. Muhlemann, *eIF4E-bound mRNPs are substrates for nonsense-mediated mRNA decay in mammalian cells.* Nat Struct Mol Biol, 2013. **20**(6): p. 710-7.
136. Zhang, S., et al., *Polysome-associated mRNAs are substrates for the nonsense-mediated mRNA decay pathway in Saccharomyces cerevisiae.* RNA, 1997. **3**(3): p. 234-44.
137. Gozalbo, D. and S. Hohmann, *Nonsense suppressors partially revert the decrease of the mRNA level of a nonsense mutant allele in yeast.* Curr Genet, 1990. **17**(1): p. 77-9.
138. Belgrader, P., J. Cheng, and L.E. Maquat, *Evidence to implicate translation by ribosomes in the mechanism by which nonsense codons reduce the nuclear level of human triosephosphate isomerase mRNA.* Proc Natl Acad Sci U S A, 1993. **90**(2): p. 482-6.
139. Gaba, A., A. Jacobson, and M.S. Sachs, *Ribosome occupancy of the yeast CPA1 upstream open reading frame termination codon modulates nonsense-mediated mRNA decay.* Mol Cell, 2005. **20**(3): p. 449-60.
140. Editors, S. *SparkNote on Molecular Biology: Translation*. 2014 02/25/14]; Available from: http://www.sparknotes.com/biology/molecular/translation.
141. Frolova, L., et al., *A highly conserved eukaryotic protein family possessing properties of polypeptide chain release factor.* Nature, 1994. **372**(6507): p. 701-3.
142. Zhouravleva, G., et al., *Termination of translation in eukaryotes is governed by two interacting polypeptide chain release factors, eRF1 and eRF3.* EMBO J, 1995. **14**(16): p. 4065-72.
143. Cheng, Z., et al., *Structural insights into eRF3 and stop codon recognition by eRF1.* Genes Dev, 2009. **23**(9): p. 1106-18.
144. Alkalaeva, E.Z., et al., *In vitro reconstitution of eukaryotic translation reveals cooperativity between release factors eRF1 and eRF3.* Cell, 2006. **125**(6): p. 1125-36.
145. Jackson, R.J., C.U. Hellen, and T.V. Pestova, *Termination and post-termination events in eukaryotic translation.* Adv Protein Chem Struct Biol, 2012. **86**: p. 45-93.
146. Salas-Marco, J. and D.M. Bedwell, *GTP hydrolysis by eRF3 facilitates stop codon decoding during eukaryotic translation termination.* Mol Cell Biol, 2004. **24**(17): p. 7769-78.
147. Hoshino, S., et al., *The eukaryotic polypeptide chain releasing factor (eRF3/GSPT) carrying the translation termination signal to the 3'-Poly(A) tail of mRNA. Direct association of erf3/GSPT with polyadenylate-binding protein.* J Biol Chem, 1999. **274**(24): p. 16677-80.
148. Cosson, B., et al., *Poly(A)-binding protein acts in translation termination via eukaryotic release factor 3 interaction and does not influence [PSI(+)] propagation.* Mol Cell Biol, 2002. **22**(10): p. 3301-15.
149. Ivanov, P.V., et al., *Interactions between UPF1, eRFs, PABP and the exon junction complex suggest an integrated model for mammalian NMD pathways.* EMBO J, 2008. **27**(5): p. 736-47.

150. Singh, G., I. Rebbapragada, and J. Lykke-Andersen, *A competition between stimulators and antagonists of Upf complex recruitment governs human nonsense-mediated mRNA decay.* PLoS Biol, 2008. **6**(4): p. e111.
151. Okada-Katsuhata, Y., et al., *N- and C-terminal Upf1 phosphorylations create binding platforms for SMG-6 and SMG-5:SMG-7 during NMD.* Nucleic Acids Res, 2012. **40**(3): p. 1251-66.
152. Cho, H., K.M. Kim, and Y.K. Kim, *Human proline-rich nuclear receptor coregulatory protein 2 mediates an interaction between mRNA surveillance machinery and decapping complex.* Mol Cell, 2009. **33**(1): p. 75-86.
153. Aitken, S.C., et al., *Relationship between the expression of estrogen-regulated genes and estrogen-stimulated proliferation of MCF-7 mammary tumor cells.* Cancer Res, 1985. **45**(6): p. 2608-2615.
154. Garneau, N., J. Wilusz, and C. Wilusz, *The highways and biways of mRNA decay.* Nat Rev Mol Cell Biol, 2007. **8**(2): p. 113-126.
155. Gudikote, J.P., et al., *RNA splicing promotes translation and RNA surveillance.* Nat Struct Mol Biol, 2005. **12**(9): p. 801-9.
156. Alonso, C.R. and M. Akam, *A Hox gene mutation that triggers nonsense-mediated RNA decay and affects alternative splicing during Drosophila development.* Nucleic Acids Res, 2003. **31**(14): p. 3873-80.
157. Bruno, I.G., et al., *Identification of a microRNA that activates gene expression by repressing nonsense-mediated RNA decay.* Mol Cell, 2011. **42**(4): p. 500-10.
158. Papagiannakopoulos, T., et al., *Pro-neural miR-128 is a glioma tumor suppressor that targets mitogenic kinases.* Oncogene, 2012. **31**(15): p. 1884-95.
159. Addington, A.M., et al., *A novel frameshift mutation in UPF3B identified in brothers affected with childhood onset schizophrenia and autism spectrum disorders.* Mol Psychiatry, 2011. **16**(3): p. 238-9.
160. Laumonnier, F., et al., *Mutations of the UPF3B gene, which encodes a protein widely expressed in neurons, are associated with nonspecific mental retardation with or without autism.* Mol Psychiatry, 2010. **15**(7): p. 767-76.
161. Huang, L., et al., *RNA homeostasis governed by cell type-specific and branched feedback loops acting on NMD.* Mol Cell, 2011. **43**(6): p. 950-61.
162. Frischmeyer, P.A. and H.C. Dietz, *Nonsense-mediated mRNA decay in health and disease.* Hum Mol Genet, 1999. **8**(10): p. 1893-900.
163. Sheppard, D.N. and M.J. Welsh, *Structure and function of the CFTR chloride channel.* Physiol Rev, 1999. **79**(1 Suppl): p. S23-45.
164. Shoshani, T., et al., *Association of a nonsense mutation (W1282X), the most common mutation in the Ashkenazi Jewish cystic fibrosis patients in Israel, with presentation of severe disease.* Am J Hum Genet, 1992. **50**(1): p. 222-8.
165. Wilschanski, M., et al., *Gentamicin-induced correction of CFTR function in patients with cystic fibrosis and CFTR stop mutations.* N Engl J Med, 2003. **349**(15): p. 1433-41.
166. Kerr, T.P., et al., *Long mutant dystrophins and variable phenotypes: evasion of nonsense-mediated decay?* Hum Genet, 2001. **109**(4): p. 402-7.
167. Alonso, J., et al., *Spectrum of Germline RB1 Gene Mutations in Spanish Retinoblastoma Patients- Phenotypic and Molecular Epidemiological Implications.* Human Mutation, 2001. **17**: p. 412-422.

168. Benz, E.J. *Treatment of beta thalassemia*. 2014 Feb 15, 2014 [cited 2013; 46.0:[Available from: http://www.uptodate.com/contents/treatment-of-beta-thalassemia?source=see_link&anchor=H10#H16.
169. Schrier, S.L. *Pathophysiology of beta thalassemia*. 2014 Dec 20, 2013 [cited 2013; 10.0:[Available from: http://www.uptodate.com/contents/pathophysiology-of-beta-thalassemia?source=see_link.
170. Huisman, T.H., *The beta- and delta-thalassemia repository*. Hemoglobin, 1992. **16**(4): p. 237-58.
171. Thein, S.L., et al., *Molecular basis for dominantly inherited inclusion body beta-thalassemia.* Proc Natl Acad Sci U S A, 1990. **87**(10): p. 3924-8.
172. Hall, G.W. and S. Thein, *Nonsense codon mutations in the terminal exon of the beta-globin gene are not associated with a reduction in beta-mRNA accumulation: a mechanism for the phenotype of dominant beta-thalassemia.* Blood, 1994. **83**(8): p. 2031-2037.
173. Galanello, R. and R. Origa, *Beta-thalassemia.* Orphanet J Rare Dis, 2010. **5**: p. 11.
174. Kinniburgh, A.J., et al., *mRNA-deficient beta o-thalassemia results from a single nucleotide deletion.* Nucleic Acids Res, 1982. **10**(18): p. 5421-7.
175. Lim, S.-K., et al., *Nonsense codons in human beta-globin mRNA result in the production of mRNA degradation products.* Molecular and Cellular Biology, 1992. **12**(3): p. 1149-1161
176. Maquat, L.E., *Translational Control of Gene Expression*, ed. N. Sonenberg, et al. 2000, Plainview, NY: Cold Spring Harbor Laboratory Press.
177. Lim, S.-K., et al., *Novel metabolism of several Beta zero-thalassemic beta-globin mRNAs in the erythroid tissues of transgenic mice.* EMBO, 1989. **8**(9): p. 2613-2619.
178. Rottman, F., A.J. Shatkin, and R.P. Perry, *Sequences containing methylated nucleotides at the 5' termini of messenger RNAs: possible implications for processing.* Cell, 1974. **3**(3): p. 197-9.
179. Lim, S.K. and L.E. Maquat, *Human beta-globin mRNAs that harbor a nonsense codon are degraded in murine erythroid tissues to intermediates lacking regions of exon I or exons I and II that have a cap-like structure at the 5' termini.* EMBO J, 1992. **11**(9): p. 3271-8.
180. Stevens, A., et al., *Beta -Globin mRNA decay in erythroid cells: UG site-preferred endonucleolytic cleavage that is augmented by a premature termination codon.* Proc Natl Acad Sci U S A, 2002. **99**(20): p. 12741-6.
181. Chernokalskaya, E., R. Dompenciel, and D.R. Schoenberg, *Cleavage properties of an estrogen-regulated polysomal ribonuclease involved in the destabilization of albumin mRNA.* Nucleic Acids Res, 1997. **25**(4): p. 735-42.
182. Chernokalskaya, E., et al., *A polysomal ribonuclease involved in the destabilization of albumin mRNA is a novel member of the peroxidase gene family.* RNA, 1998. **4**(12): p. 1537-48.
183. Lasham, A., et al., *A rapid and sensitive method to detect siRNA-mediated mRNA cleavage in vivo using 5' RACE and a molecular beacon probe.* Nucleic Acids Res, 2010. **38**(3): p. e19.

184. Schoenberg, D.R. and L.E. Maquat, *Regulation of cytoplasmic mRNA decay.* Nat Rev Genet, 2012. **13**(4): p. 246-59.
185. Youseff, B.H., J.A. Dougherty, and C.A. Rappleye, *Reverse genetics through random mutagenesis in Histoplasma capsulatum.* BMC Microbiol, 2009. **9**: p. 236.
186. Bio-Rad Laboratories, I., *Hallmarks of an optimized qPCR assay.* 2012.
187. Pfaffl, M.W., *A new mathematical model for relative quantification in real-time RT-PCR.* Nucleic Acids Res, 2001. **29**(9): p. e45.
188. Molas, M.L. and J.Z. Kiss, *The effect of column purification on cDNA indirect labelling for microarrays.* Plant Methods, 2007. **3**: p. 9.
189. Livak, K.J. and T.D. Schmittgen, *Analysis of relative gene expression data using real-time quantitative PCR and the 2(-Delta Delta C(T)) Method.* Methods, 2001. **25**(4): p. 402-8.
190. Pfaffl, S.L., *Relative Quantification*, in *Real-time PCR (Advanced Methods)*, M.T. Dorak, Editor. 2006, Taylor & Francis Group: New York, NY. p. 63-82.
191. Karginov, F.V., et al., *Diverse endonucleolytic cleavage sites in the mammalian transcriptome depend upon microRNAs, Drosha, and additional nucleases.* Mol Cell, 2010. **38**(6): p. 781-8.
192. Schoenberg, D.R., *Mechanisms of endonuclease-mediated mRNA decay.* Wiley Interdiscip Rev RNA, 2011. **2**(4): p. 582-600.
193. Hanson, M.N. and D.R. Schoenberg, *Application of ligation-mediated reverse transcription polymerase chain reaction to the identification of in vivo endonuclease-generated messenger RNA decay intermediates.* Methods Mol Biol, 2004. **257**: p. 213-22.
194. Bremer, K.A., A. Stevens, and D.R. Schoenberg, *An endonuclease activity similar to Xenopus PMR1 catalyzes the degradation of normal and nonsense-containing human beta-globin mRNA in erythroid cells.* RNA, 2003. **9**(9): p. 1157-67.
195. Wang, J., et al., *A quality control pathway that down-regulates aberrant T-cell receptor (TCR) transcripts by a mechanism requiring UPF2 and translation.* J Biol Chem, 2002. **277**(21): p. 18489-93.
196. Otsuka, Y. and D.R. Schoenberg, *Approaches for studying PMR1 endonuclease-mediated mRNA decay.* Methods Enzymol, 2008. **448**: p. 241-63.
197. Trcek, T., et al., *Temporal and spatial characterization of nonsense-mediated mRNA decay.* Genes Dev, 2013. **27**(5): p. 541-51.
198. Otsuka, Y., N.L. Kedersha, and D.R. Schoenberg, *Identification of a cytoplasmic complex that adds a cap onto 5'-monophosphate RNA.* Mol Cell Biol, 2009. **29**(8): p. 2155-67.
199. Ross, J., *mRNA stability in mammalian cells.* Microbiol Rev, 1995. **59**(3): p. 423-50.
200. Poddie, D., et al., *delta-Globin gene structure and expression in the K562 cell line.* Hemoglobin, 2003. **27**(4): p. 219-28.
201. Matsushita, K., et al., *Zc3h12a is an RNase essential for controlling immune responses by regulating mRNA decay.* Nature, 2009. **458**(7242): p. 1185-90.
202. Mukherjee, C., et al., *Identification of cytoplasmic capping targets reveals a role for cap homeostasis in translation and mRNA stability.* Cell Rep, 2012. **2**(3): p. 674-84.

203. Shiraki, T., et al., *Cap analysis gene expression for high-throughput analysis of transcriptional starting point and identification of promoter usage.* Proc Natl Acad Sci U S A, 2003. **100**(26): p. 15776-81.